NOAA Technical Memorandum NESS 90

LAKE ERIE ICE: WINTER 1975-76

Washington, D.C.
August 1977

noaa NATIONAL OCEANIC AND ATMOSPHERIC ADMINISTRATION / National Environmental Satellite Service

NOAA TECHNICAL MEMORANDUMS

National Environmental Satellite Service Series

The National Environmental Satellite Service (NESS) is responsible for the establishment and operation of the environmental satellite [illegible] of NOAA.

NOAA Technical Memorandums fac[illegible] material that may be preliminary in nature and so may be published formal[illegible]lications 1 through 20 and 22 through 25 are in the earlier ESSA Nationa[illegible]chnical Memorandum (NESCTM) series. The current NOAA Technical Memo[illegible]and subsequent issuances.

Publications listed below are av[illegible]al Information Service, U.S. Department of Commerce, Sills Bldg., 528[illegible]a. 22151. Prices on request. Order by accession number (given in paren[illegible]dums not listed below can be obtained from Environmental Data Service (D831), [illegible], Washington, D.C. 20235.

NESS 49 Operational Processing of Solar Proton Monitor Data. Louis Rubin, Henry L. Phillips, and Stanley R. Brown, August 1973, 17 pp. (COM-73-11647/AS)

NESS 50 An Examination of Tropical Cloud Clusters Using Simultaneously Observed Brightness and High Resolution Infrared Data From Satellites. Arnold Gruber, September 1973, 22 pp. (COM-73-11941/4AS)

NESS 51 SKYLAB Earth Resources Experiment Package Experiments in Oceanography and Marine Science. A. L. Grabham and John W. Sherman, III, September 1973, 72 pp. (COM 74-11740/AS)

NESS 52 Operational Products From ITOS Scanning Radiometer Data. Edward F. Conlan, October 1973, 57 pp. (COM-74-10040)

NESS 53 Catalog of Operational Satellite Products. Eugene R. Hoppe and Abraham L. Ruiz (Editors), March 1974, 91 pp. (COM-74-11339/AS)

NESS 54 A Method of Converting the SMS/GOES WEFAX Frequency (1691 MHz) to the Existing APT/WEFAX Frequency (137 MHz). John J. Nagle, April 1974, 18 pp. (COM-74-11294/AS)

NESS 55 Publications and Final Reports on Contracts and Grants, 1973. NESS, April 1974, 8 pp. (COM-74-11108/AS)

NESS 56 What Are You Looking at When You Say This Area Is a Suspect Area for Severe Weather? Arthur H. Smith, Jr., February 1974, 15 pp. (COM-74-11333/AS)

NESS 57 Nimbus-5 Sounder Data Processing System, Part I: Measurement Characteristics and Data Reduction Procedures. W.L. Smith, H. M. Woolf, P. G. Abel, C. M. Hayden, M. Chalfant, and N. Grody, June 1974, 99 pp. (COM-74-11436/AS)

NESS 58 The Role of Satellites in Snow and Ice Measurements. Donald R. Wiesnet, August 1974, 12 pp. (COM-74-11747/AS)

NESS 59 Use of Geostationary-Satellite Cloud Vectors to Estimate Tropical Cyclone Intensity. Carl. O. Erickson, September 1974, 37 pp. (COM-74-11762/AS)

NESS 60 The Operation of the NOAA Polar Satellite System. Joseph J. Fortuna and Larry N. Hambrick, November 1974, 127 pp. (COM-75-10390/AS)

NESS 61 Potential Value of Earth Satellite Measurements to Oceanographic Research in the Southern Ocean. E. Paul McClain, January 1975, 18 pp. (COM-75-10479/AS)

NESS 62 A Comparison of Infrared Imagery and Video Pictures in the Estimation of Daily Rainfall From Satellite Data. Walton A. Follansbee and Vincent J. Oliver, January 1975, 14 pp. (COM-75-10435/AS)

NESS 63 Snow Depth and Snow Extent Using VHRR Data From the NOAA-2 Satellite. David F. McGinnis, Jr., John A. Pritchard, and Donald R. Wiesnet, February 1975, 10 pp. (COM-75-10482/AS)

NESS 64 Central Processing and Analysis of Geostationary Satellite Data. Charles F. Bristor (Editor), March 1975, 155 pp. (COM-75-10853/AS)

NESS 65 Geographical Relations Between a Satellite and a Point Viewed Perpendicular to the Satellite Velocity Vector (Side Scan). Irwin Ruff and Arnold Gruber, March 1975, 14 pp. (COM-75-10678/AS)

NESS 66 A Summary of the Radiometric Technology Model of the Ocean Surface in the Microwave Region. John C. Alishouse, March 1975, 24 pp. (COM-75-10849/AS)

(Continued on inside back cover)

NOAA Technical Memorandum NESS 90

LAKE ERIE ICE: WINTER 1975-76

Jenifer H. Wartha

Washington, D.C.
August 1977

UNITED STATES
DEPARTMENT OF COMMERCE
Juanita M. Kreps, Secretary

NATIONAL OCEANIC AND
ATMOSPHERIC ADMINISTRATION
Richard A. Frank, Administrator

National Environmental
Satellite Service
David S. Johnson, Director

CONTENTS

LAKE ERIE ICE: WINTER 1975-76

Jenifer H. Wartha
National Environmental Satellite Service, NOAA
Washington, D.C.

ABSTRACT. Ice conditions on Lake Erie depicted mainly from satellite imagery were observed during the winter of 1975-76. The formation, movement, and decay of lake ice were traced at intervals of about 3 days from December 28, 1975, to April 19, 1976. Wind speeds and directions were correlated with ice movement, and air temperatures were related to ice formation and dissipation. Ice conditions were generally normal; however, ice persisted in the eastern end of the lake until mid-April. This unusually late date for clearing was caused more by winds concentrating the ice than by very cold weather.

INTRODUCTION

Lake Erie, more thermally dynamic than the remaining Great Lakes because of its shallowness, has been selected for these ice studies. This is the second in a series of ice reports on Lake Erie. Last year's report (McMillan and Forsyth, 1975) included satellite data from only one source, the Very High Resolution Radiometer (VHRR) carried by the National Oceanic and Atmospheric Administration's (NOAA) polar orbiting satellite, NOAA-4. This report includes satellite data from the NOAA-4 VHRR, NOAA's Geostationary Operational Environmental Satellite (GOES), and the National Aeronautics and Space Administration's (NASA) Landsat; Canadian aerial ice reconnaissance, and aircraft Side Looking Airborne Radar (SLAR) systems. These data are used to trace the development, movement, and dissipation of lake ice from December 28, 1975, to April 19, 1976, at intervals of about 3 days.

The 1974-75 ice season was considered to be milder than normal (Leshkevich, 1976) and milder than the 1975-76 ice season. This statement is based on freezing degree day accumulations calculated by the author. During the 1975-76 ice season, temperatures in the second half of December, January, and the first half of April were generally below normal; February and March were above normal.

Local daily mean weather conditions for stations surrounding Lake Erie are used. Air temperatures at these stations are correlated with ice formation and dissipation; wind speeds and directions are related to ice movement.

DATA SOURCES

Images from three different satellites (NOAA-4 VHRR, GOES, and Landsat), and from SLAR and Canadian ice flights were chosen for viewing ice on Lake Erie during December 1975-April 1976.

Satellites

The NOAA GOES satellite orbital motion matches that of the Earth; thus, the two GOES satellites appear stationary over fixed points above the Equator. Orbiting at an altitude of 36,000 km and positioned over the Equator at longitude 75°W, GOES-I provides visible images at various selectable resolutions of the Great Lakes area. The visible sensors of the Visible and Infrared Spin Scan Radiometer (VISSR) aboard the GOES respond to energy in the 0.55- to 0.75-μm range and transmit images to ground stations every half hour during daylight. Most of the illustrations in this report are 1-km resolution GOES visible-range images in which the ice on Lake Erie is clearly discernible. GOES infrared images are not used because the resolution, 8 km, is too low.

The Very High Resolution Radiometer (VHRR) carried by the NOAA-4 polar orbiting satellite senses energy in the visible (0.6 to 0.7 μm) and thermal infrared (IR) (10.5 to 12.5 μm) spectral regions at a resolution of 1 km. The satellite views an area at approximately 9 a.m. local solar time each day from an altitude of 1,500 km. Visible images covering the United States are available once a day; IR data are available twice daily at 9 a.m. and 9 p.m. local solar time. On the IR images warm features are assigned dark-gray shades while cold features are assigned light-gray shades. Therefore, the cold clouds and ice appear lighter than the warmer lake and river waters. In this report, computer-enhanced VHRR visible and IR images are used to depict lake ice.

Landsat: NASA's Earth Resources Technology Satellites (ERTS) were renamed Landsat 1 and 2. Aboard Landsat, the multispectral scanners (MSS) which detect light reflected from the Earth provide images from a 920-km altitude with an 80-m ground resolution; each frame covers a 185- by 185-km area on the Earth's surface. The imagery can be obtained in four different spectral bands: band 4 (0.5 to 0.6 μm), band 5 (0.6 to 0.7 μm), band 6 (0.7 to 0.8 μm), and band 7 (0.8 to 1.1 μm). Only band 5 Landsat images are used in this study. The major disadvantage of Landsat is that imagery is available only once every 18 days (9 days when both Landsat 1 and 2 are operating).

Aircraft

The Side Looking Airborne Radar (SLAR) AN/APS-94C system is mounted aboard a U.S. Coast Guard C-130-B aircraft. SLAR has the ability to penetrate most weather. The imagery from SLAR can be used to determine roughness or topography of the ice surface and to estimate ice thickness. The SLAR system operates in the X-band at a frequency of 9.245 GHz (3.245-cm wavelength). SLAR vertical range resolution is 80 m; azimuth resolution varies from 45 m at 5-km range to 450 m at 50-km range (Schertler et al., 1975). SLAR interpretation charts and prints are included in this report. The SLAR system involves a cooperative effort among the NASA Lewis Research Center in

Cleveland, Ohio, NOAA, and the U.S. Coast Guard as part of the Winter Navigation Extension Program for the Great Lakes.

Canadian Flights: The Atmospheric Environmental Service of Canada sponsors flights over the Great Lakes in response to U.S. Coast Guard requirements. An Airborne Radiation Thermometer (ART) aboard a DC-3 aircraft is used to determine surface-water temperatures. However, the ice thickness, concentration, and extent are determined chiefly by visual observations. The ice observers aboard the aircraft transmit information over facsimile to ice breakers below the flight path. The ice observers also formulate ice forecasts based on visual observations.

Other Sources

Local climatological data for Buffalo, N.Y., Erie, Pa., Cleveland and Toledo, Ohio, and Detroit, Mich., were provided by the Environmental Data Service (EDS) in Asheville, N.C.

SUMMARY OF ICE GROWTH, MOVEMENT, AND DECAY

On December 28, 1975, ice could be detected adhering to the western shore of Lake Erie. This ice was blown offshore after December 28 by westerly winds but by January 10, 1976, had become refrozen to shore. Five days later (Jan. 15), ice had developed along the north shore. Within a few days the ice extended across the lake from midnorth shore (Port Stanley) to mid-south shore (Ashtabula). New ice also formed and attached to the old ice west of Pelee Point leaving an area of open water between the two newly formed ice structures.

Almost 100% of Lake Erie was ice covered by January 19. As expected, the thinnest ice occurred near the east end (Long Point) in the deepest part of the lake. Ten days later (Jan. 29), the ice cover split into two large pieces: the western piece was confined by Pelee Island and Kelleys Island south of Pelee Point; the other piece partially covered the remainder of the lake. The predominant westerly winds before January 29 caused the ice in the western part of Lake Erie to drift eastward to the Pelee-Kelleys island barrier. Meanwhile, the ice east of these islands drifted eastward causing a lead to form adjacent to the islands.

On February 2, the lake was 100% ice covered in response to very low temperatures (-14° to -16°C). Refreezing had occurred along the western shore and had welded the two major ice areas together. Again westerly winds were so persistent that by February 8 the eastward ice drift had widened the lead near the islands. Temperatures were generally 5° to 10°C from February 10 until the end of the month. This warming caused melting, and westerly winds compressed the ice eastward.

The west end of Lake Erie was ice free at the beginning of March. However, the ice remained in the eastern portion until mid-April because the persistent westerly winds did not allow the ice to drift offshore. The entire lake was ice free by April 19, a full month later than the previous year.

A bathymetric chart of Lake Erie is shown in figure 1. Although the maximum depth is 64 m in the eastern basin, the average lake depth is only 18 m. The shallowest water is located along the perimeter of the lake and west of Pelee Island; it is less than or equal to 7.6 m deep.

On December 28, 1975, Erie, Cleveland, Toledo, and Detroit reported air temperatures of -2.2°, -2.2° -8.9°, and -4.4°C, respectively. In figure 2, ice concentration of 50 to 100% has formed west of Pelee Point and in the southern half of Lake St. Clair. Ice with 20 to 60% concentration has formed west of Long Point where the shallow bottom is less than 15.3 m deep and extends as a ridge almost entirely across the lake. Open measured radiant water temperatures ranged from 1.5° to 4.8°C.

Air temperatures at Buffalo, Erie, Cleveland, Toledo, and Detroit were consistently below freezing for 2 1/2 weeks prior to January 4. Though cloud cover hinders interpretation of features in the satellite image of figure 3, ice (labeled) can be detected in the western end of Lake Erie on January 4.

Air temperatures at the land stations were still below freezing (-14.4° to -10°C) on January 8, and in figure 4A the ice (labeled A) in the western end of Lake Erie appears more concentrated than it did on January 4. Note the lead parallel to the north and west shores west of Pelee Point, and the open water or transparent ice on the west shore of Lake St. Clair. The predominant 9-kt westerly and northwesterly winds reported at the land stations have blown the ice offshore. Clouds cover the southeastern part of the lake.

Figure 4B, the Landsat image acquired on January 8 agrees well with the GOES image of figure 4A except that the detail is far superior owing to the better resolution of Landsat (80 m versus 1,000 m). Very thin, newly formed ice extending almost to shore west of Pelee Point and thin fast ice along the shore just east of Pelee Point can be seen here, but are not visible in the GOES image. An interpretation of this image is that ice formed, was blown offshore by the northwesterly and westerly winds, and new ice formed between the older offshore ice and the shore. Later this new ice formation broke away from shore and cracks that occurred in the ice structure extended from the older ice and continued into the newly formed ice.

Separated by a small lead are two major ice areas west of Pelee Point: one larger area (labeled 1) compacted against the south shore of the west end of Lake Erie and a smaller area (labeled 2) east of the larger one. The islands running longitudinally from Pelee Point to Sandusky seem to confine the ice.

Owing to current speeds as high as 6 kt, the Detroit River seldom freezes over. The river appears very dark in the Landsat image and is probably ice free.

Air temperatures remaining low (about -10°C at the reporting land stations) on January 10 contributed to the growth of new ice (C in the GOES image of figure 5) along the north and south shores and to the formation of new ice (B)

adjacent to the west end ice (A). Winds from the south at 9 kt have produced an apparent small lead parallel to the south shore between Cleveland and Erie.

West end ice (A) in figure 6 has been transported offshore by westerly winds at 17 kt on January 14. The new ice (B) formerly attached to the eastern part of the ice west of Pelee Point has moved eastward under the influence of the wind.

In the GOES image of figure 7A, ice that formed along the north shore (at C) on January 10 has widened but does not appear more concentrated. Air temperatures were -5.5°C on January 15. The eastern tip of Lake Erie near Buffalo is covered by ice (D). This ice does not look new, but it was previously undetected probably because of cloud cover.

The extent of the north shore ice (C) is more easily seen in the VHRR computer-enhanced visible-range satellite image of figure 7B. Also, the older ice (A) previously blown offshore west of Pelee Point appears whiter or older than the new ice (E) which has formed between it and the western shore. The lead between the two areas of A (1 and 2) is still unchanged from January 8.

Figure 7C is a NOAA-4 VHRR computer-enhanced infrared image acquired simultaneously with the visible image of figure 7B. The IR image shows that the older ice (A) is colder (whiter) than the newer north shore ice (C). The open water is the warmest surface in the image.

Temperatures were still low enough to form and maintain ice on January 17; they ranged from -14.4° to -10.6°C. In the GOES image of figure 8A, new ice (F) has formed across the width of the lake west of Erie, Pa. Winds from the north at 9 kt have created a lead parallel to the north shore.

The NOAA-4 VHRR computer-enhanced (visible) image in figure 8B compares well with the GOES image; the same ice features (A, 1 and 2, B, C, E, and F) and the north shore lead are discernible. Older ice again appears colder than the newer ice and the water areas appear warmest in the NOAA-4 VHRR (IR) image of figure 8C.

Comparisons between Landsat imagery in figure 8D and GOES and the VHRR imagery in figures 8A, 8B, and 8C agree very well except that Landsat imagery is more detailed. The Detroit River remains ice free. Thermal pollution, due to the dumping of industrial wastes from the automobile plants and to boat traffic, probably contributes to the ice-free conditions of the river.

At point 3 in figure 8D, a lead has developed where ice was blown offshore by westerly winds on January 16 and by northerly winds on January 17. Refreezing has occurred along shore in response to the low temperatures. The two previously separated ice areas at A in figure 4B in the western end of the lake have united. Details of the irregular ice features can be discerned at B in Landsat imagery (fig. 8D), but not in the VHRR (figs. 8B, 8C) or GOES imagery (fig. 8A) because of cloudiness. Thin transparent ice at E extending to the shore can be seen in the GOES and VHRR images. The black ice (4 in fig. 8D) is very new transparent ice formed between the ice at E which adheres

to shore and the ice at A. The black ice can also be detected in the VHRR (visible) image.

Winds were light and variable at 2 to 4 kt and temperatures ranged from -17° to -14°C at the reporting stations on January 18. In figure 9, Lake Erie is almost 100% frozen except possibly in area G, which may be open water, but probably is covered by thin ice. Lake surface temperatures have lowered to 0°C, and ice has formed on the surface for the reasons explained below.

The maximum density of freshwater is reached when the temperature is 4°C. Further loss of heat to the atmosphere cools the surface water below 4°C. Since water at 0°C is less dense than water at 4°C, it remains in equilibrium on top of the 4°C water. This process of cooling continues until the surface water reaches 0°C. At this point ice forms at the surface.

Winds from the south at 10 to 17 kt have moved the ice off the south shore in the GOES image taken on January 19 (fig. 10A). The most outstanding feature is the lead paralleling the south coast. In the NOAA-4 VHRR (visible) image from January 19 (fig. 10B), the same features as those in the GOES image are observed. However, the detail is superior on the VHRR image.

In figure 11, January 22, ice has broken away from the northwest coast in response to winds from the northwest at 9 kt. Ice appears the least concentrated over the deepest part (K) of Lake Erie. It is expected that freezing occurs here more slowly than the rest of the lake. Air temperatures at the land stations ranged from -14.4° to -9.4°C.

On January 26, a SLAR image and interpretation chart (fig. 12) were produced. Many features are discernible in this high-resolution image. Winds were from the south at Buffalo and Erie and from the west at about 9 kt at Cleveland, Toledo, and Detroit. Temperatures were above freezing for the first time this month: Buffalo, Erie, Cleveland, Toledo, and Detroit reported 5.0°, 3.3°, 3.9°, 0.6°, and 2.8°C, respectively. The wide lead parallel to the south shore probably is due to temperature and wind conditions. Most of the lake is covered by ice 13- to 20-cm thick and 90% concentrated. Again there is open water over the deepest part of the lake.

In figure 13, January 29, a large lead extending from Sandusky on the south shore north to Pelee Point (between ice A and B) and along part of the north shore can be discerned. Westerly winds at 9 kt in combination with the island obstructions caused this lead.

Figures 14A and 14B are GOES images taken 2 1/2 hours apart on February 2. Temperatures at the land stations were -16.1° to -14.4°C. Winds from the west at 17 kt are displacing the ice eastward. At 1600 GMT (12 noon EDT) in figure 14A the entire lake appears frozen. However, by 1830 GMT (2:30 p.m. EDT) in figure 14B a thin lead developed along the north shore, possibly because strong winds moved the ice offshore.

The NOAA-4 VHRR computer-enhanced (visible) image (fig. 14C) confirms cloud movement from the northwest and the lead along the north shore. In figure 14D, a VHRR computer-enhanced (IR) image for the same time as figure 14C, the

area along the north shore is warmer than the remainder of the ice covered lake. This factor supports analysis of the presence of a lead along shore.

Westerly winds at 17 kt on February 2, coupled with southerly winds at 10 kt on February 3, caused leads to develop on February 3 (fig. 15A). On the north shore there is an eastward ice displacement. On the south shore between Cleveland and Sandusky, ice was displaced northward and a lead developed between the two large ice areas divided at the islands near Pelee Point and south to Sandusky. These leads refroze because of low temperatures (-9.4°C). The two ice areas are designated A and H. H represents a fusion of the previous B, C, D, F, and G areas.

The westerly and southerly wind-induced leads are confirmed by the VHRR computer-enhanced (visible) image of figure 15B; also note a thin lead at the extreme west end on the west and south shores. This feature was not visible on the GOES image. In figure 15C, the NOAA-4 VHRR (IR) image of February 3, the lake appears warmest (darkest) where there is open water near Long Point and along the leads and coldest (whitest) west of Pelee Point where the ice (A) is the oldest.

On February 6, snow was falling at Buffalo, Erie, Cleveland, and Toledo. Temperatures were -9°C, and the wind was from the west and northwest at 9 kt. The GOES image (fig. 16) indicates that snow covered the entire frozen lake surface except for the lead between the two ice areas and the lead paralleling the north shore.

The GOES image for February 7 is shown in figure 17. Snow has ceased falling, and the leads seen on February 6 are wider than they first appeared. Fog or clouds dominate the middle of Lake Erie. Air temperatures ranged from -10.6° to -6.1°C, and wind velocities were generally 13 kt from the west at Buffalo and Cleveland and from the southwest at Erie, Toledo, and Detroit.

Figure 18 is a GOES image taken on February 9. Westerly winds at 13 kt on February 8 widened the lead between the two major ice areas by pushing the ice east of Pelee Point farther to the east.

Between February 10 and 12, temperatures at the land stations were 0.6° to 7.2°C; hence, melting occurred and caused a wider gap between the two ice areas seen in figure 19A, a GOES image for February 12. Clouds cover the eastern two-thirds of the lake. Winds were generally from the south on the 10th and 12th and from the west on the 11th at 13 kt on all 3 days.

The SLAR image and interpretation chart of figure 19B clearly depict the extent of open water. Open-water conditions from Pelee Point south to Sandusky are 64 km in width. Near Long Point open water extends 32 km eastward. Ice concentration is mostly 90% in the two ice areas.

Fast ice along the south shore between Sandusky and Cleveland appears on the Landsat image of figure 19C as well as the SLAR image, but is not apparent on the GOES image. Extensive ice cover can be seen under thin clouds over the middle of the lake.

Figure 20A is a GOES image from February 14. Winds became light and variable, and temperatures averaged about 2.2°C after February 10. A large high-pressure system dominates the lakes as indicated by the lack of clouds over Lake Erie, and by local EDS records. Temperatures indicated melting conditions along the north coast and between areas A and H. The VHRR (visible) image (fig. 20B) is virtually identical with the GOES image except the Detroit River is clearly ice free. The VHRR (IR) image (fig. 20C) shows that the coldest, hence thickest, ice is located in the west end of Lake Erie and in Lake St. Clair. The Detroit River is the warmest feature.

A SLAR image and interpretation chart of Lake Erie for February 17 are shown in figure 21A. Temperatures of approximately 5.3°C have caused further melting along the south shore and between A and H. The ice in the western end of the lake is thicker than the more extensive ice in its eastern end. An area of open water is visible north of Long Point.

The drawing from the Canadian ice reconnaissance flight (fig. 21B) substantiates the presence of the SLAR-indicated open-water areas. However, ice concentrations estimated by the Canadians differ from the SLAR interpretation by approximately ±10%. Ice thicknesses are greater than 30 cm west of Pelee Point and in the eastern tip.

Above freezing temperatures (3°C) melted the ice extensively by February 20, and a larger gap exists between the two ice areas. (See the GOES image of figure 22A.) In the Canadian ice chart (fig. 22B) open-water areas along the north coast are the same as those on the GOES image. The ice in the eastern end is mostly 80 to 90% concentrated; its thickness ranges from 10 cm to greater than 30 cm. The ice in the western end is mainly 50 to 80% concentrated and is not so thick (10 to 15 cm). The western end ice is thinner than it was 3 days ago.

Figure 23 is a SLAR image and interpretation chart of the west end of Lake Erie on February 21. High temperatures were maintained, and melting occurred; ice in the west end of Lake St. Clair receded and decayed.

Persistent westerly winds and above-freezing temperatures before February 23 caused eastward movement of the two ice areas and considerable melting in the February 23 GOES image (fig. 24A). In the NOAA-4 VHRR (visible) image (fig. 24B), ice in Lake St. Clair (J) also has been pushed to the east shore by westerly winds. The NOAA-4 VHRR (IR) image (fig. 24C) shows that the open-water areas of the lake are much warmer than the ice areas. Note that the cloud tops are cooler than the ice and can be distinguished from the lake ice on this image.

Figure 25 is a SLAR image and interpretation chart for February 25. Winds from the south at 13 kt have moved the ice throughout the lake to the north shores; compare this with positions of the ice in the lake on February 23. The ice concentration is also lower, a factor that allows the ice to drift more rapidly under wind stress. The open-water area between the two ice areas is approximately 160 km wide. Temperatures were approximately 13°C.

Winds from the south at 9 kt on February 29 continued to keep the ice in western Lake Erie compacted along the north shore. (See figure 26, a SLAR

interpretation chart for this date.) All the remaining ice is thin because of the high temperatures, but concentration is 90%. The central area of the lake is not shown in the SLAR interpretation chart.

Figure 27 is a SLAR image and interpretation chart of the west end of Lake Erie for March 4. Ice formerly attached to the north shore of the west end ice, although melted somewhat, has been transported westward by the predominantly 9-kt easterly winds during the past few days. Temperatures have remained 8° to 14°C.

Winds from the west at 13 kt have kept Lake St. Clair ice compressed against the eastern shore on March 6 (SLAR image and interpretation chart, fig. 28A). The Canadian chart (fig. 28B) verifies ice-free conditions in the western half of the lake where surface-water temperatures were 1.4° to 2.8°C according to Airborne Radiation Thermometer (ART) readings. The remaining ice has decayed in the eastern end; it is less concentrated and less extensive than previously.

Owing to frequent storms and snow melt, early spring river runoff is high. Since in winter there is little vegetation to prevent soil erosion, sediment transport into the Detroit River and ultimately into Lake Erie is high. Sediment in the western end of Lake Erie appears lighter than the surrounding water on March 9 (GOES image, fig. 29A). The only ice remaining is in the eastern end; it has moved further east because of predominant westerly winds over the past few days. In the SLAR image and interpretation chart of figure 29B, open water is visible in the entire west end of the lake and in Lake St. Clair.

Figures 30A, B, C, and D are GOES, VHRR (visible), Landsat, and SLAR image and interpretation chart, respectively, for March 11. Sediment in the west end plus the ice plug at Buffalo and broken floes in the eastern end are the dominant features in the GOES image (fig. 30A). Only the ice appears clearly in the VHRR (visible) image (fig. 30B). The sediment is not visible on this computer-enhanced, rectified image. The Landsat image (fig. 30C) of the west end of Lake Erie shows that extensive mixing of sediment has occurred in the western end. The high concentration of sediment in southeastern Lake St. Clair can be seen draining through the Detroit River into the south shore of the western end of Lake Erie. Note the high turbidity of the Toledo harbor and Sandusky harbor areas. The SLAR image and interpretation chart (fig. 30D) of the east end of Lake Erie reveal that thin- to medium-thickness ice at 70 to 100% concentration remains in the eastern end.

On March 15 temperatures were not so high as before March 6; however, they were usually above freezing. Broken pieces of ice from the east end of Lake Erie have dissipated somewhat and have been compacted into the eastern end of the lake (GOES image, fig. 31A).

A VHRR computer-enhanced, rectified (visible) image (fig. 31B) provides better detail than the GOES image and shows that much of the ice along the south shore has melted since March 11.

The SLAR image and interpretation chart of the east end of Lake Erie (fig. 31C) disclose that ice in the eastern end is 100% concentrated and thin to

medium in thickness. A second mass of ice, 10% concentrated, is attached to this ice.

The SLAR image and interpretation chart of March 19 (fig. 32A) show ice in the eastern part of the lake is 15 to 51 cm thick, and 100% concentrated. The second area of ice cover, 10% concentrated, is still attached to the ice in the eastern end, but has moved further north under the influence of 16-kt southerly winds.

The Canadian chart of Lake Erie for March 19 (fig. 32B) corresponds exactly to the extent and location of the ice viewed by SLAR. However, concentrations and thicknesses of ice differ from the SLAR interpretation. The Canadians estimated the ice to be less thick than the SLAR interpreters, and the area of ice cover attached to the ice in the eastern end was thought to be more concentrated (40 to 60%) than in the SLAR interpretation (10%). Surface water temperatures ranged from 0.4° to 1.7°C; air temperatures ranged from 8.3° to 15.6°C.

The GOES image of March 24 (fig. 33A) reveals that ice remains in the eastern tip of Lake Erie despite above-freezing temperatures. Ice in the eastern end appears very white in contrast to the blackness of the water in the computer-enhanced, rectified image of figure 33B (VHRR visible); it is 13 to 41 cm thick and 100% concentrated according to the SLAR image and interpretation chart (fig. 33C).

By March 26, southerly winds at 11 kt had caused the ice to move northward producing a small lead along the south edge of the ice and extending through the middle of the ice floe in the SLAR image and interpretation chart of the eastern end of Lake Erie (fig. 34) from March 26.

By April 3, the ice (GOES image, fig. 35A) had diminished because of the high temperatures. However, the predominant west winds between March 31 and April 2 kept the ice compacted against the eastern and northern shores. The SLAR image and interpretation chart of figure 35B reveal that the surface of the ice in the eastern tip is rougher and possibly more concentrated along the southern half than along the northern half.

Figure 36A is a VHRR computer-enhanced, rectified (visible) image taken on April 5. Winds from the north at 10 kt on March 4 moved the ice off the north shore. The lead along the north shore is now 20% concentrated according to the SLAR image and interpretation chart of the east end of Lake Erie (fig. 36B). The ice floe is 15 to 46 cm thick and 90 to 100% concentrated.

The NOAA-4 VHRR (visible) image of April 9 is shown in figure 37A. Northerly winds at 9 kt have transported the ice further off the north shore. The ice is rapidly melting now. The SLAR image and interpretation chart of eastern Lake Erie (fig. 37B) disclose that the ice is 5 to 41 cm thick and 80 to 90% concentrated.

Figure 38, a GOES image for April 14, shows continued rapid melting in the eastern tip of Lake Erie. Temperatures were approximately 12°C at the reporting land stations.

The GOES image of April 19 (fig. 39) is the last used in this report. The entire lake was finally ice free. This late date for clearing was very unusual for Lake Erie; it was caused more by wind concentrating the ice than by unusually cold weather.

ACKNOWLEDGMENTS

The author sincerely thanks Dave McGinnis, Don Wiesnet, Frank Kniskern, and Stanley Schneider for their advice and criticism, and Dave Forsyth for his assistance in supplying VHRR images. Gratitude is expressed to Mary Young, who typed the paper.

REFERENCES

Leshkevich, G., 1976: Great Lakes ice cover, winter 1974-1975. NOAA Technical Report ERL 370-GLERL 11, GLERL Contribution Number 78, Boulder, Colo., 39 pp.

McMillan, M., and Forsyth, D., 1976: Satellite images of Lake Erie ice: January-March 1975. NOAA Technical Memorandum NESS 80, Washington, D.C., 14 pp.

Schertler, R., Mueller, R., Jirberg, R., Cooper, D., Heighway, J., Holmes, A., Gedney, R., and Mark, H., 1975: Great Lakes all-weather ice information system. NASA Technical Memorandum NASA TM X-71815, 13 pp.

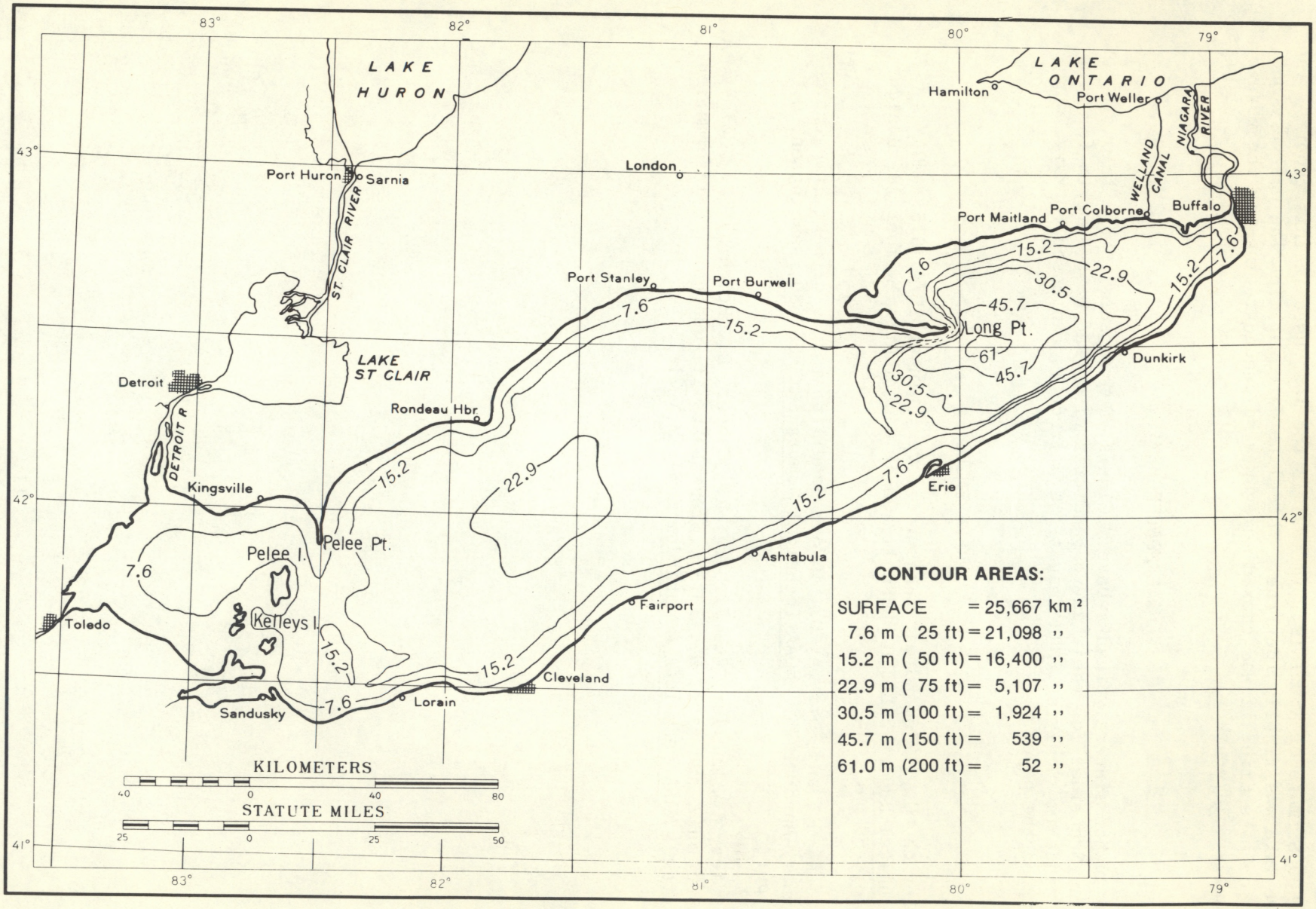

Figure 1.--Bathymetric chart of Lake Erie.

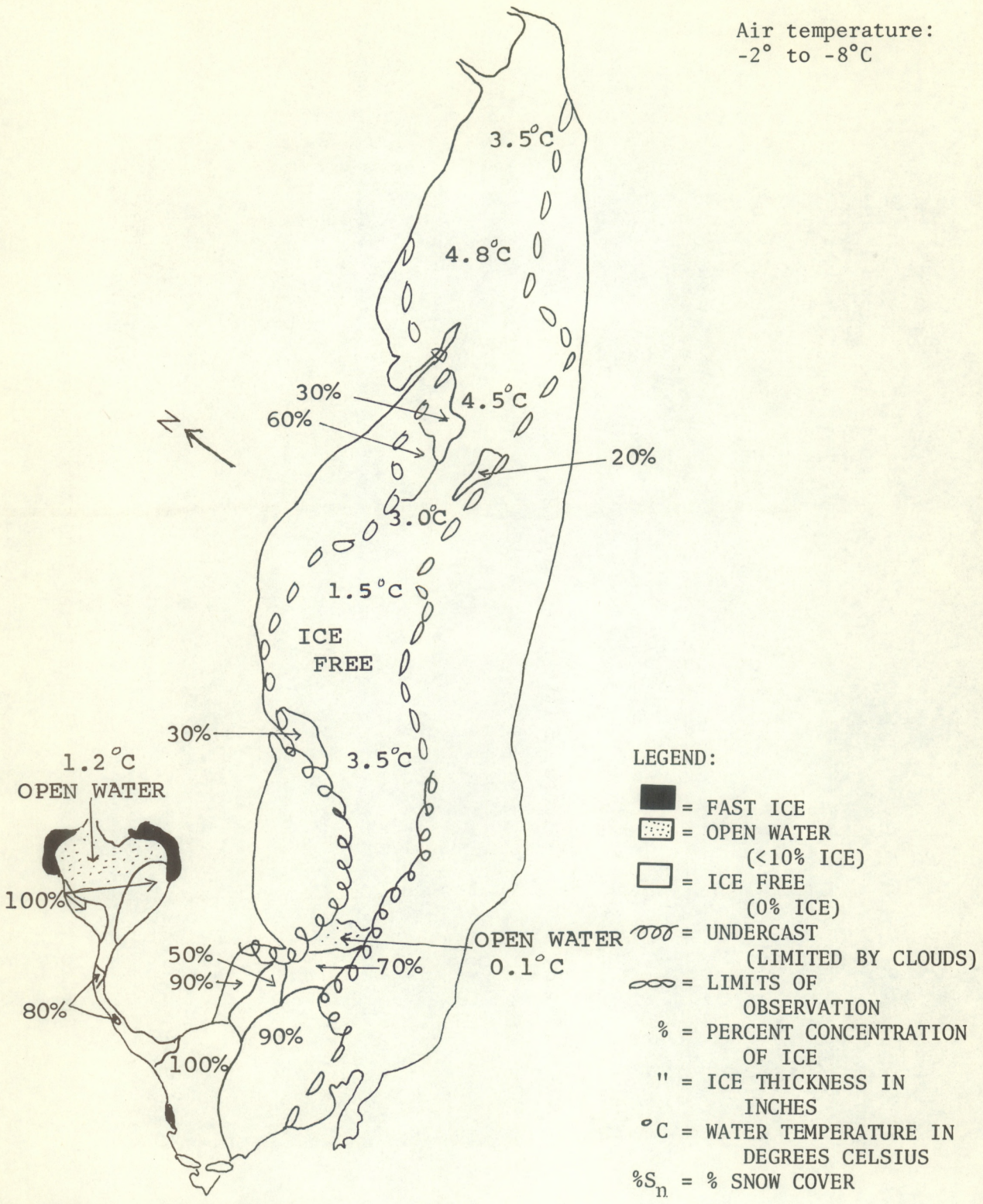

Figure 2.--Chart showing Lake Erie ice and water temperatures from the flight on December 28, 1975. (Data from Atmospheric Environmental Service of Canada.)

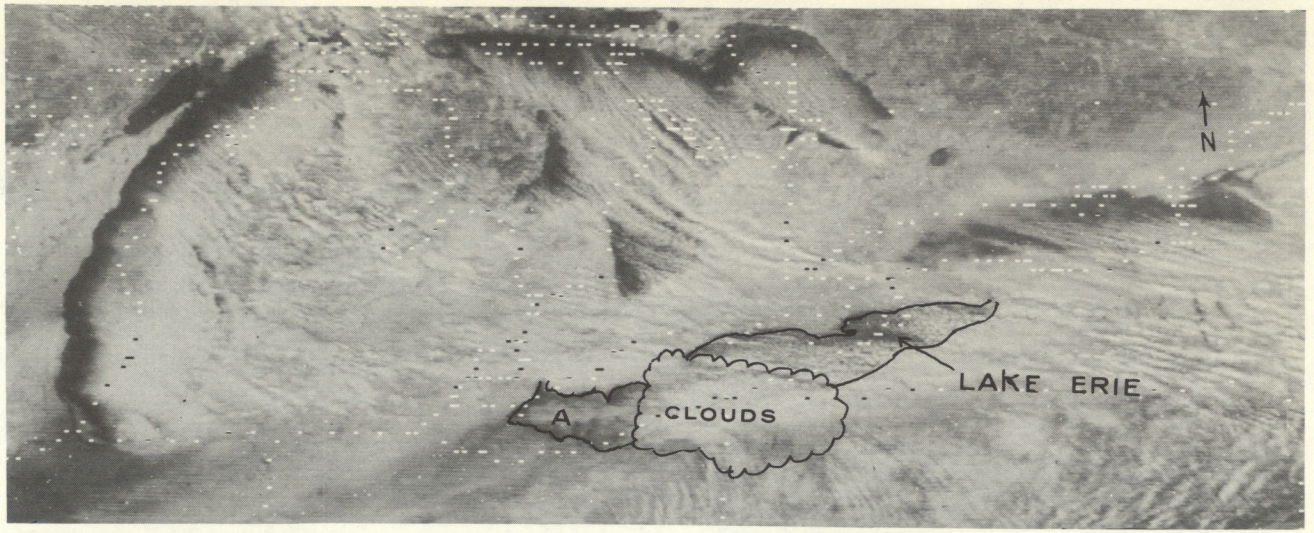

Figure 3.--GOES image of Lake Erie, 1800 GMT, January 4, 1976.

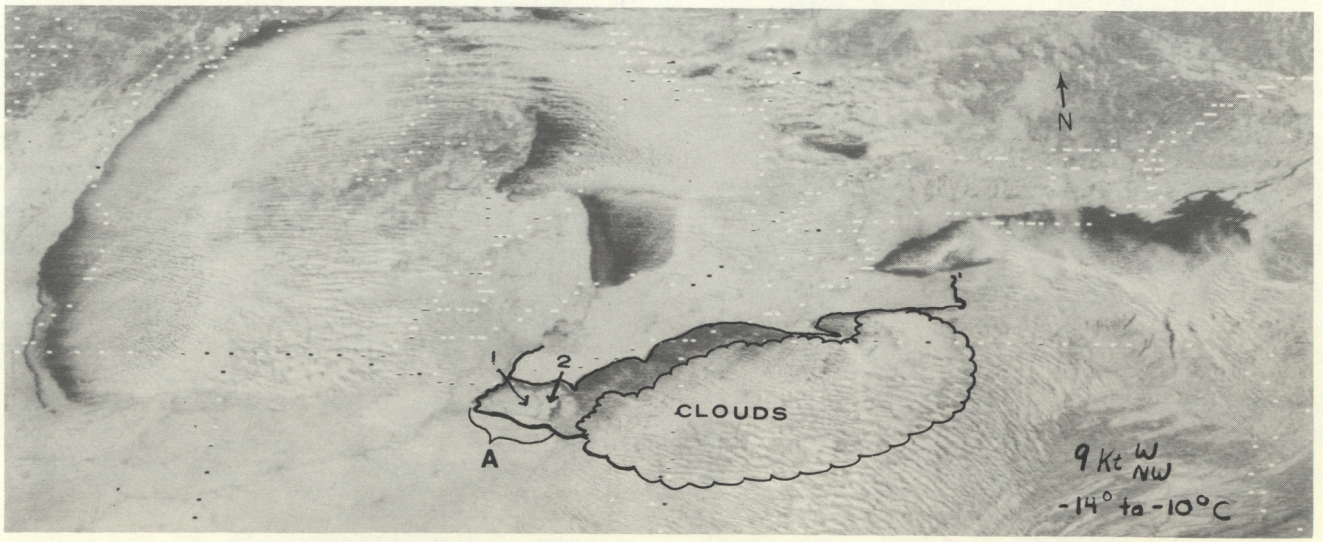

Figure 4A.--GOES image of Lake Erie, 1900 GMT, January 8, 1976.

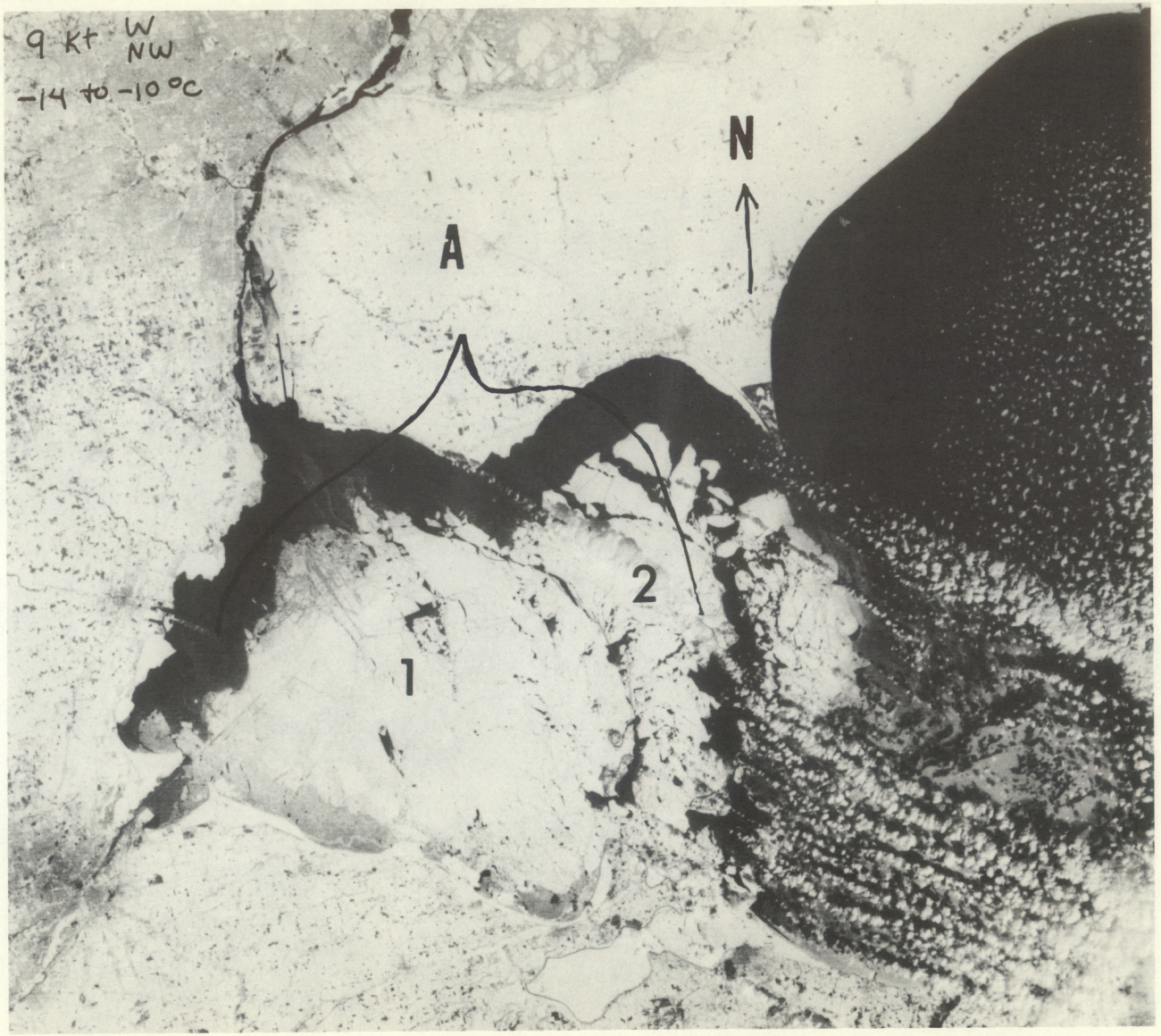

Figure 4B.--Landsat image of western Lake Erie, January 8, 1976.

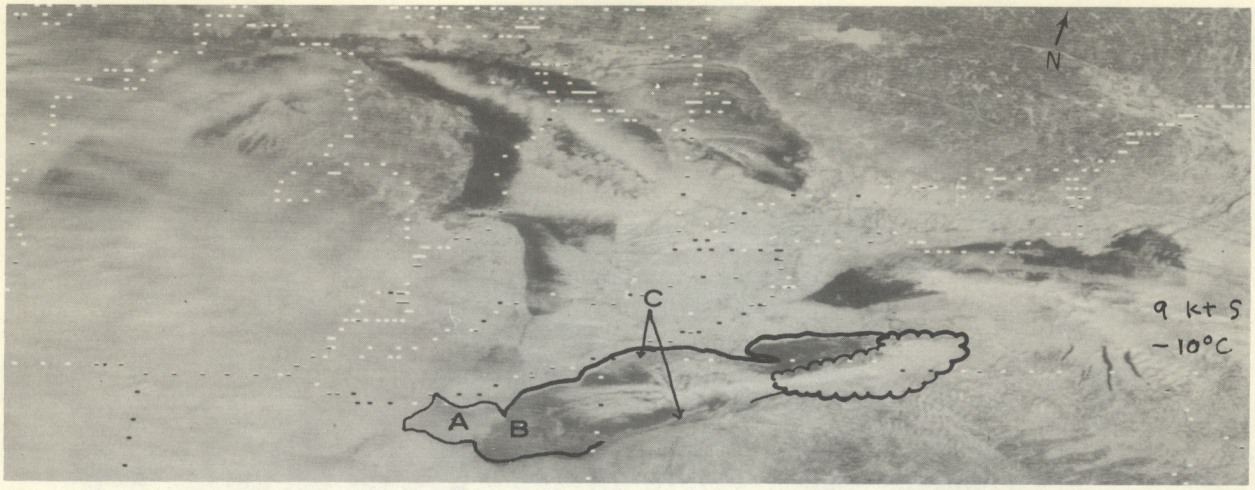

Figure 5.--GOES image of Lake Erie, 1630 GMT, January 10, 1976.

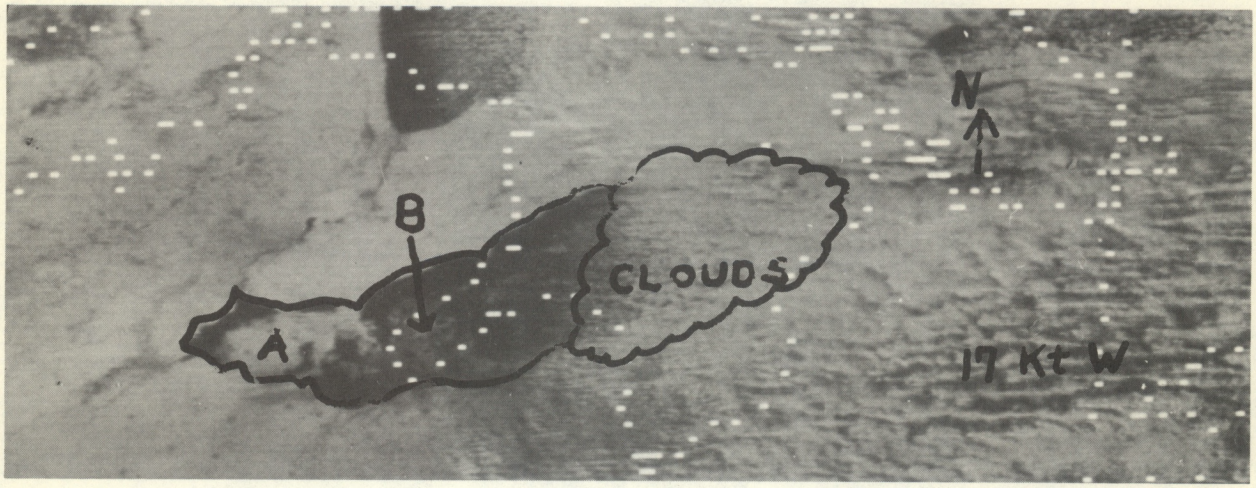

Figure 6.--GOES image of Lake Erie, 2000 GMT, January 14, 1976.

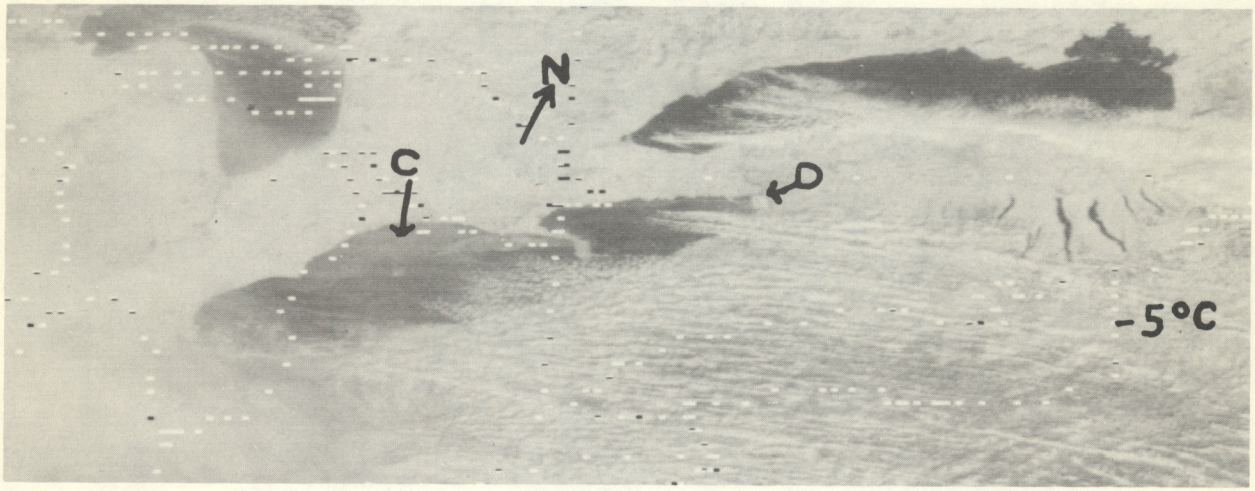

Figure 7A.--GOES image of Lake Erie, 1600 GMT, January 15, 1976.

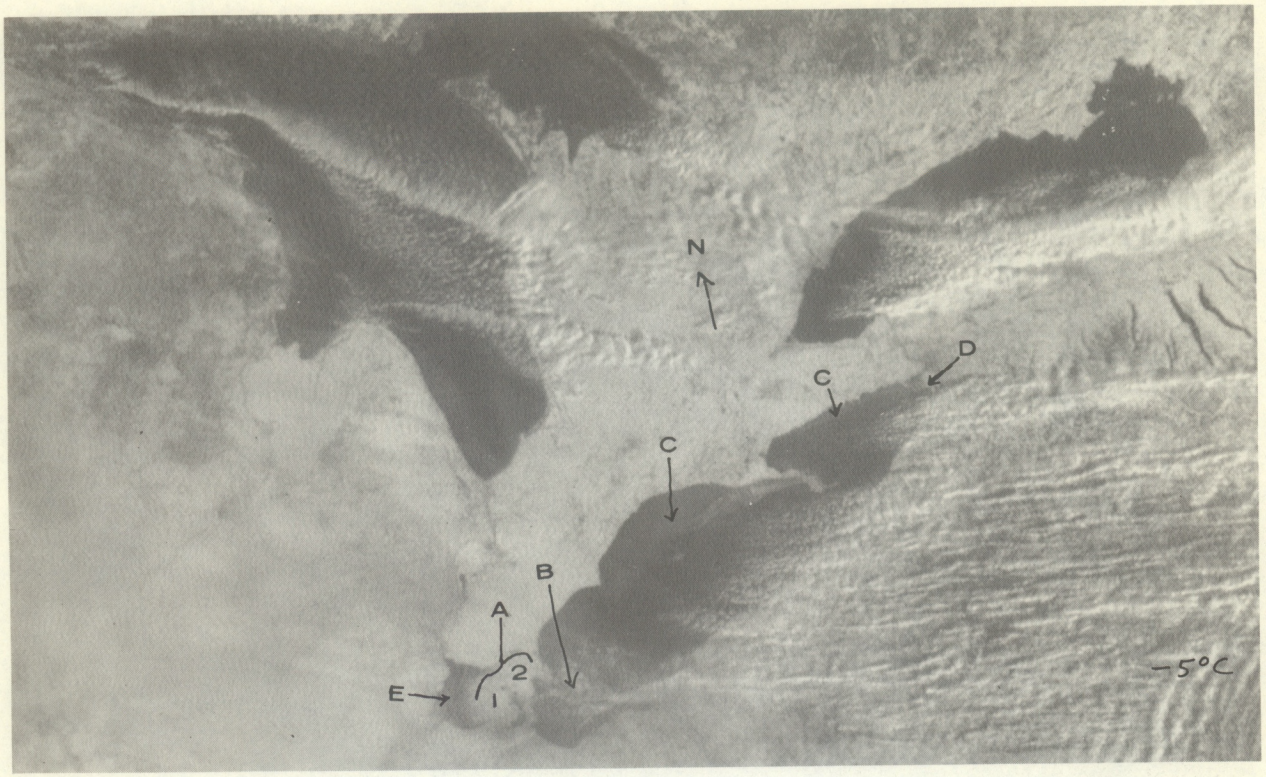

Figure 7B.--NOAA-4 VHRR (visible) image of Lake Erie, January 15, 1976.

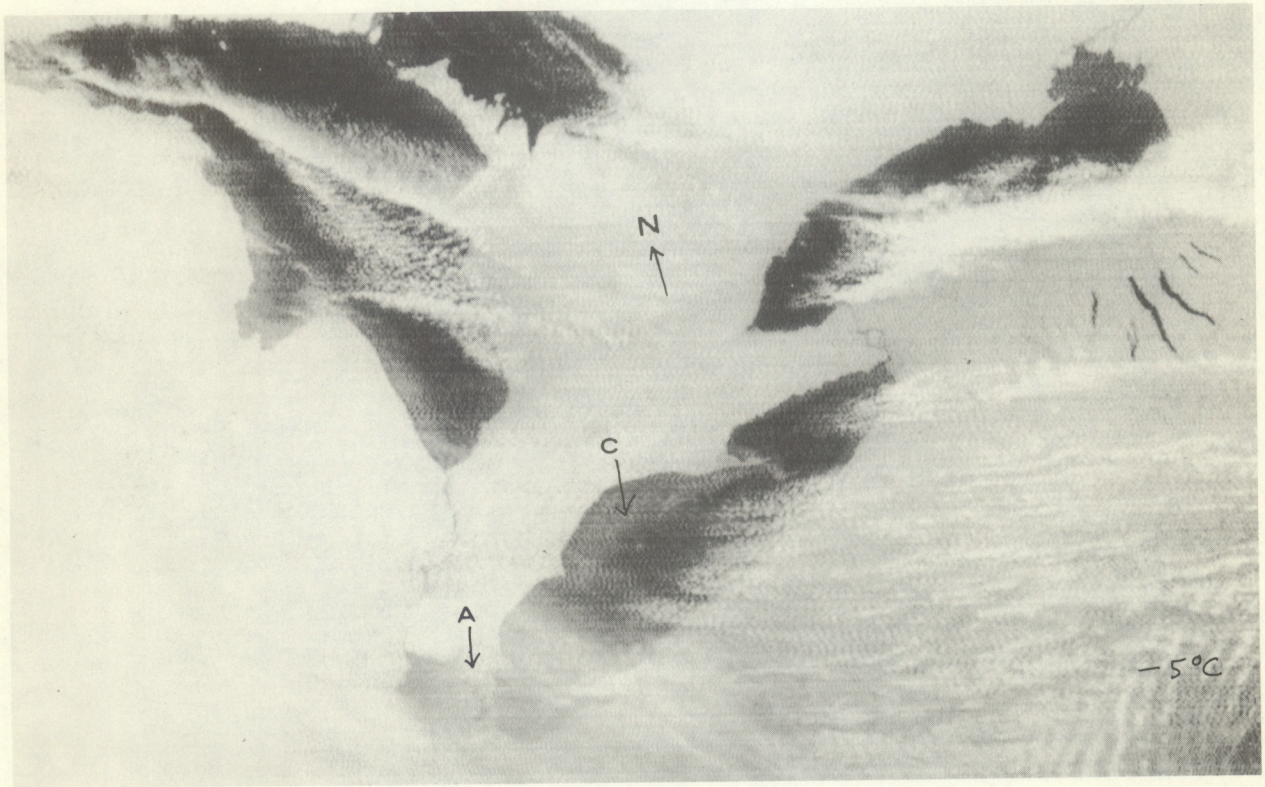

Figure 7C.--NOAA-4 VHRR (IR) image of Lake Erie, January 15, 1976.

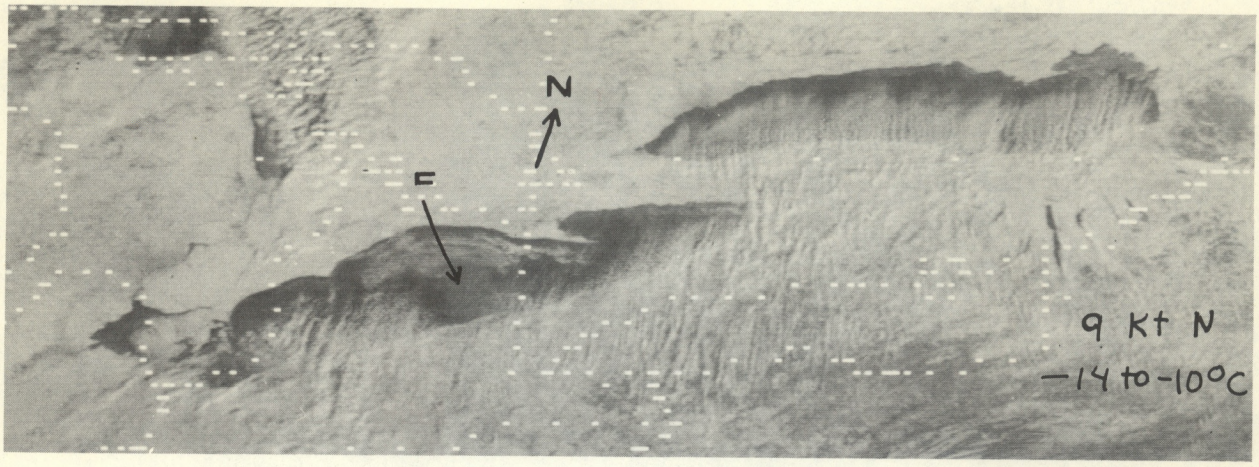

Figure 8A.--GOES image of Lake Erie, 1500 GMT, January 17, 1976.

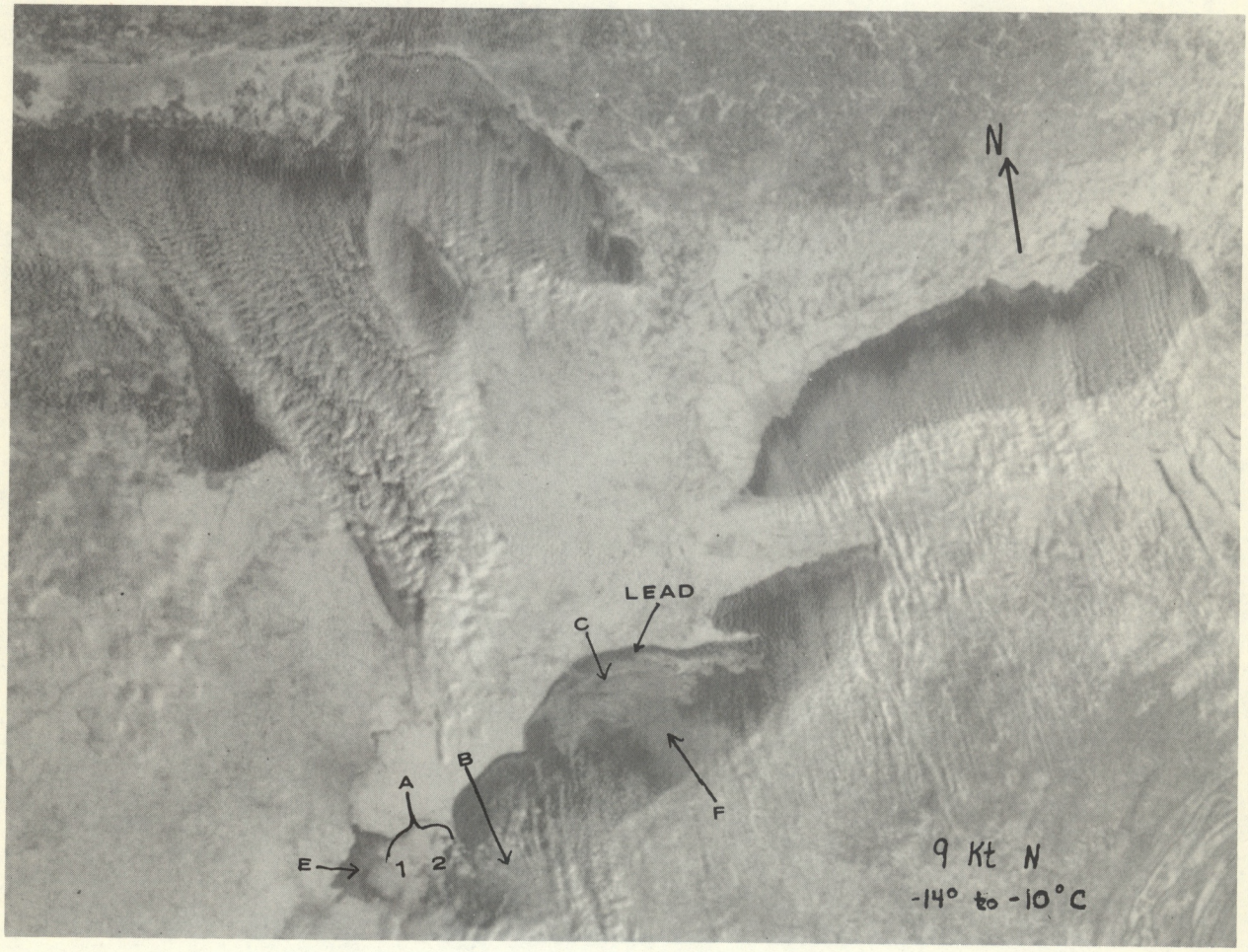

Figure 8B.--NOAA-4 VHRR (visible) image of Lake Erie, January 17, 1976.

Figure 8C.--NOAA-4 VHRR (IR) image of Lake Erie, January 17, 1976.

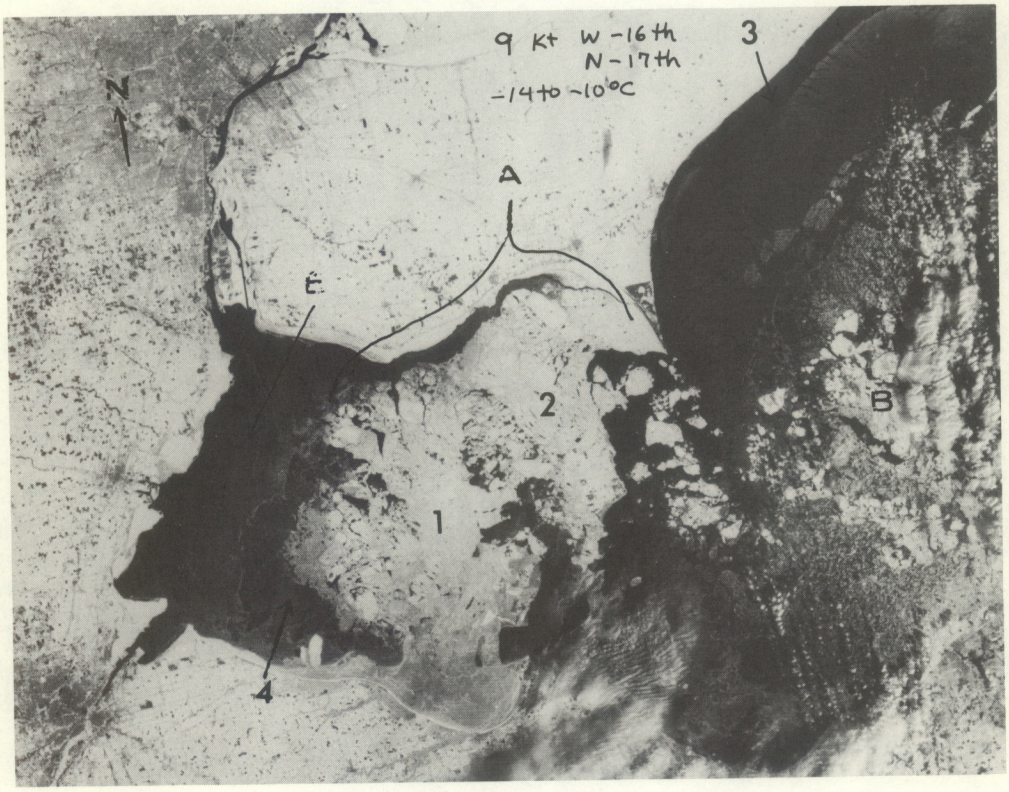

Figure 8D.--Landsat image of the western end of Lake Erie, January 17, 1976.

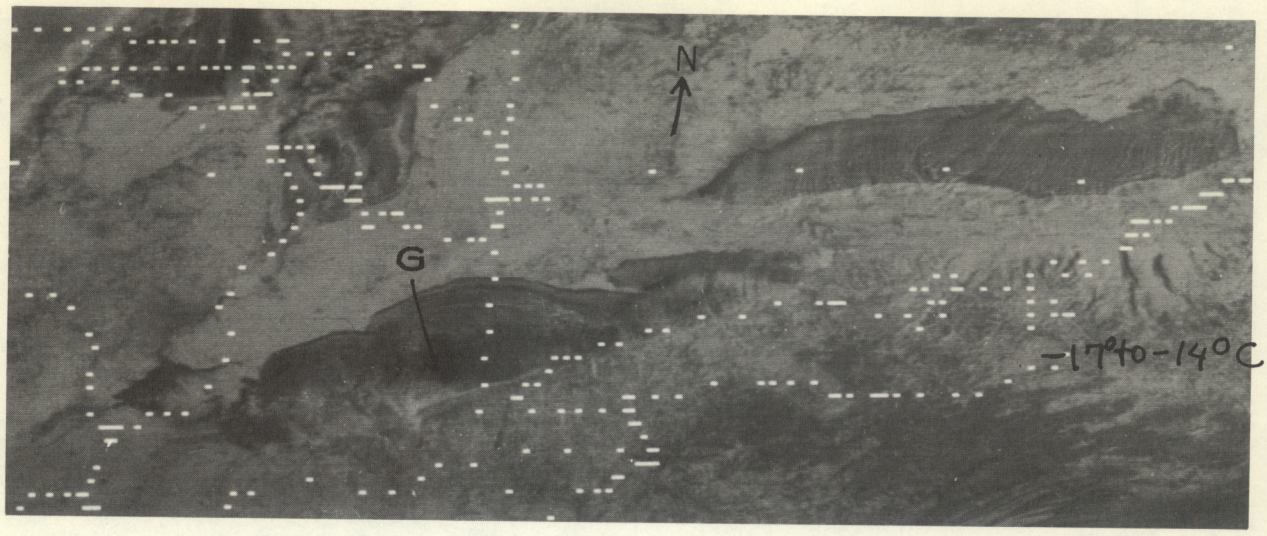

Figure 9.--GOES image of Lake Erie, 1430 GMT, January 18, 1976.

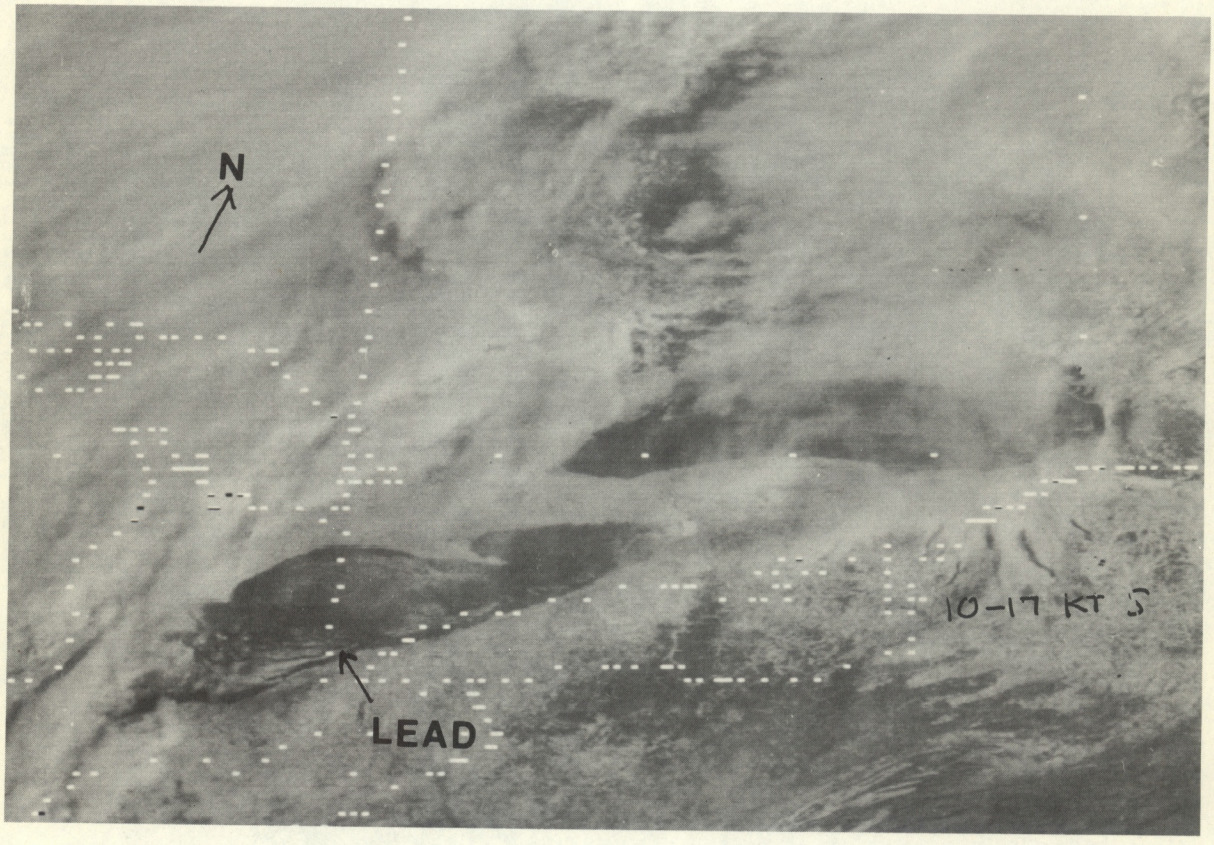

Figure 10A.--GOES image of Lake Erie, 1500 GMT, January 19, 1976.

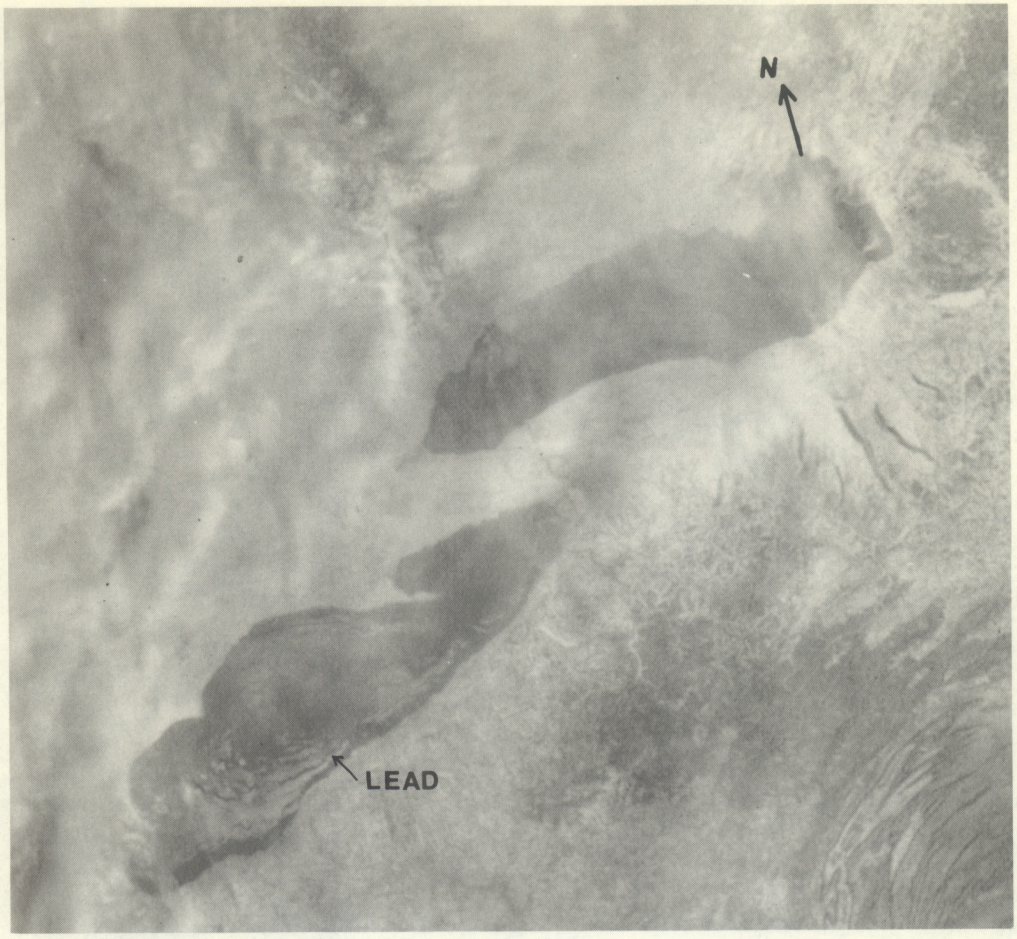

Figure 10B.--NOAA-4 VHRR (visible) image of Lake Erie, January 19, 1976.

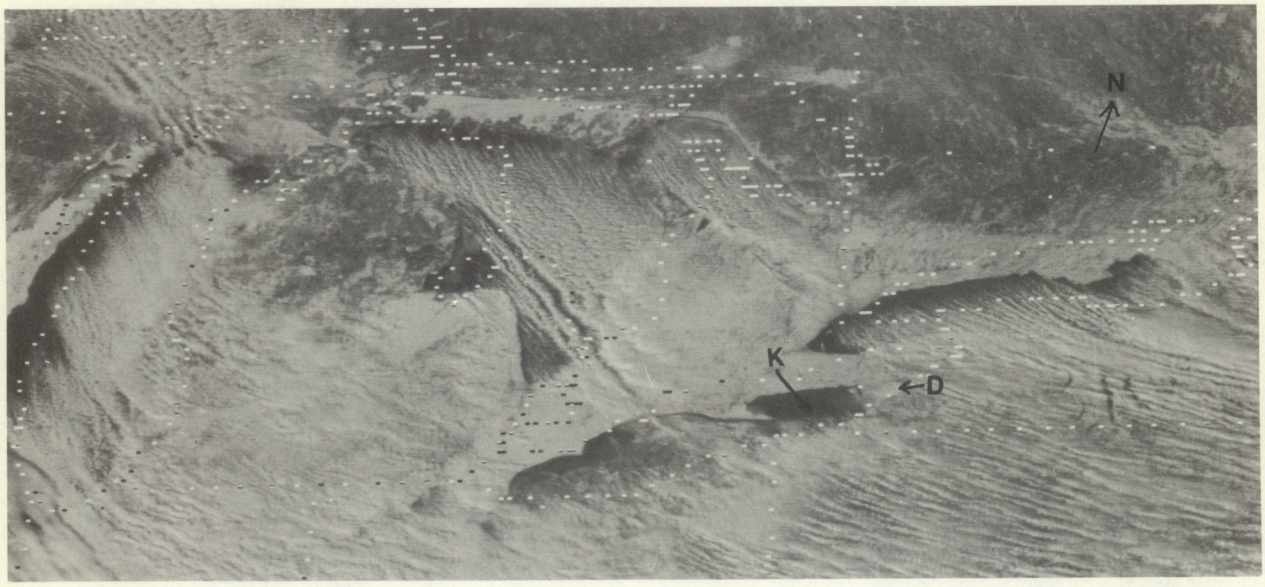

Figure 11.--GOES image of Lake Erie, 1930 GMT, January 22, 1976.

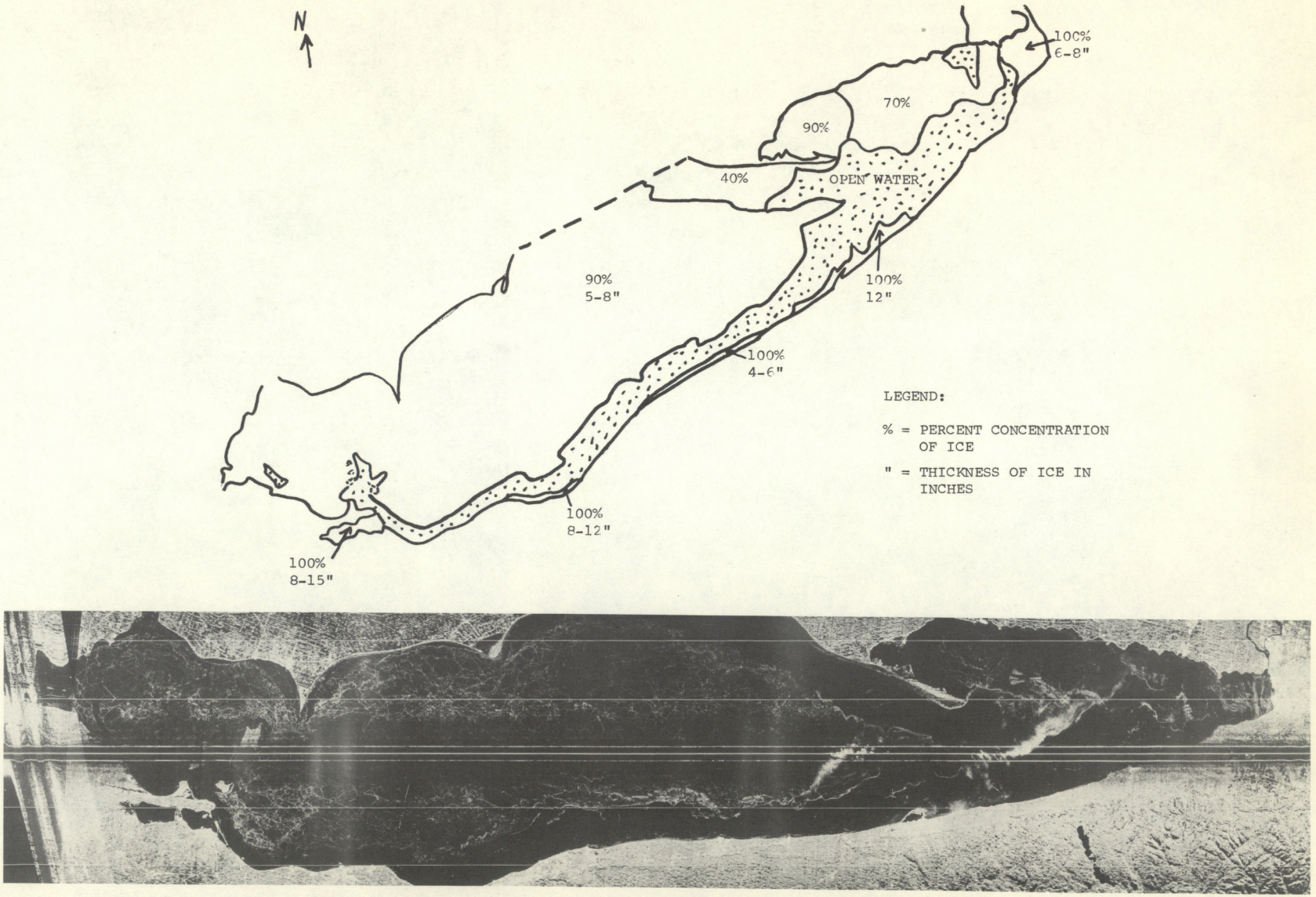

Figure 12.--SLAR image and interpretation chart of Lake Erie, January 26, 1976.

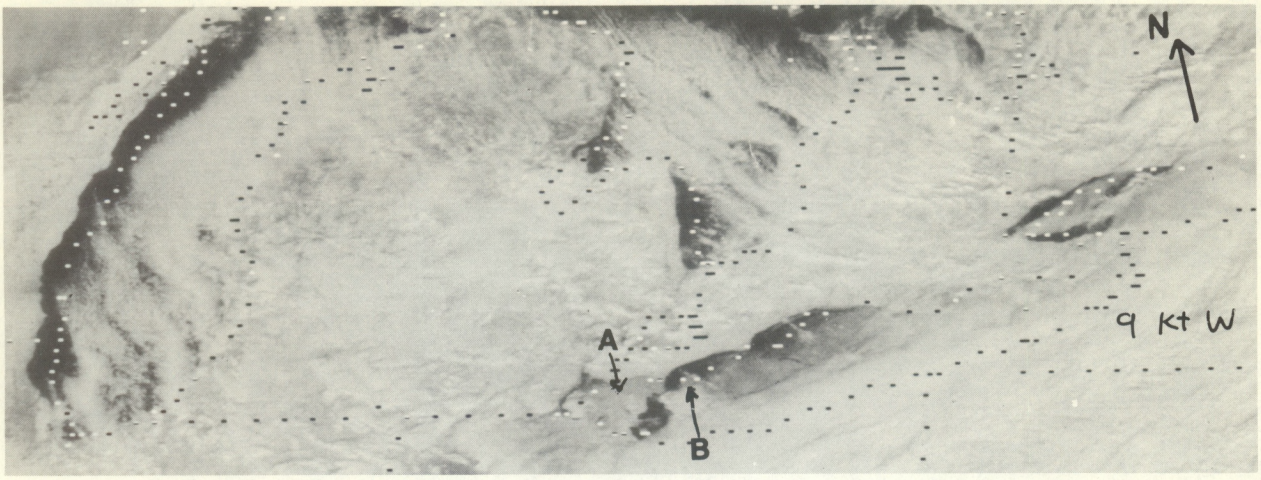

Figure 13.--GOES image of Lake Erie, 1630 GMT, January 29, 1976.

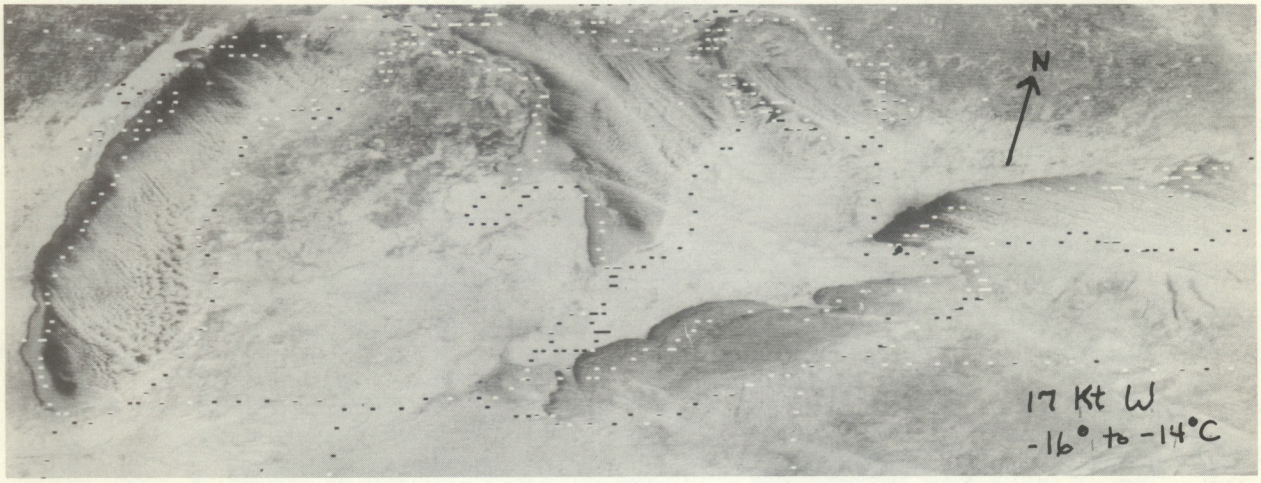

Figure 14A.--GOES image of Lake Erie, 1600 GMT, February 2, 1976.

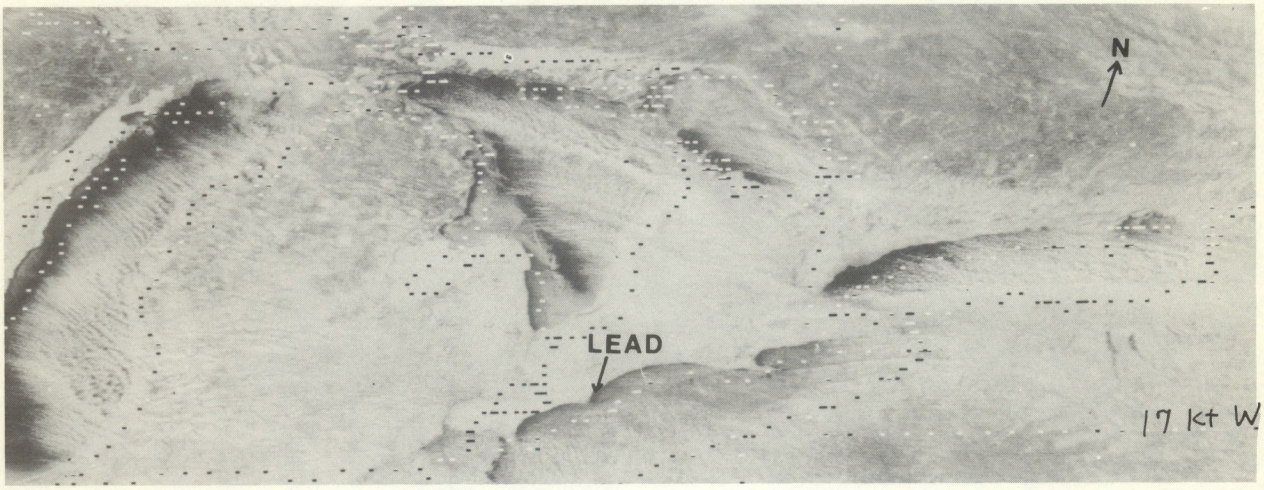

Figure 14B.--GOES image of Lake Erie, 1830 GMT, February 2, 1976.

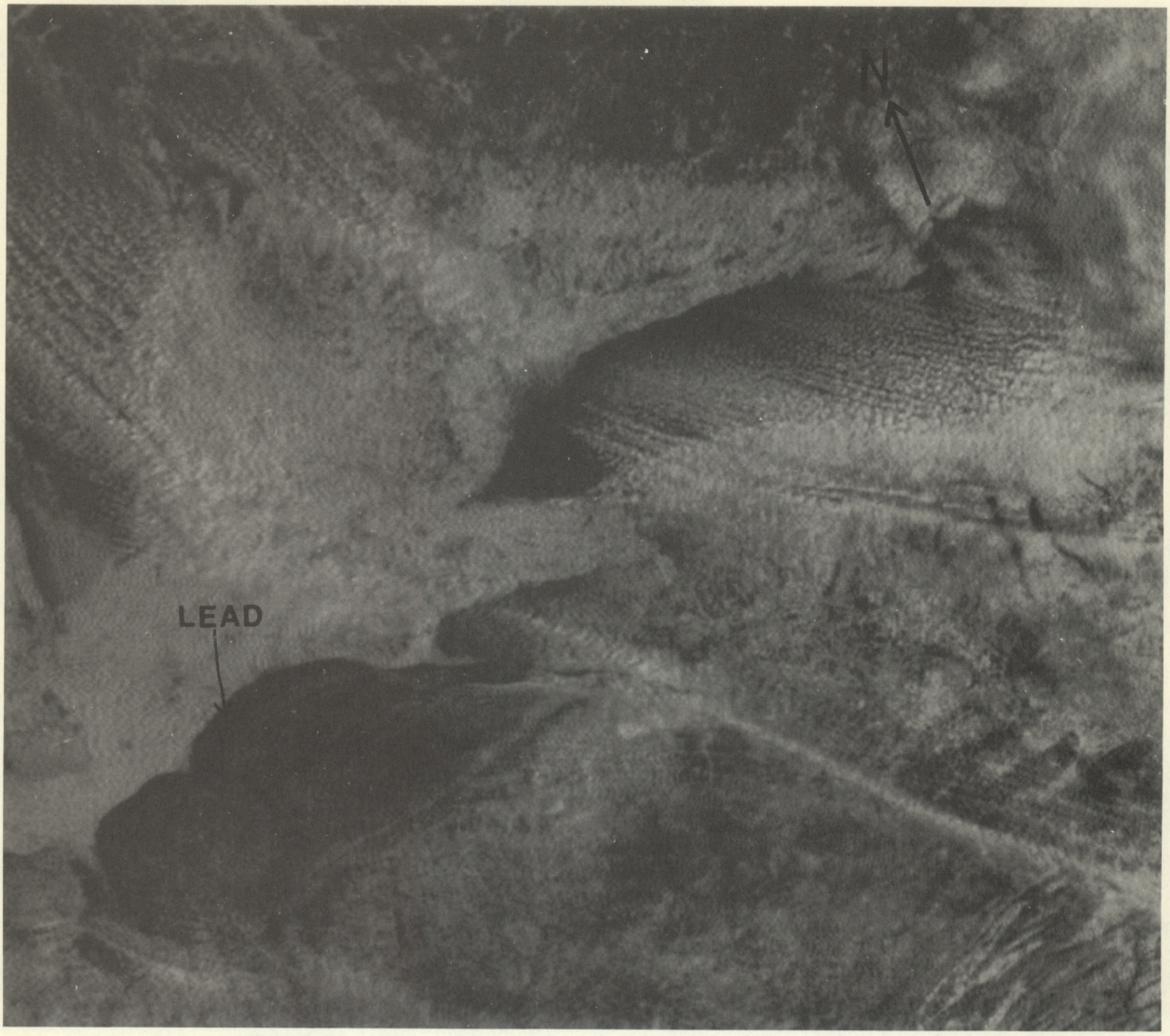

Figure 14C.--NOAA-4 VHRR (visible) image of Lake Erie, February 2, 1976.

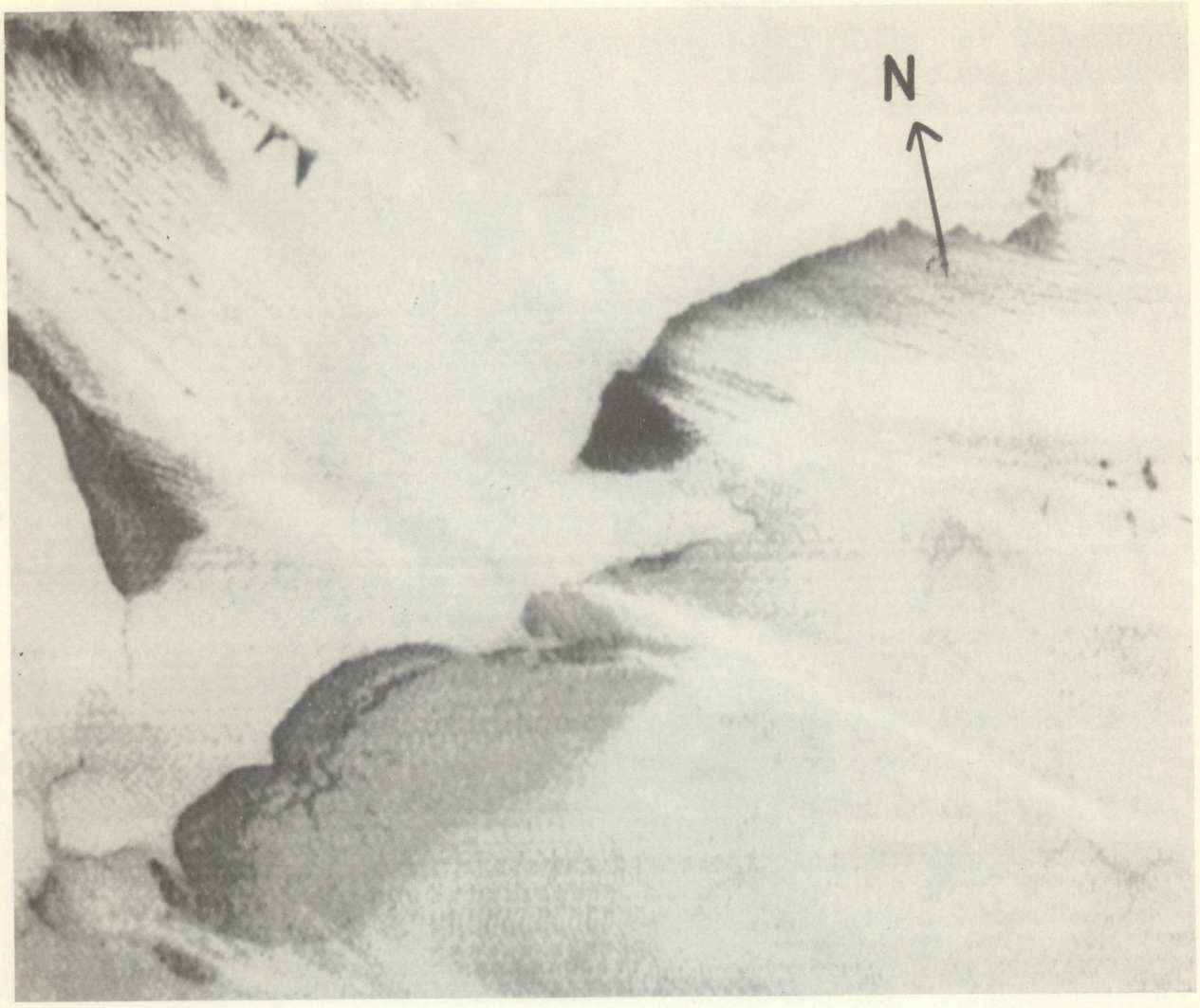

Figure 14D.--NOAA-4 VHRR (IR) image of Lake Erie, February 2, 1976.

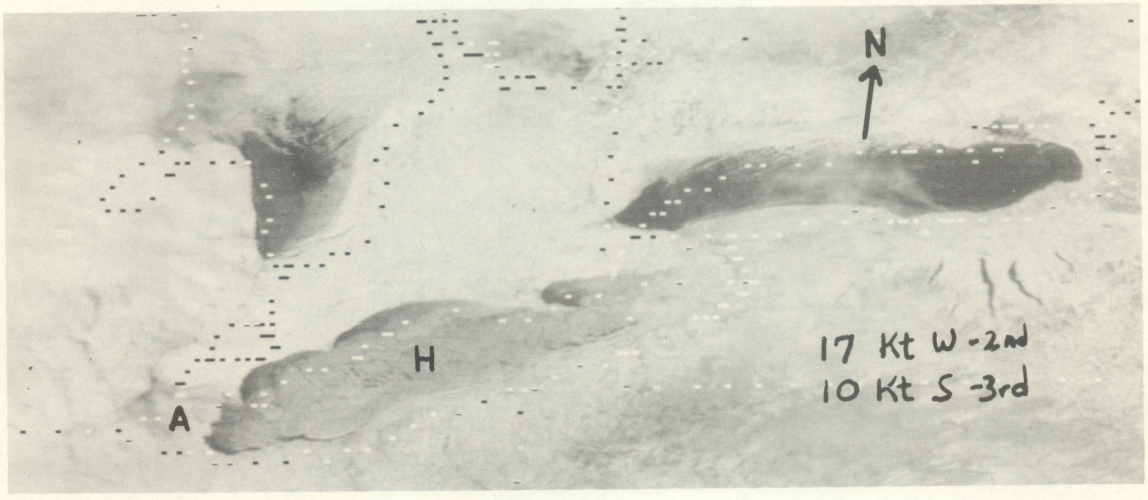

Figure 15A.--GOES image of Lake Erie, 1830 GMT, February 3, 1976.

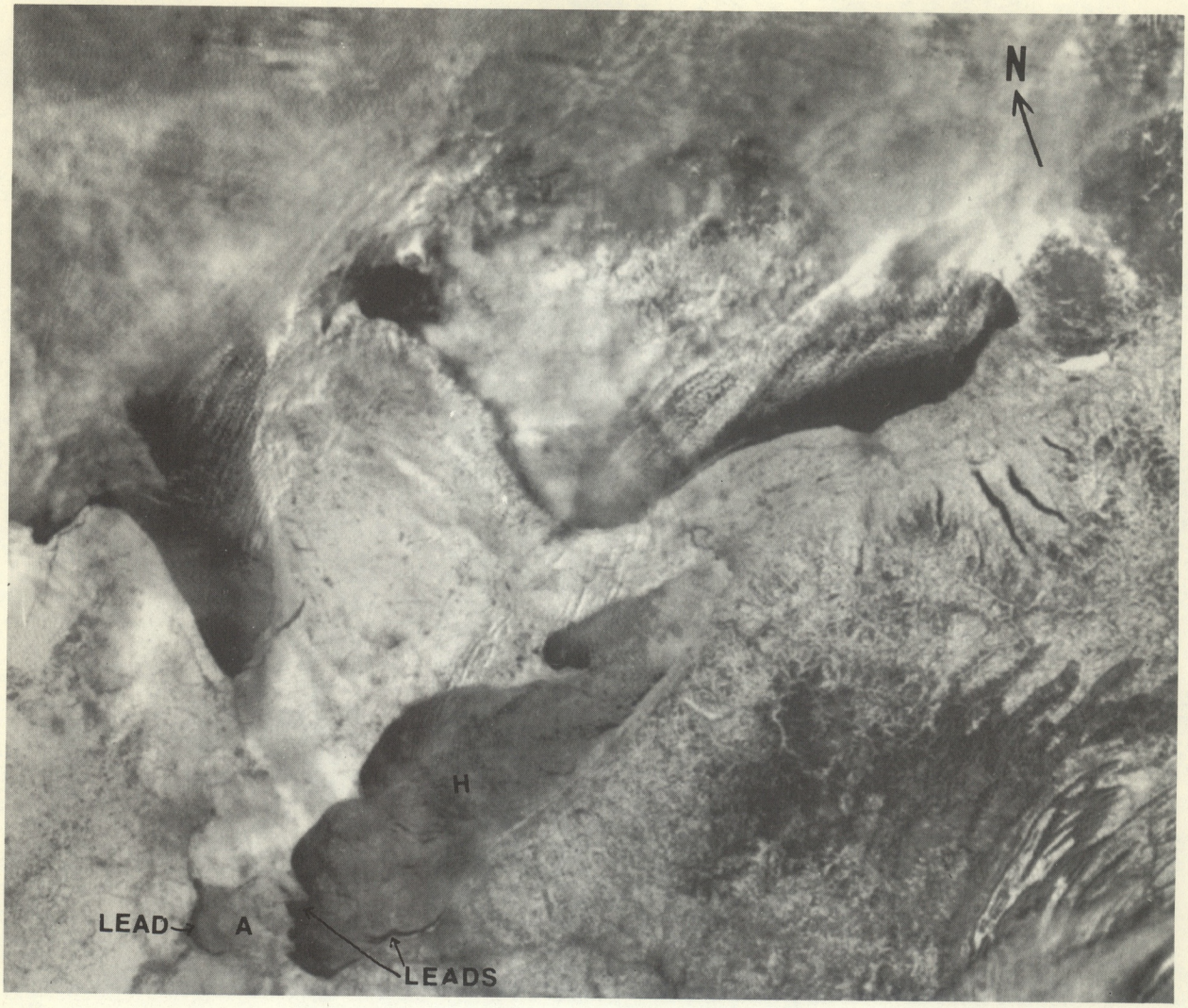

Figure 15B.--NOAA-4 VHRR (visible) image of Lake Erie, February 3, 1976.

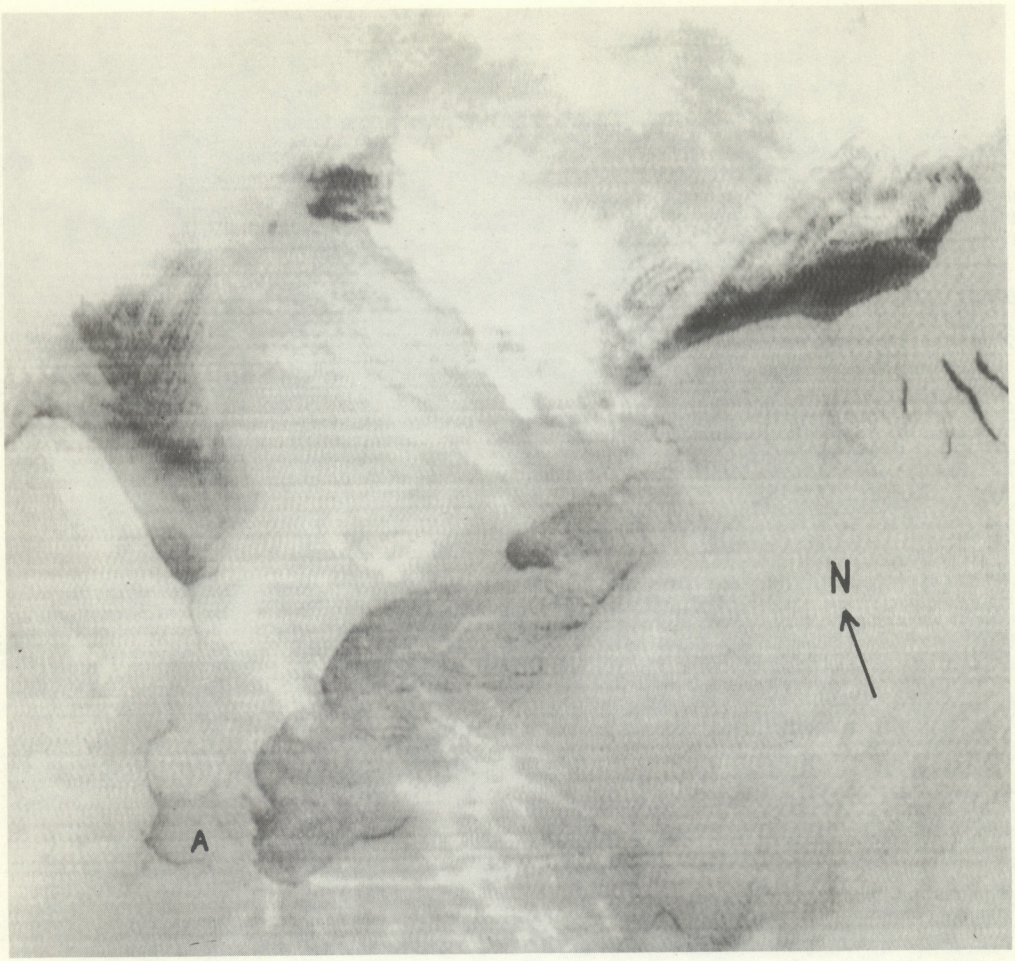

Figure 15C.--NOAA-4 VHRR (IR) image of Lake Erie, February 3, 1976.

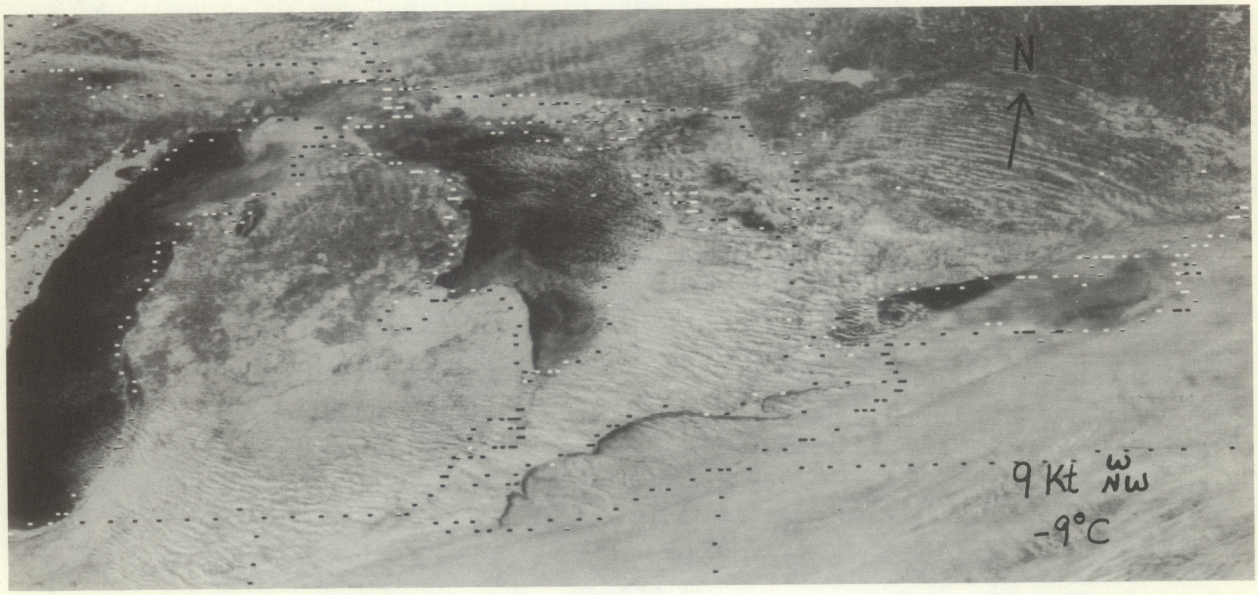

Figure 16.--GOES image of Lake Erie, 1900 GMT, February 6, 1976.

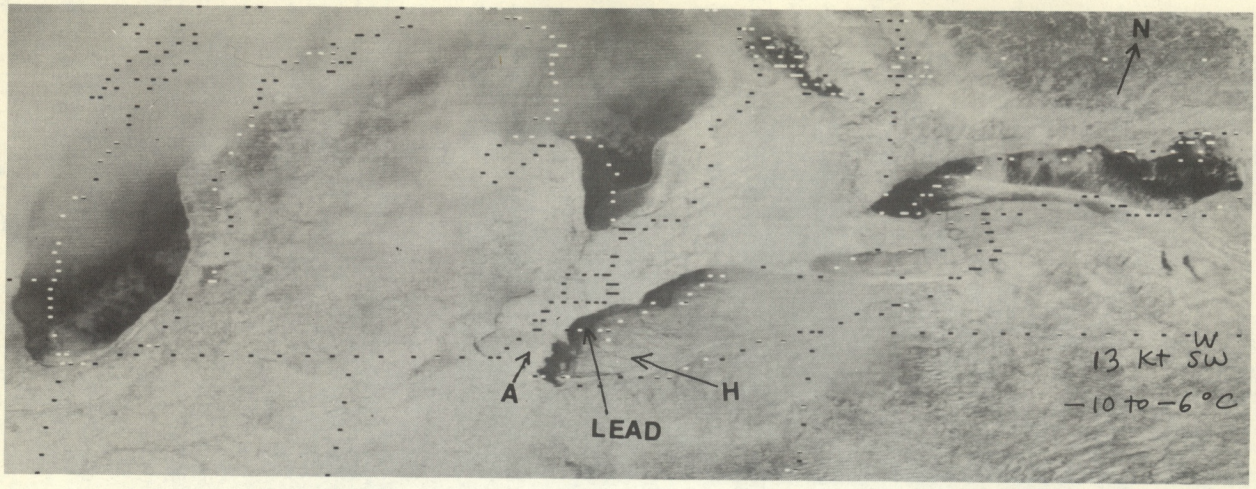

Figure 17.--GOES image of Lake Erie, 1630 GMT, February 7, 1976.

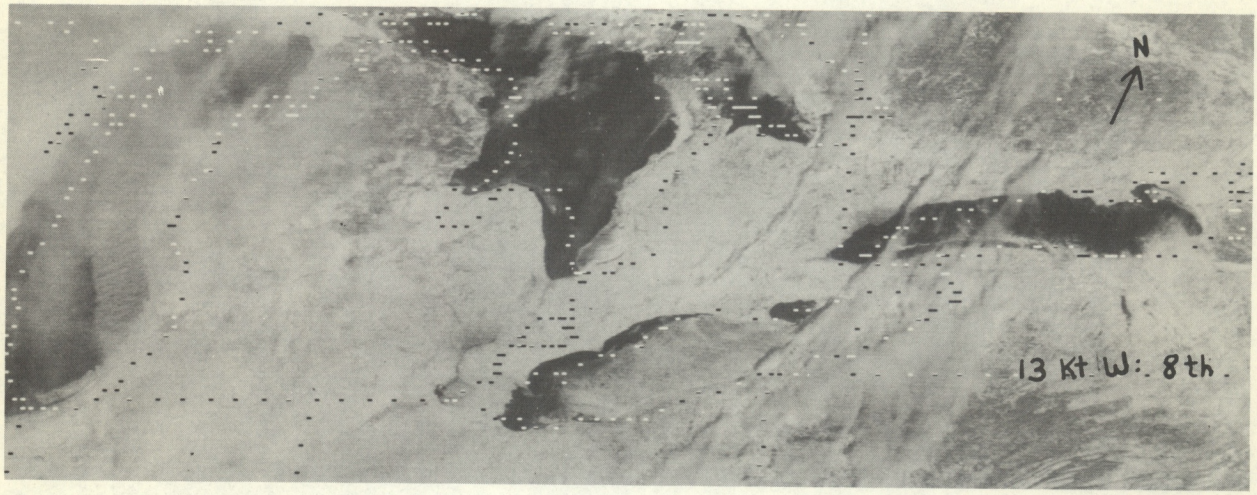

Figure 18.--GOES image of Lake Erie, 1601 GMT, February 9, 1976.

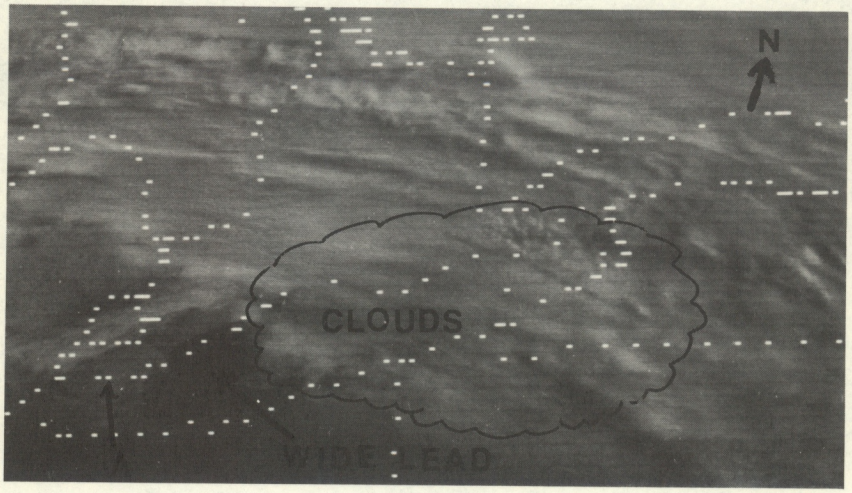

Figure 19A.--GOES image of Lake Erie, 2130 GMT, February 12, 1976.

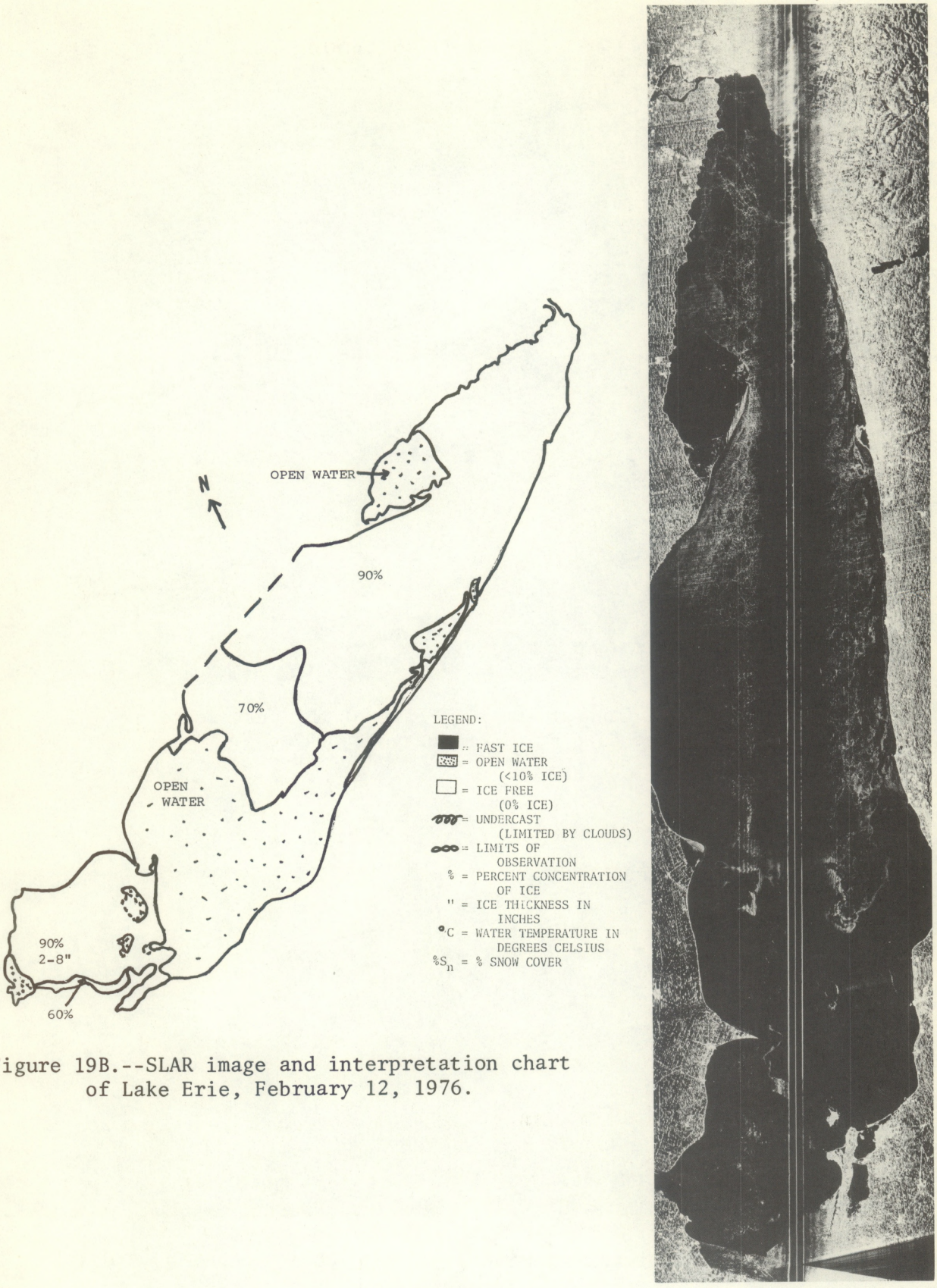

Figure 19B.--SLAR image and interpretation chart of Lake Erie, February 12, 1976.

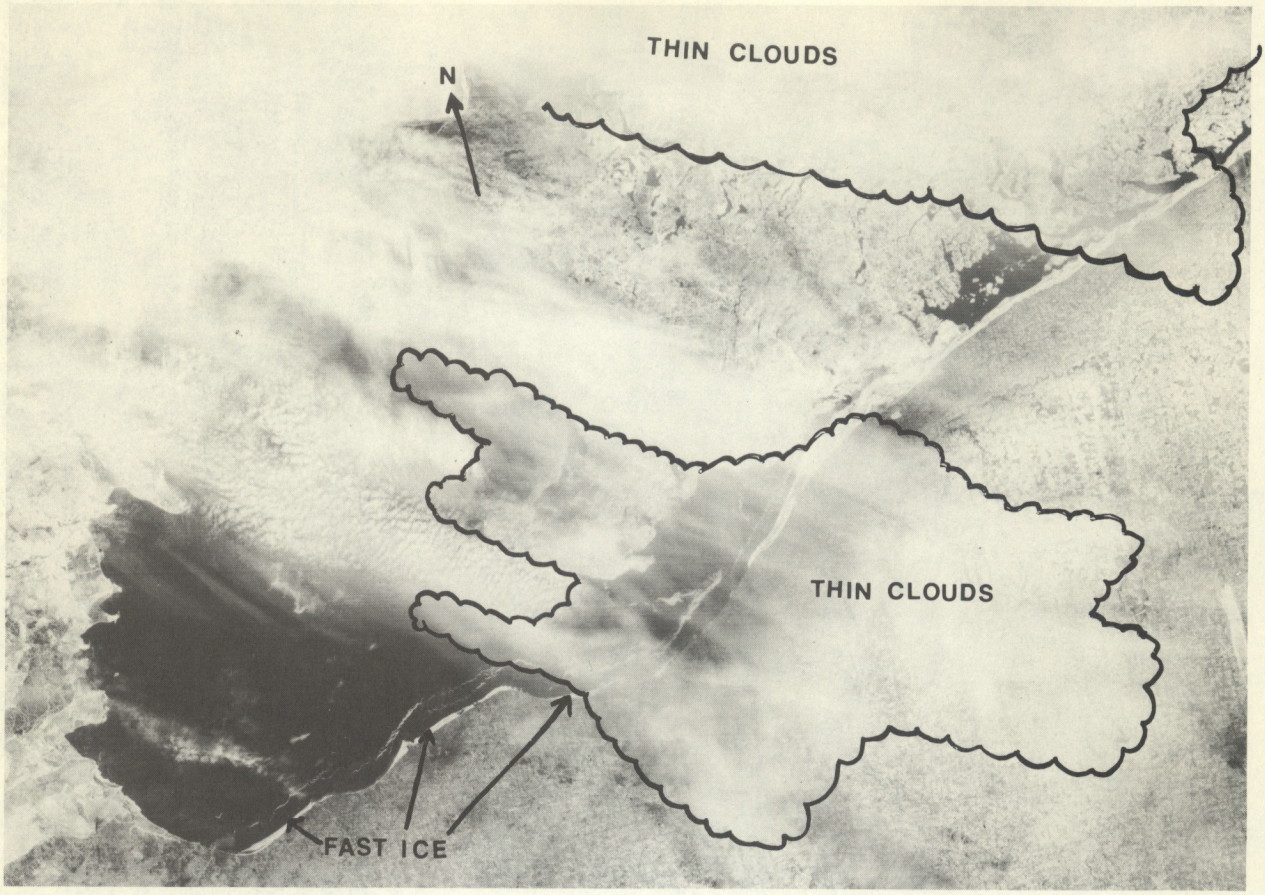

Figure 19C.--Landsat image of part of the west section of Lake Erie, February 12, 1976.

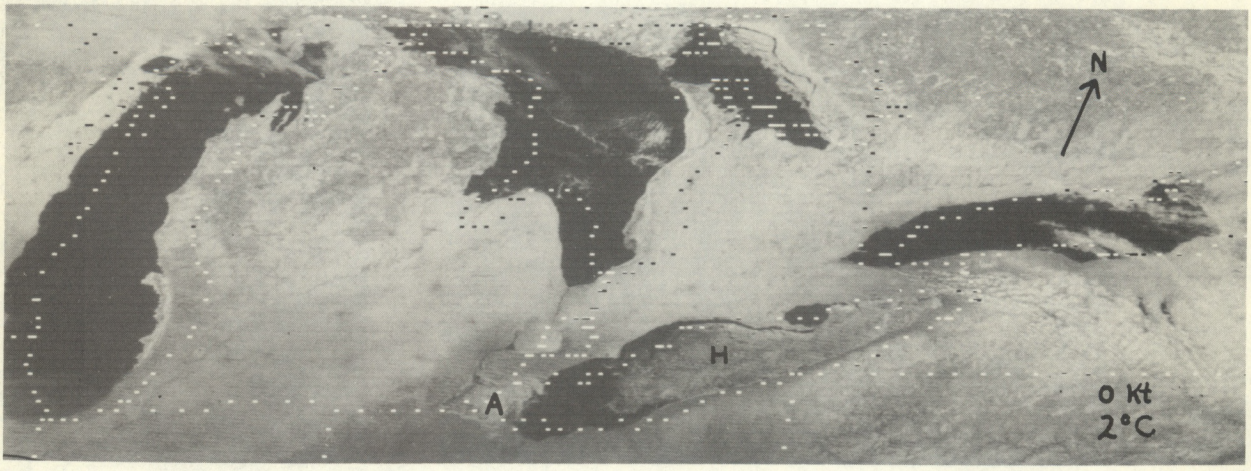

Figure 20A.--GOES image of Lake Erie, 1700 GMT, February 14, 1976.

Figure 20B.--NOAA-4 VHRR (visible) image of Lake Erie, February 14, 1976.

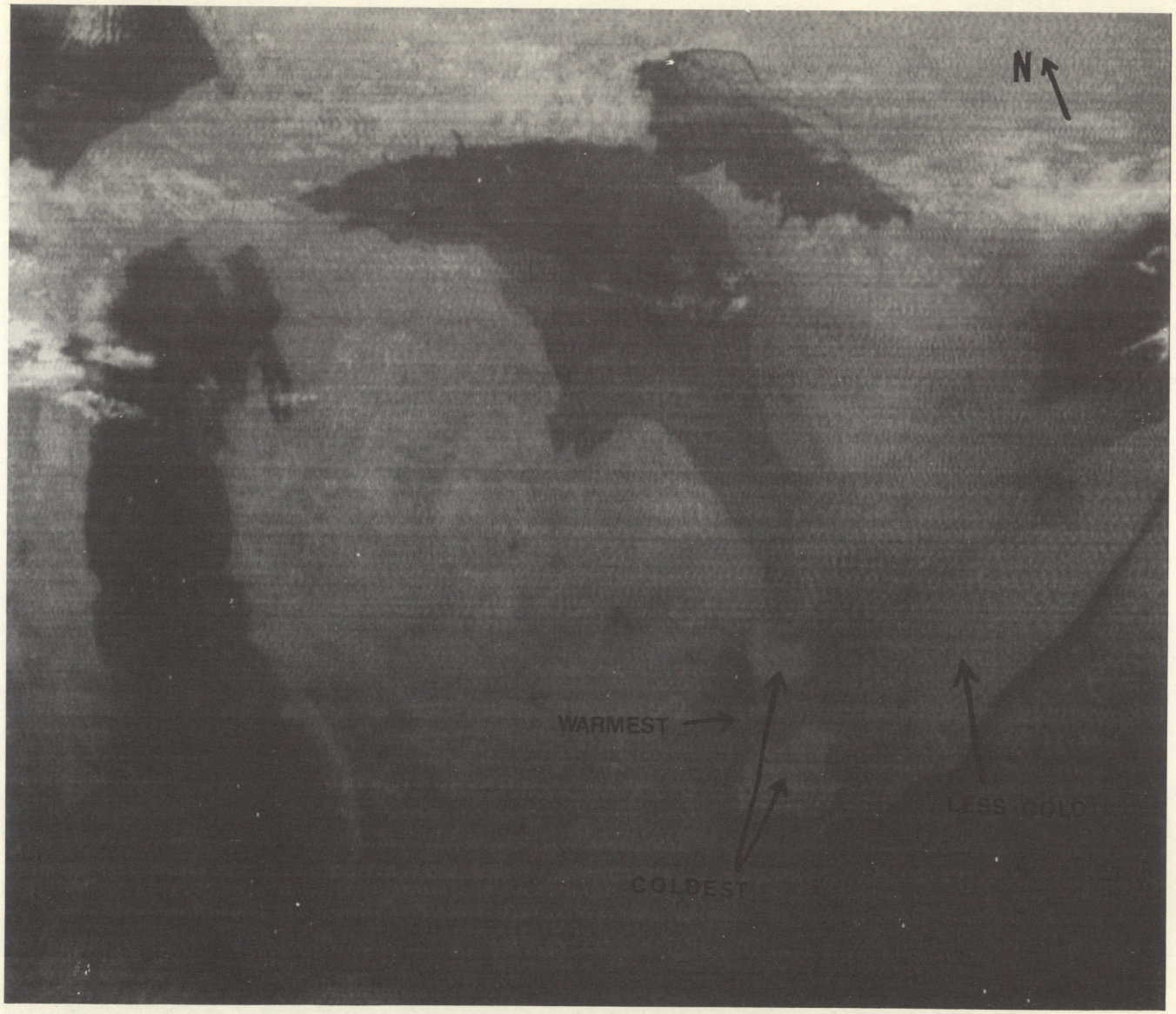

Figure 20C.--NOAA-4 VHRR (IR) image of Lake Erie, February 14, 1976.

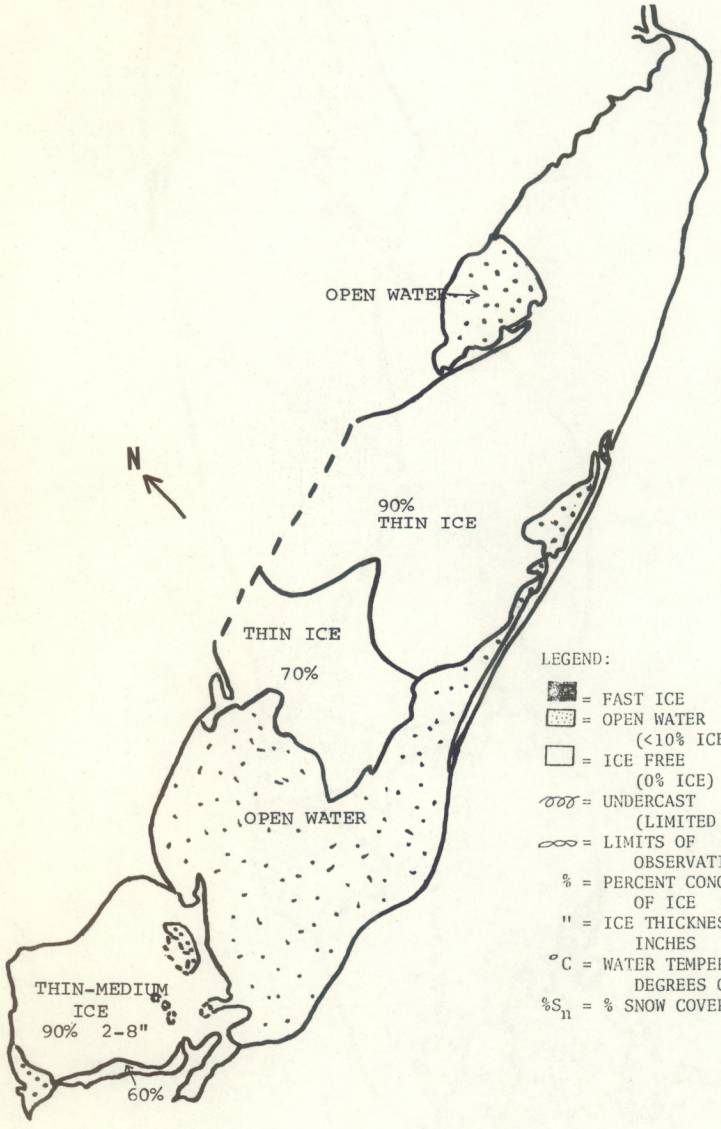

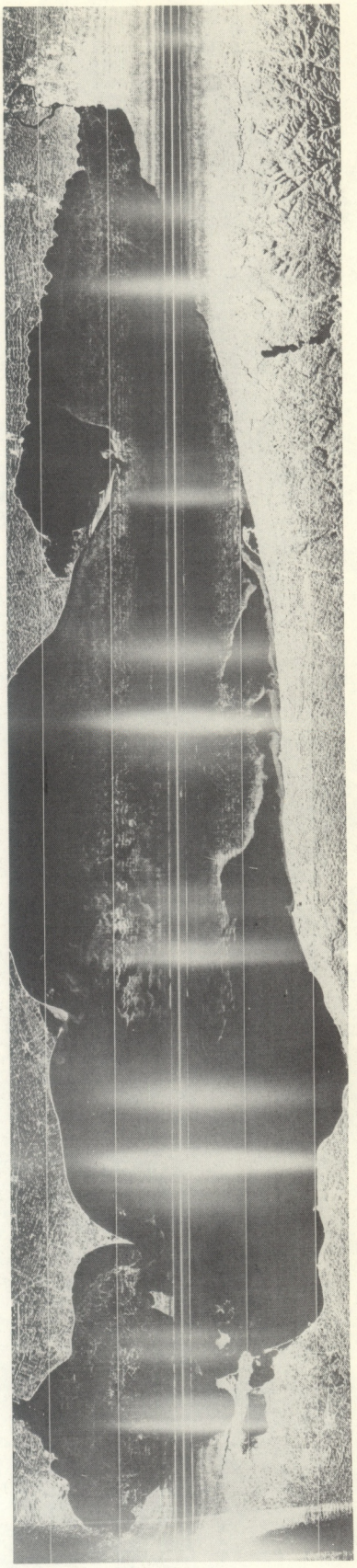

Figure 21A.--SLAR image and interpretation chart of Lake Erie, February 17, 1976.

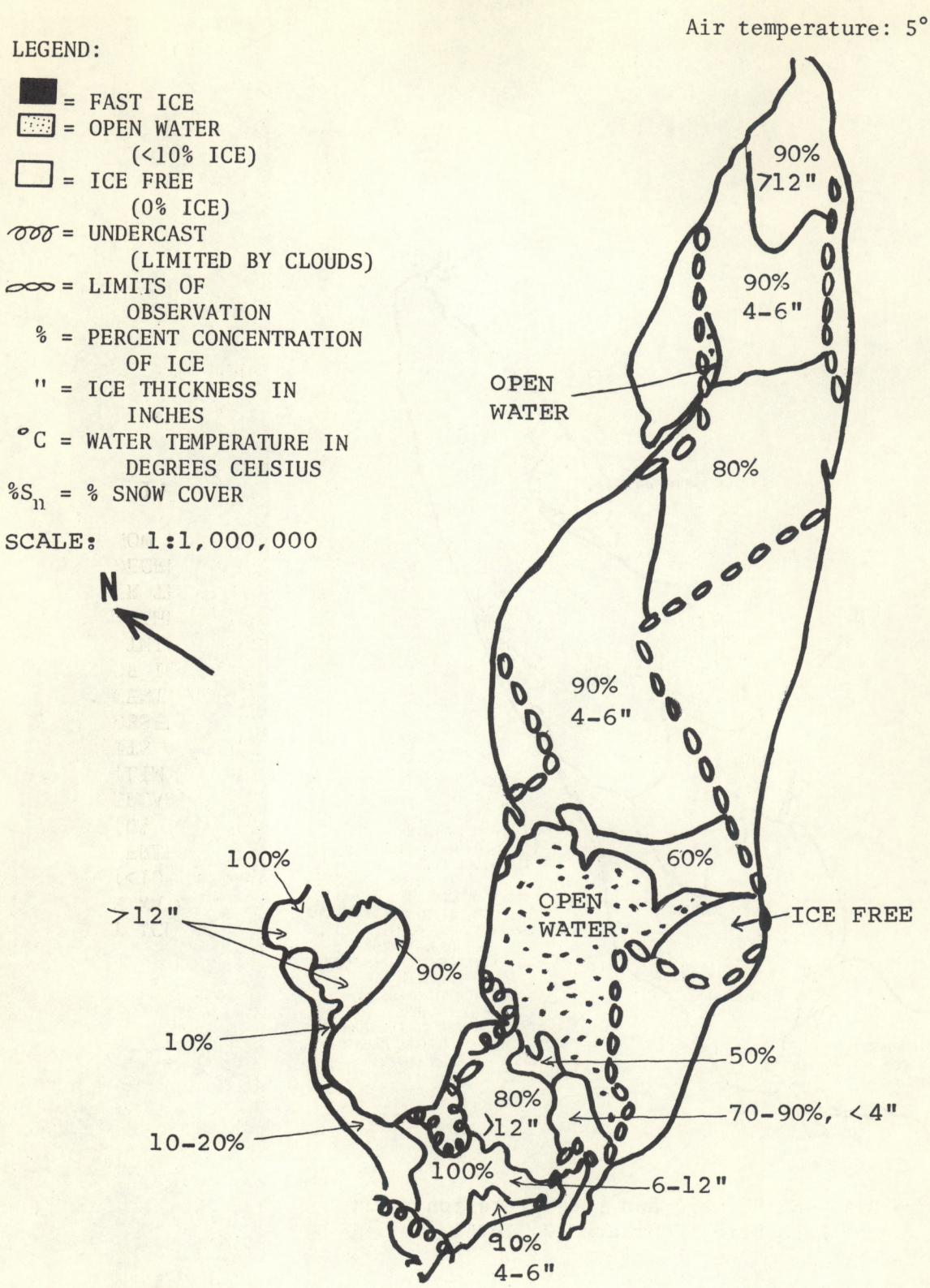

Figure 21B.--Chart showing Lake Erie ice and water temperatures, February 17, 1976. (Data from Atmospheric Environmental Service of Canada.)

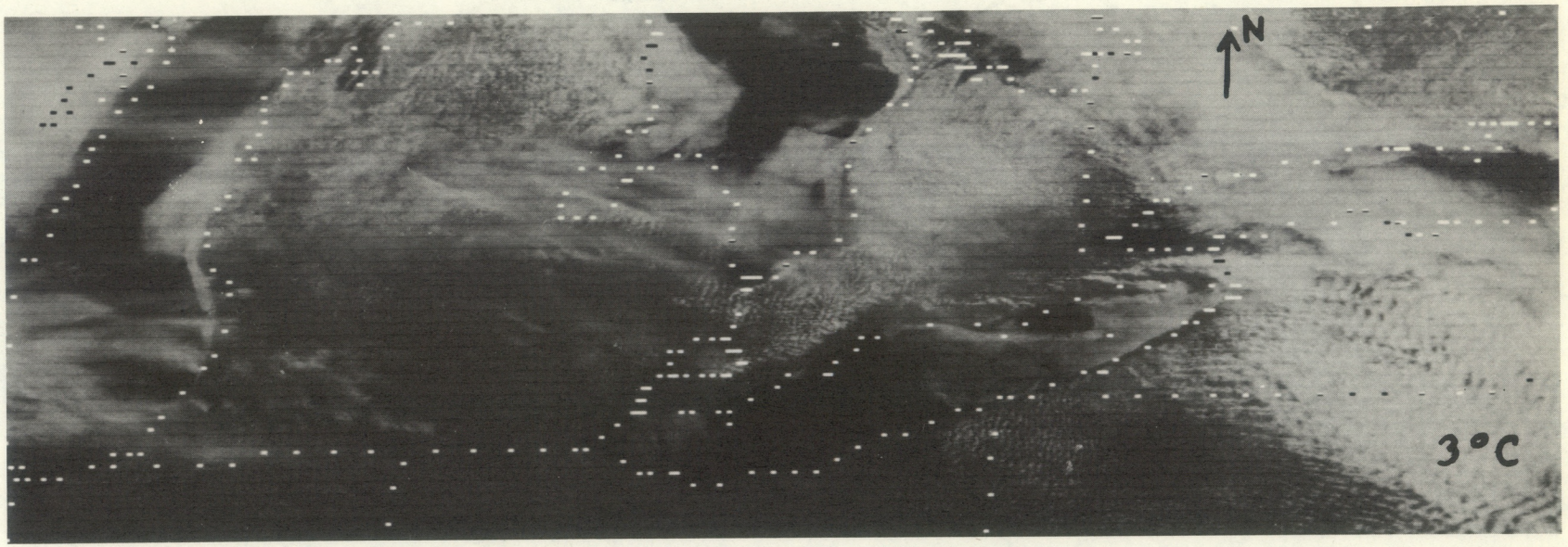

Figure 22A.--GOES image of Lake Erie, 2000 GMT, February 20, 1976.

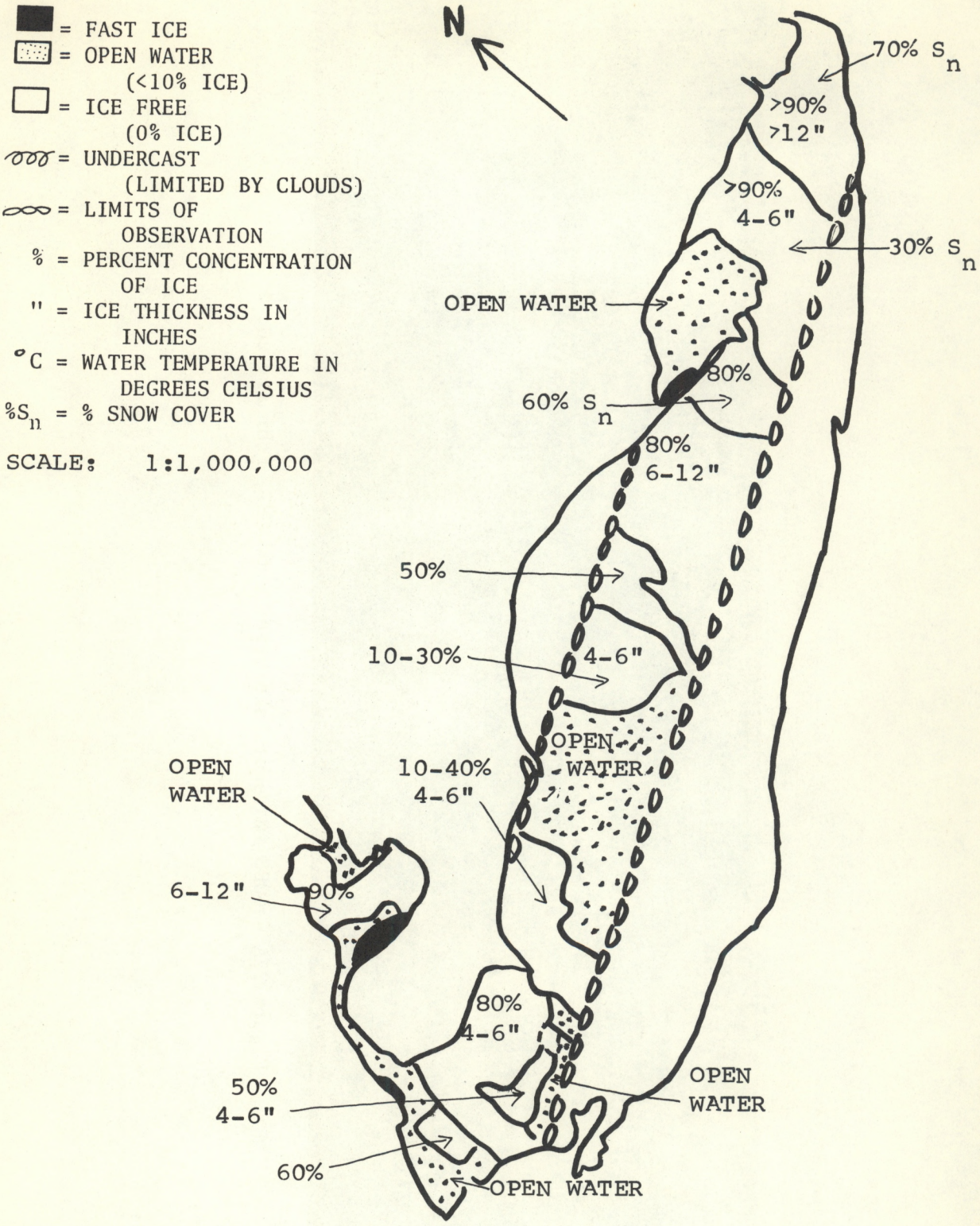

Figure 22B.--Chart showing Lake Erie ice, February 20, 1976. (Data from Atmospheric Environmental Service of Canada.)

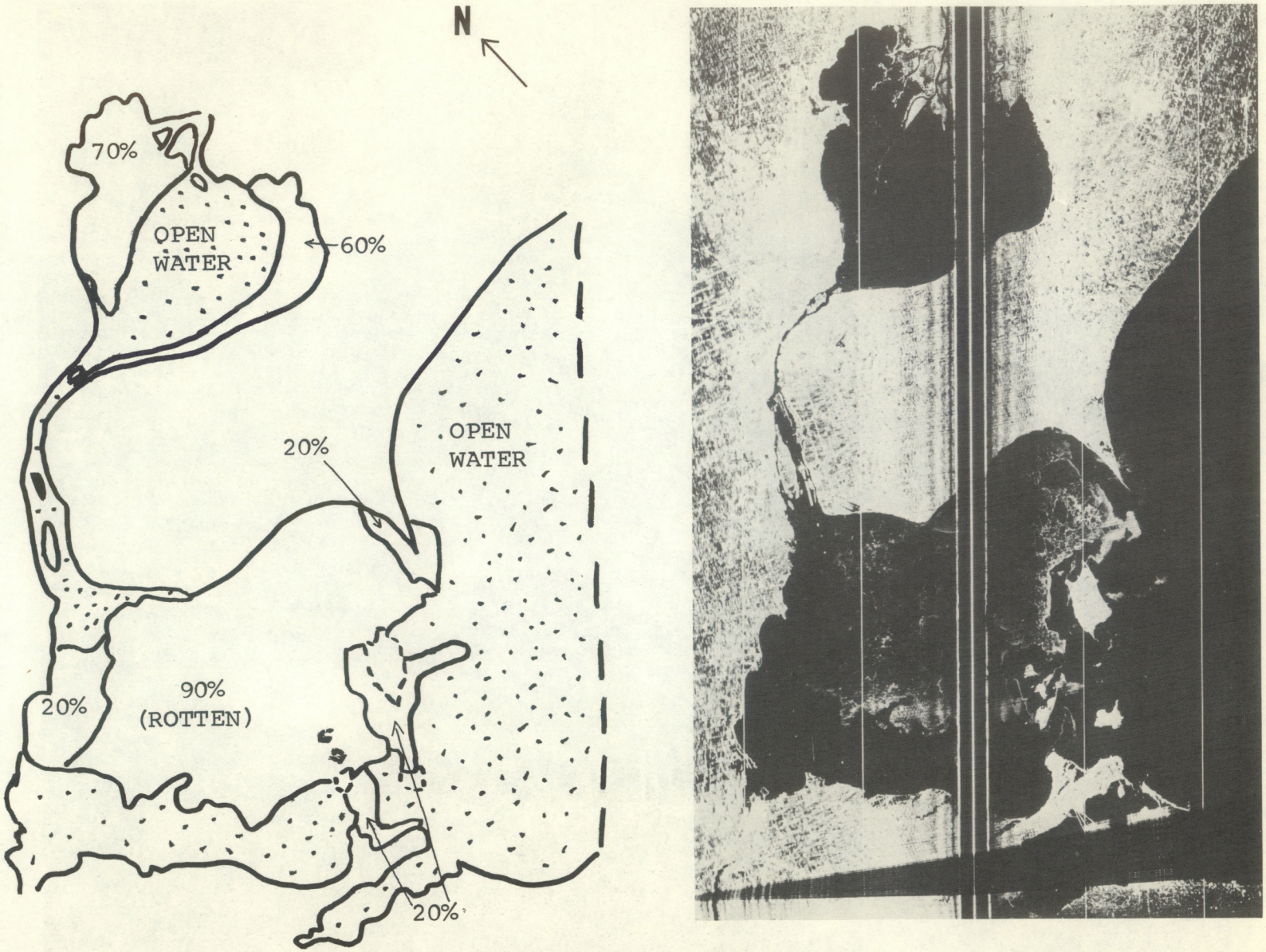

Figure 23.--SLAR image and interpretation chart of the west end of Lake Erie, February 21, 1976.

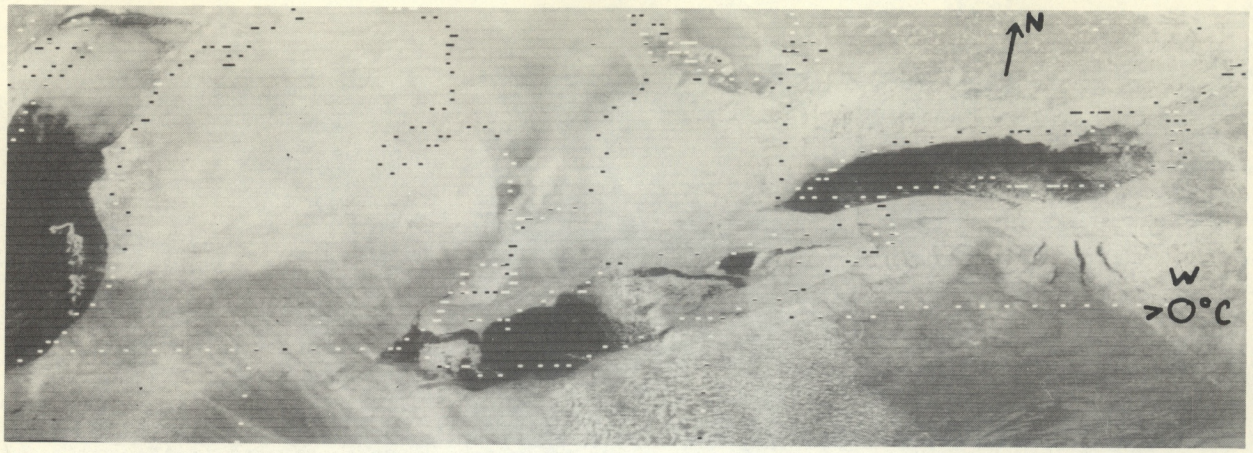

Figure 24A.--GOES image of Lake Erie, 1700 GMT, February 23, 1976.

Figure 24B.--NOAA-4 VHRR (visible) image of Lake Erie, February 23, 1976.

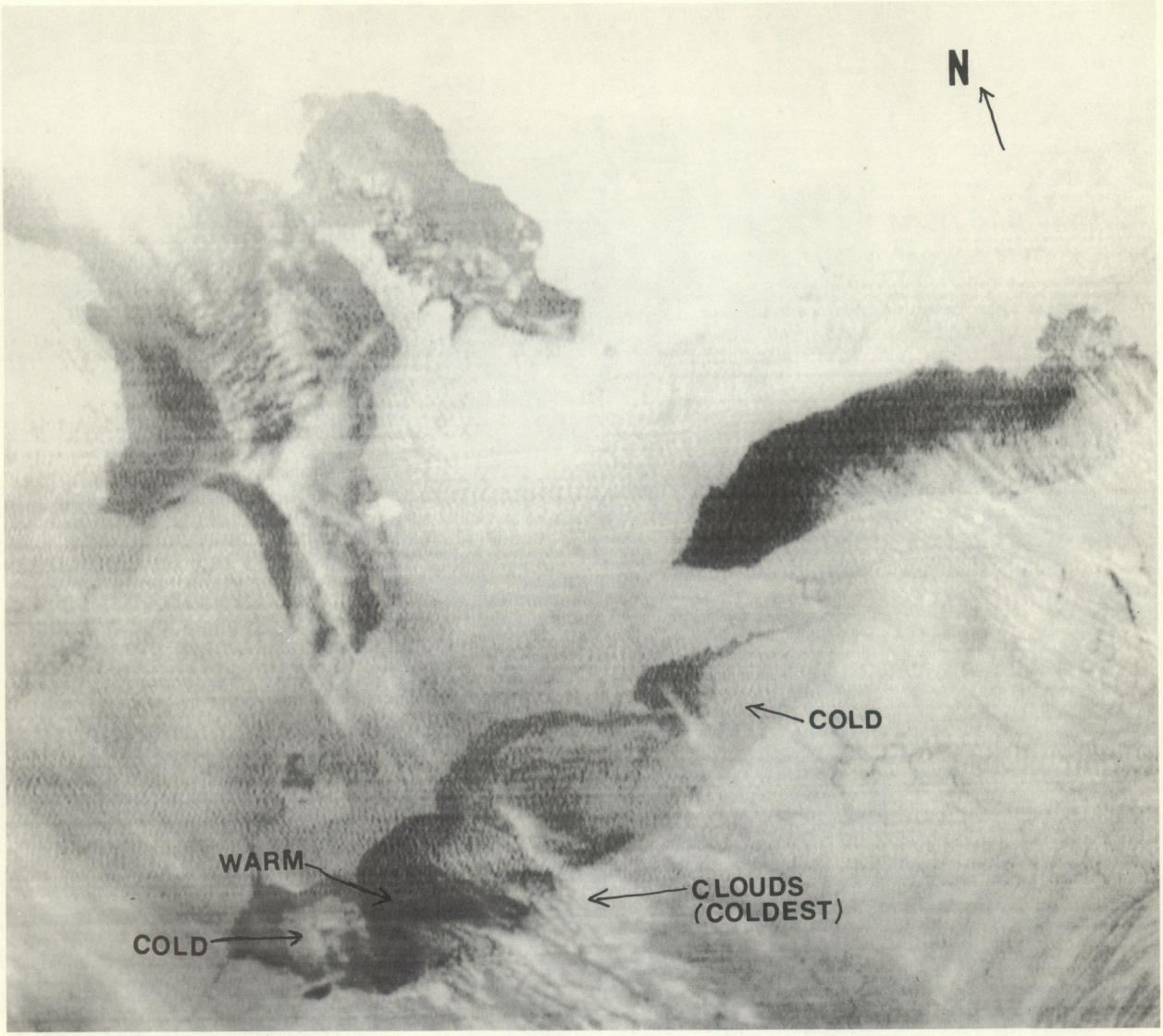

Figure 24C.--NOAA-4 VHRR (IR) image of Lake Erie, February 23, 1976.

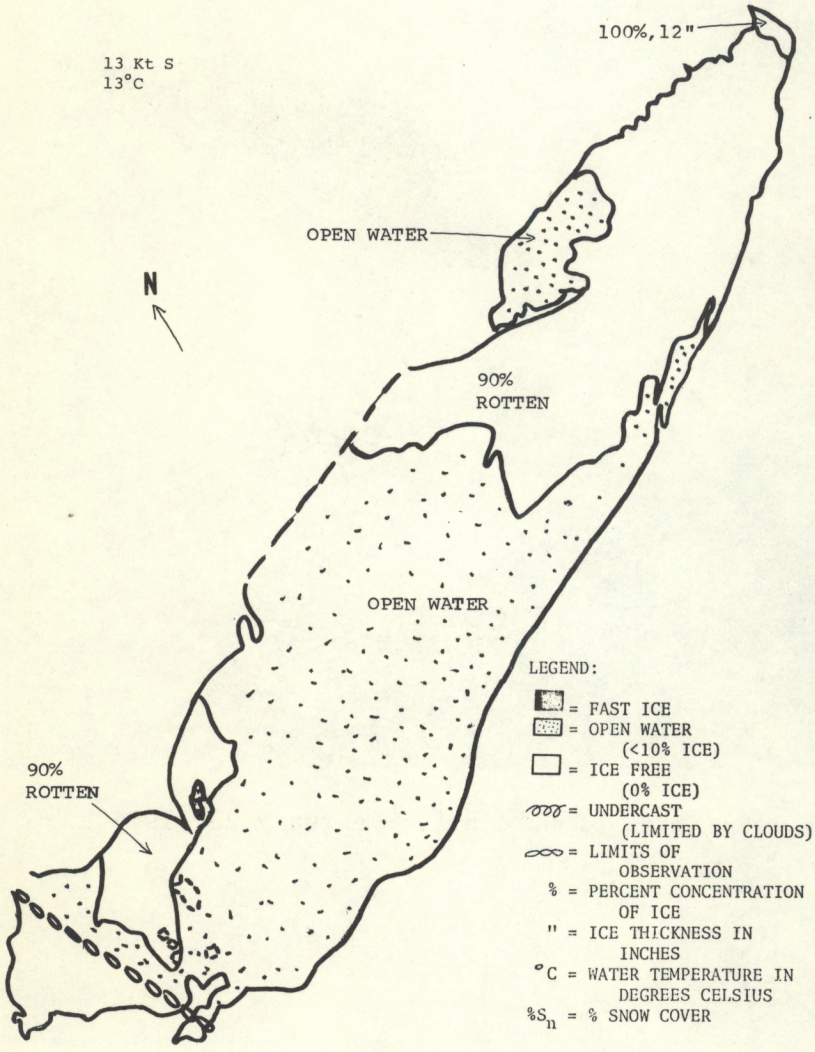

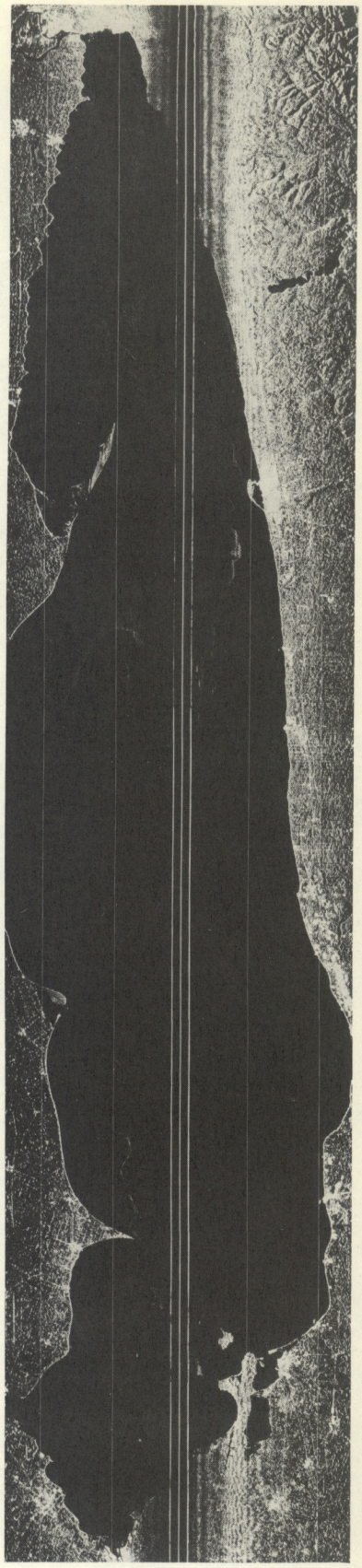

Figure 25.--SLAR image and interpretation chart of Lake Erie, February 25, 1976.

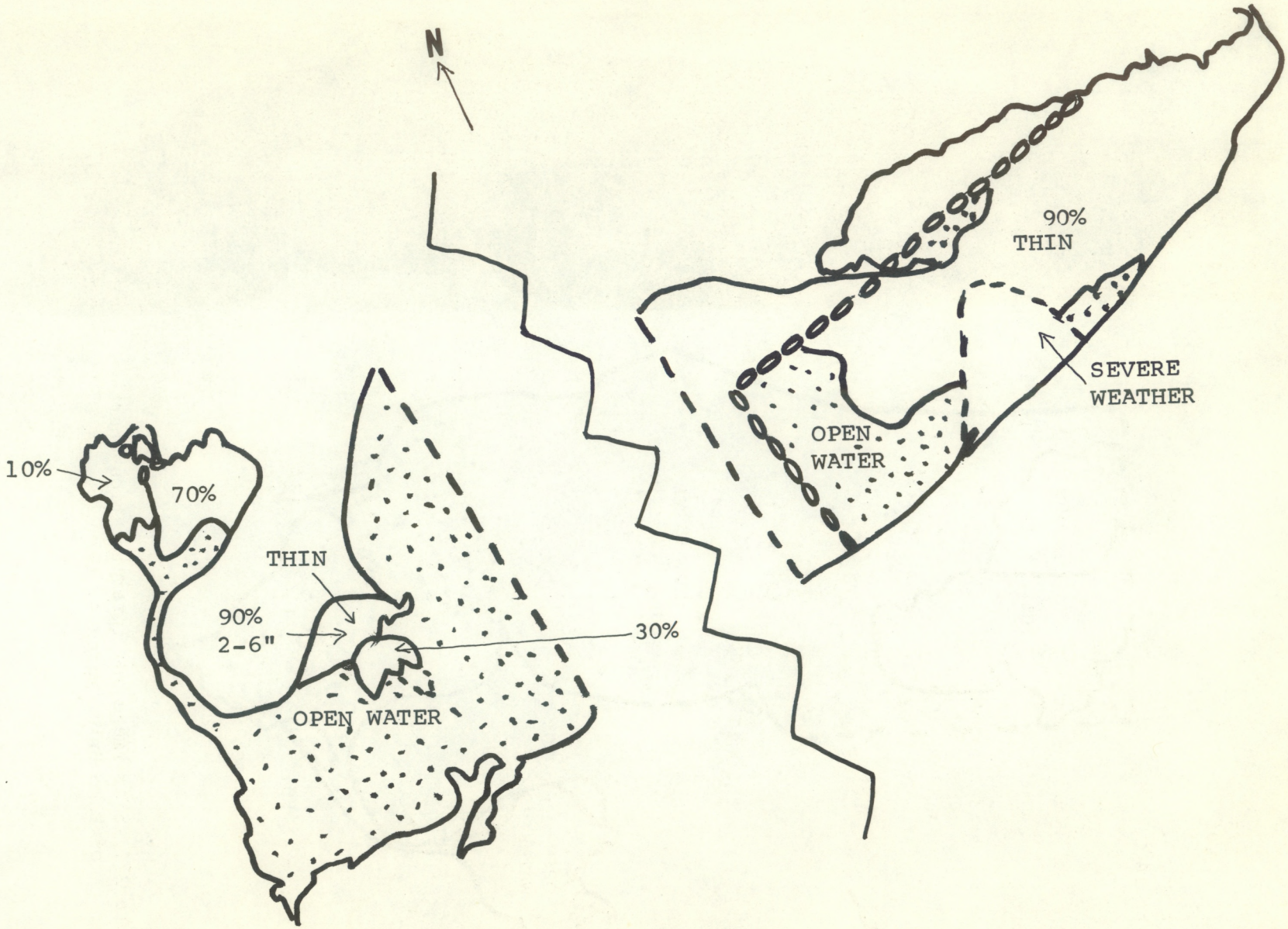

Figure 26.--Interpretation chart of Lake Erie for SLAR image taken February 29, 1976.

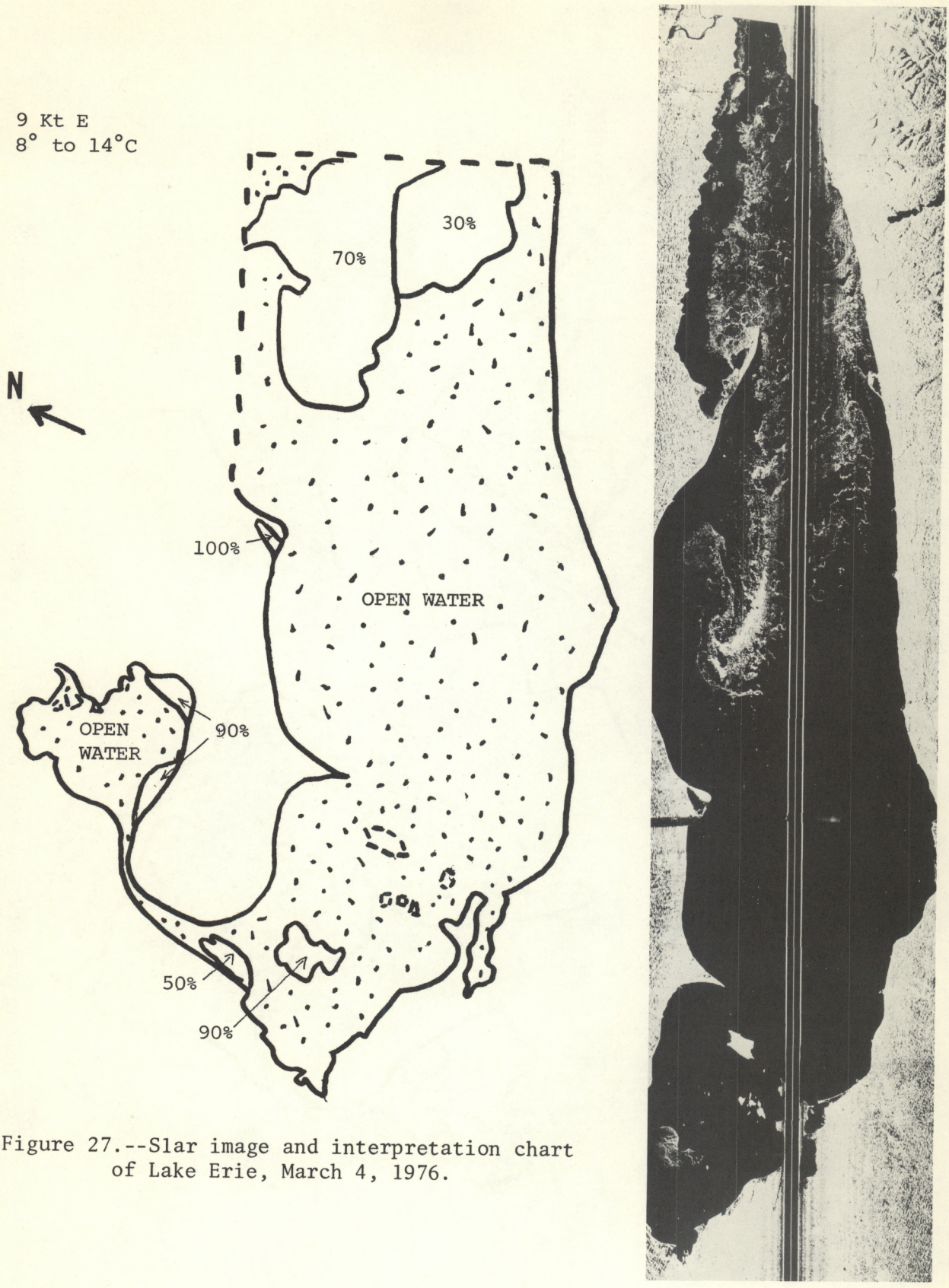

Figure 27.--Slar image and interpretation chart of Lake Erie, March 4, 1976.

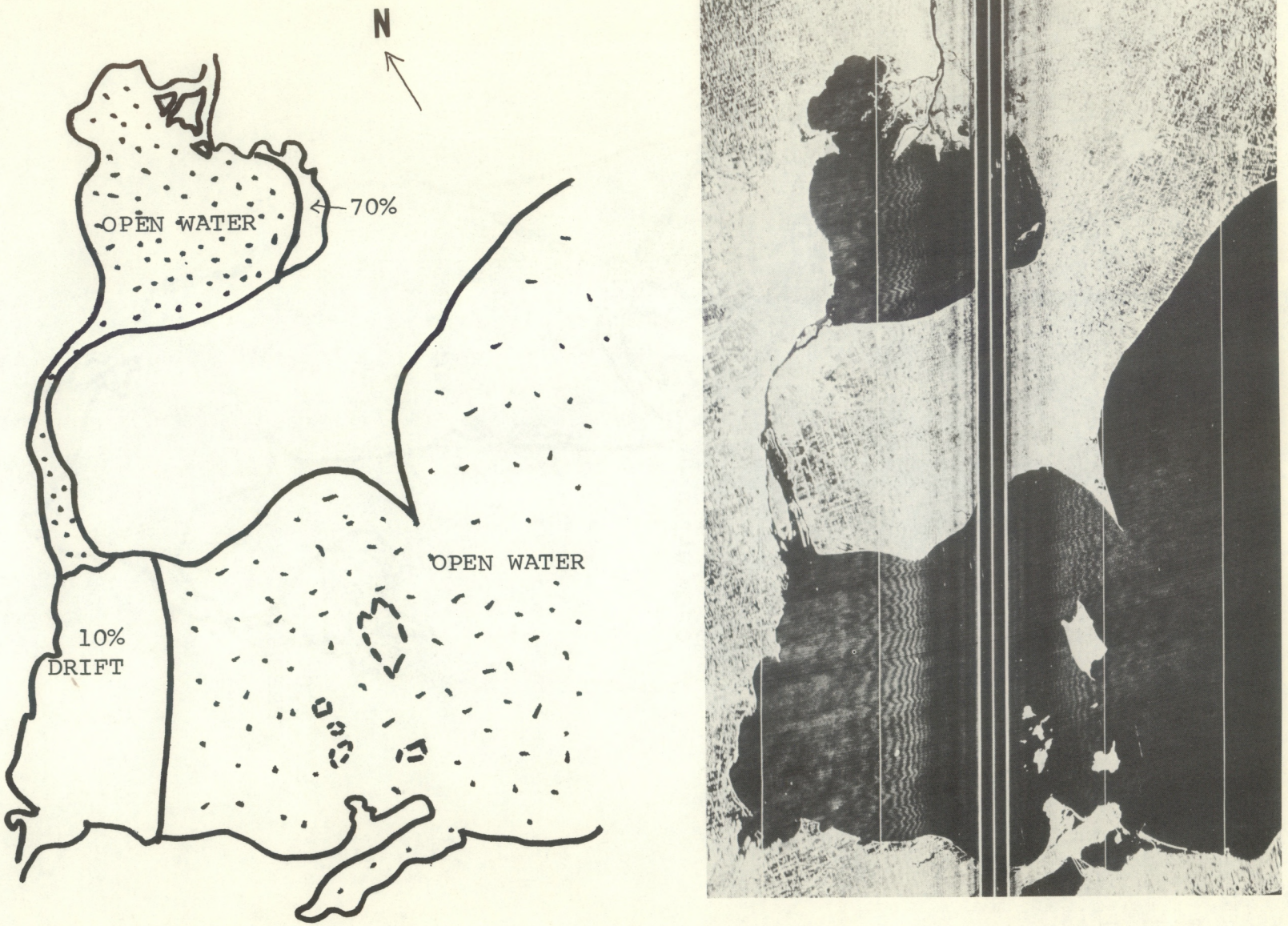

Figure 28A.--SLAR image and interpretation chart of the west end of Lake Erie, March 6, 1976.

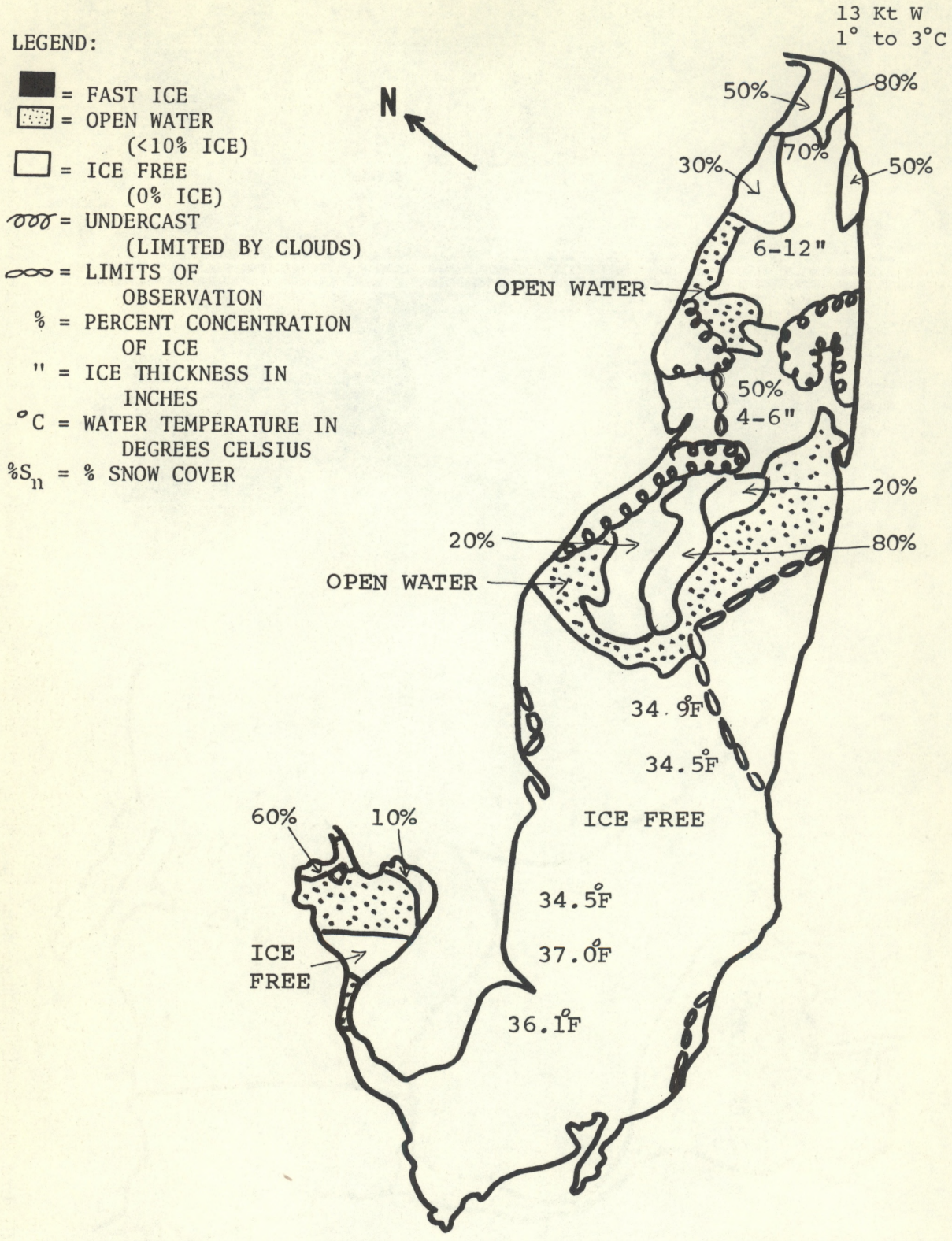

Figure 28B.--Chart showing Lake Erie ice and water temperatures, March 6, 1976. (Data from Atmospheric Environmental Service of Canada.)

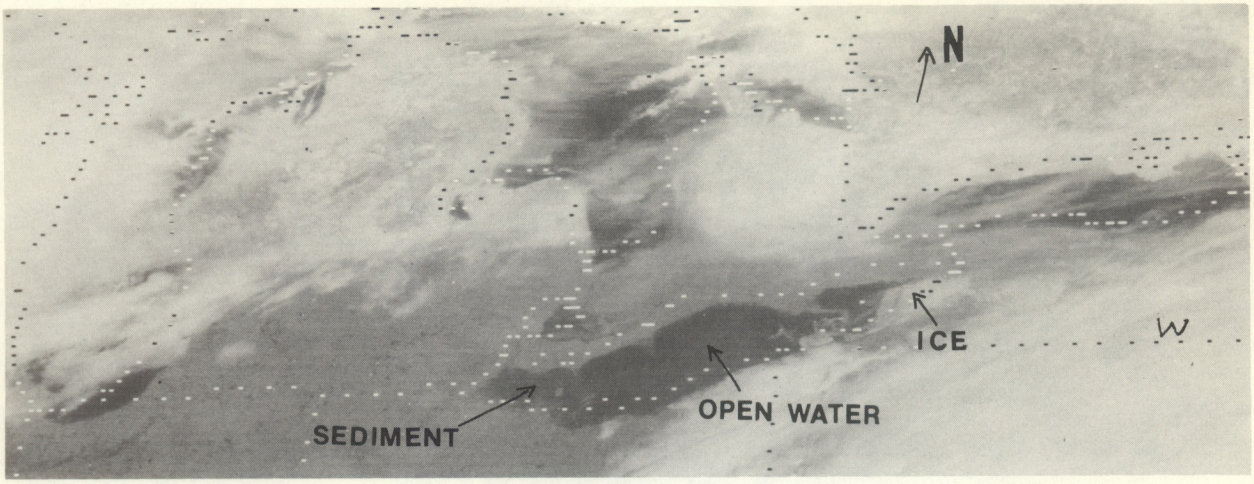

Figure 29A.--GOES image of Lake Erie, 1630 GMT, March 9, 1976.

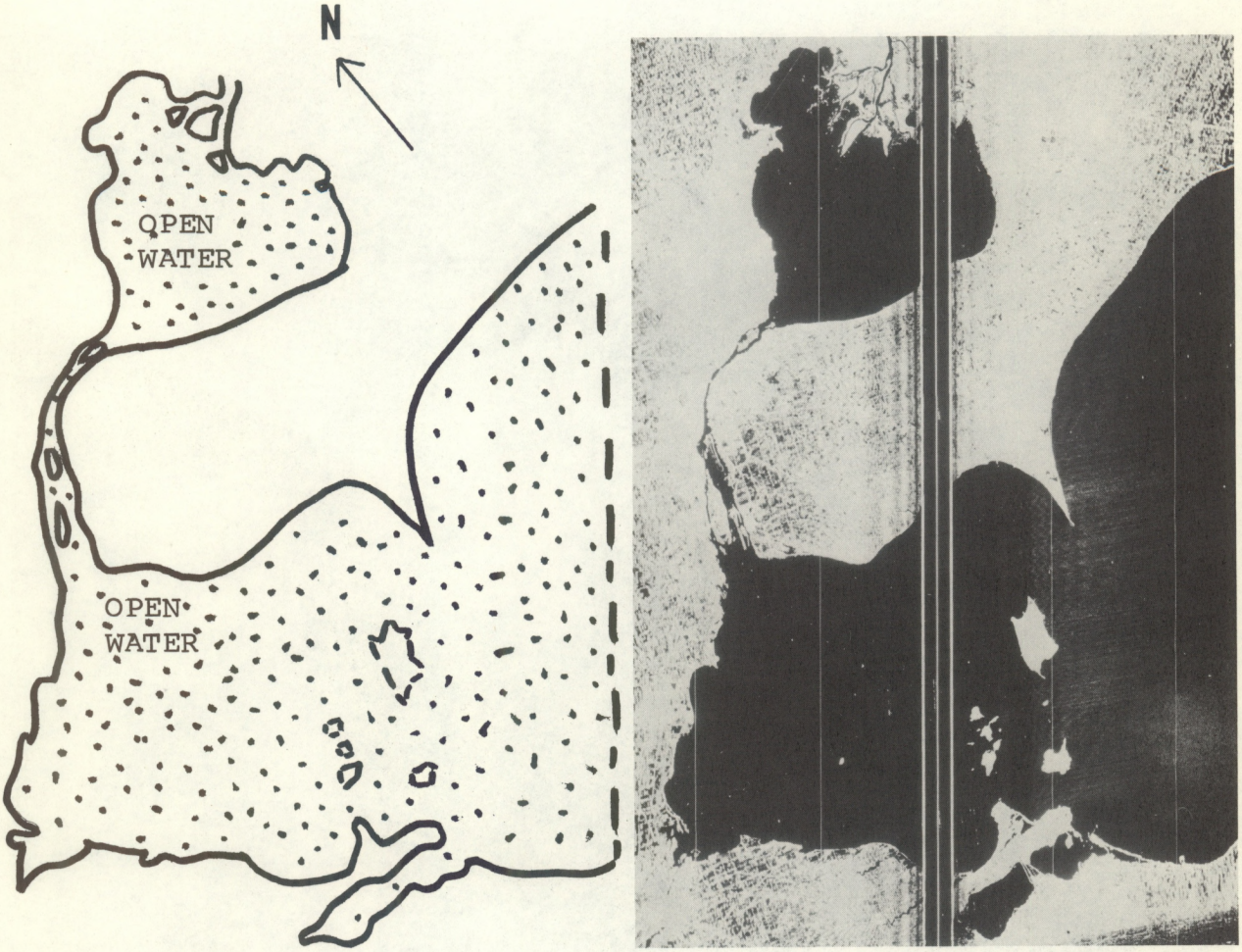

Figure 29B.--SLAR image and interpretation chart of the west end of Lake Erie, March 9, 1976.

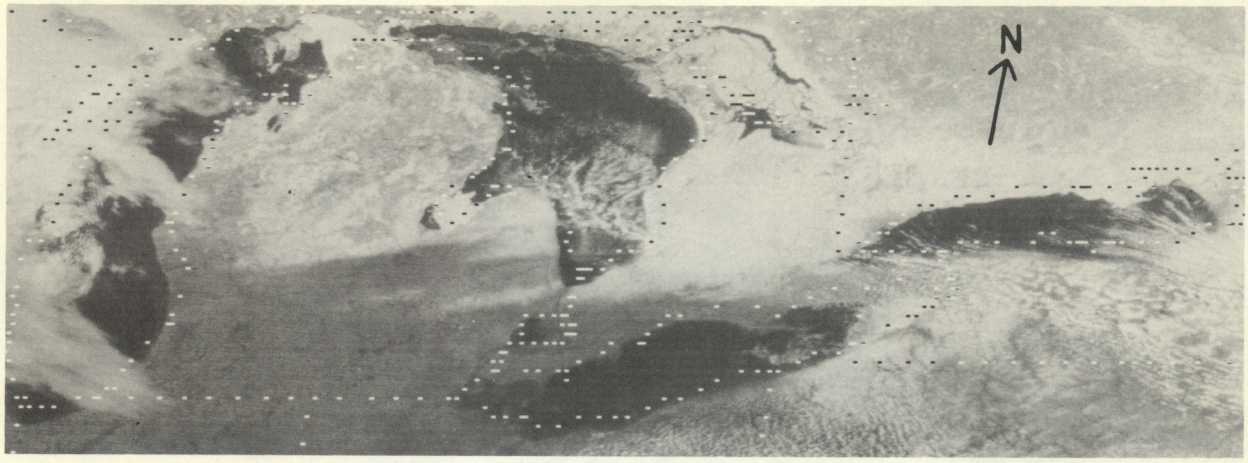

Figure 30A.--GOES image of Lake Erie, 1600 GMT, March 11, 1976.

Figure 30B.--NOAA-4 VHRR (visible) image of Lake Erie, March 11, 1976.

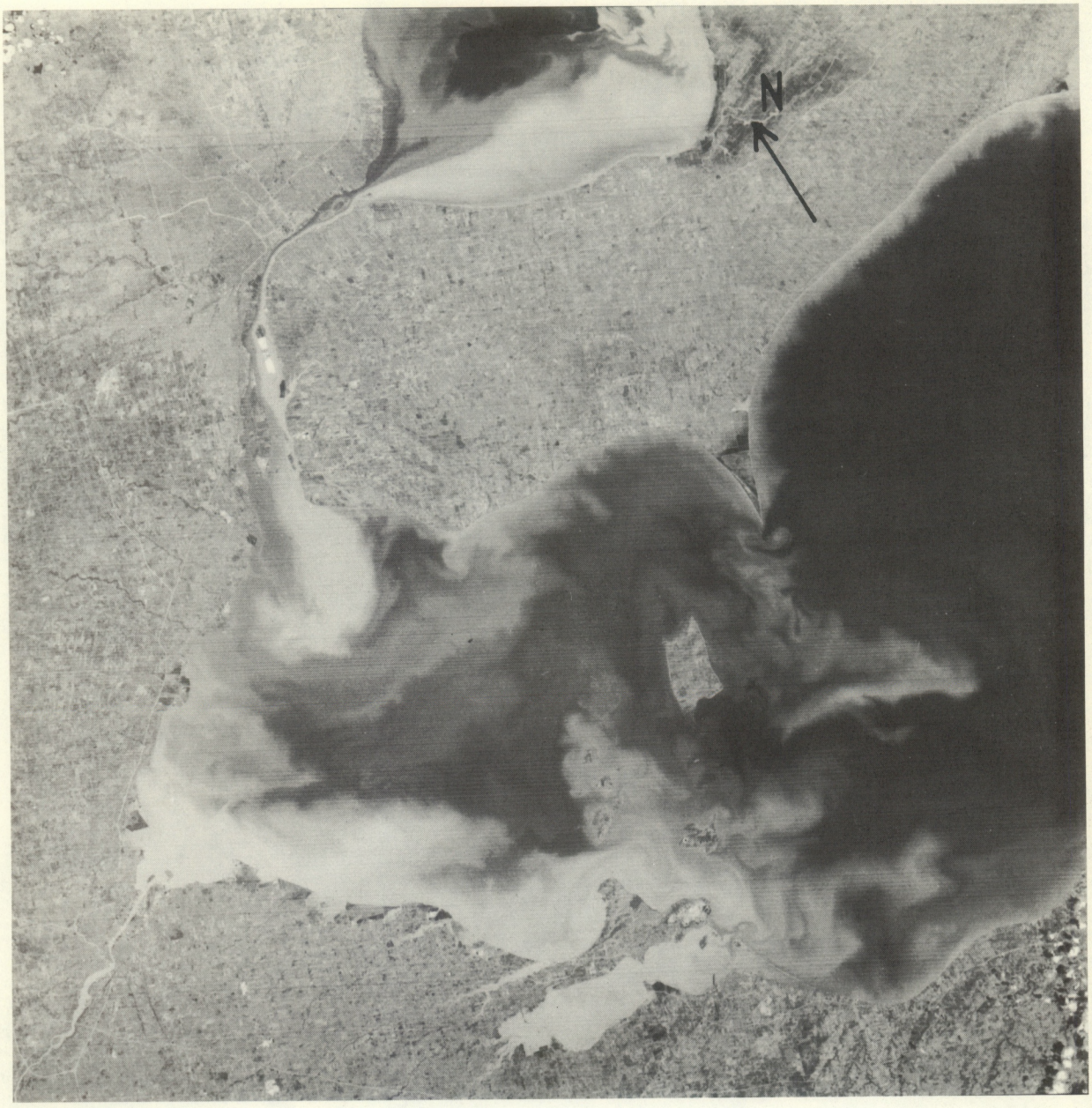

Figure 30C.--Landsat image of the west end of Lake Erie, March 11, 1976.

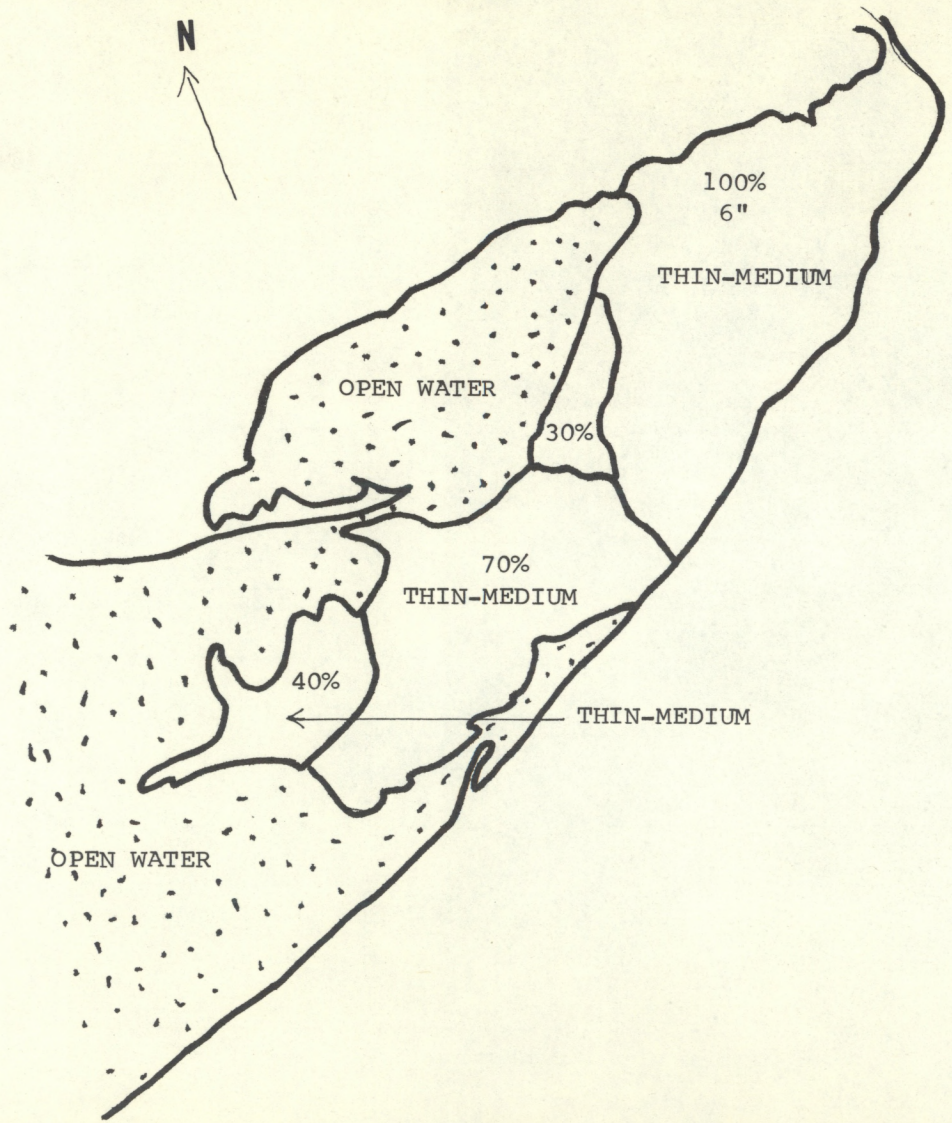

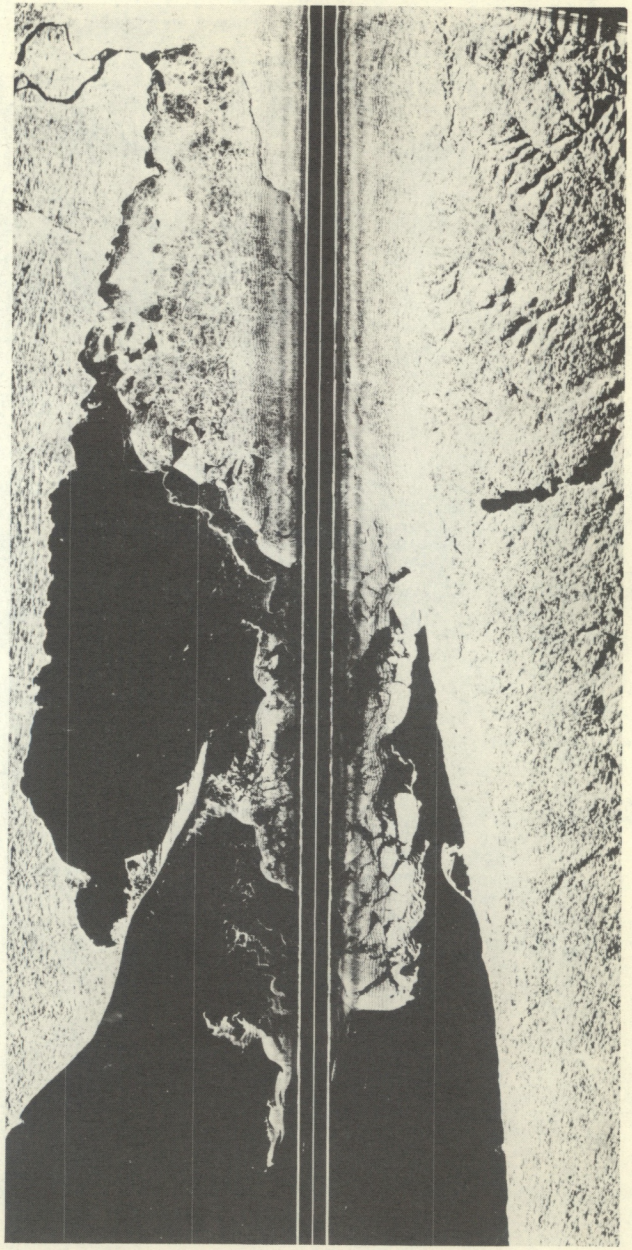

Figure 30D.--SLAR image and interpretation chart of the east end of Lake Erie, March 11, 1976.

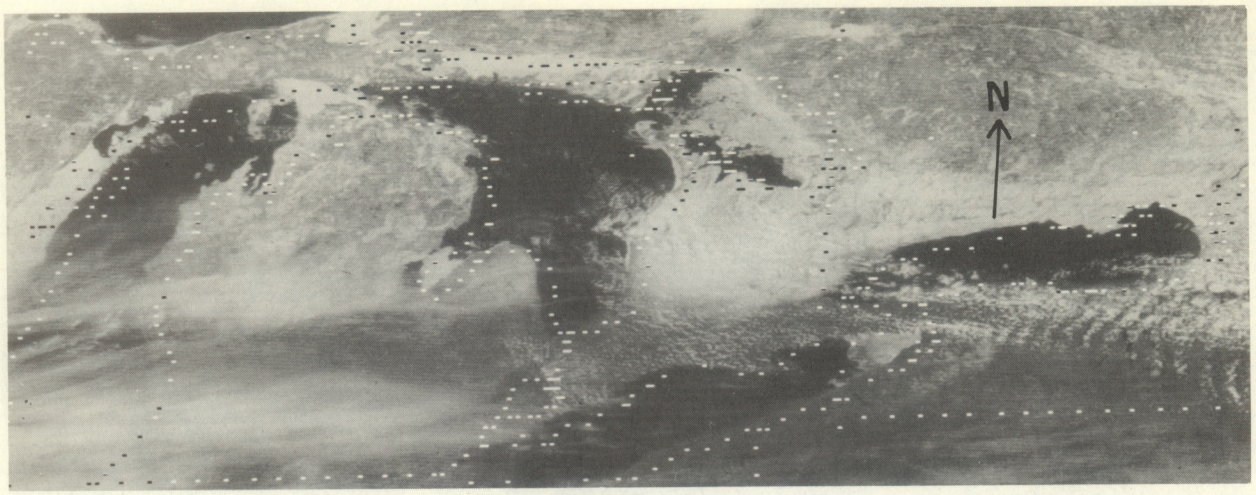

Figure 31A.--GOES image of Lake Erie, 1930 GMT, March 15, 1976.

Figure 31B.--NOAA-4 VHRR (visible) image of Lake Erie, March 15, 1976.

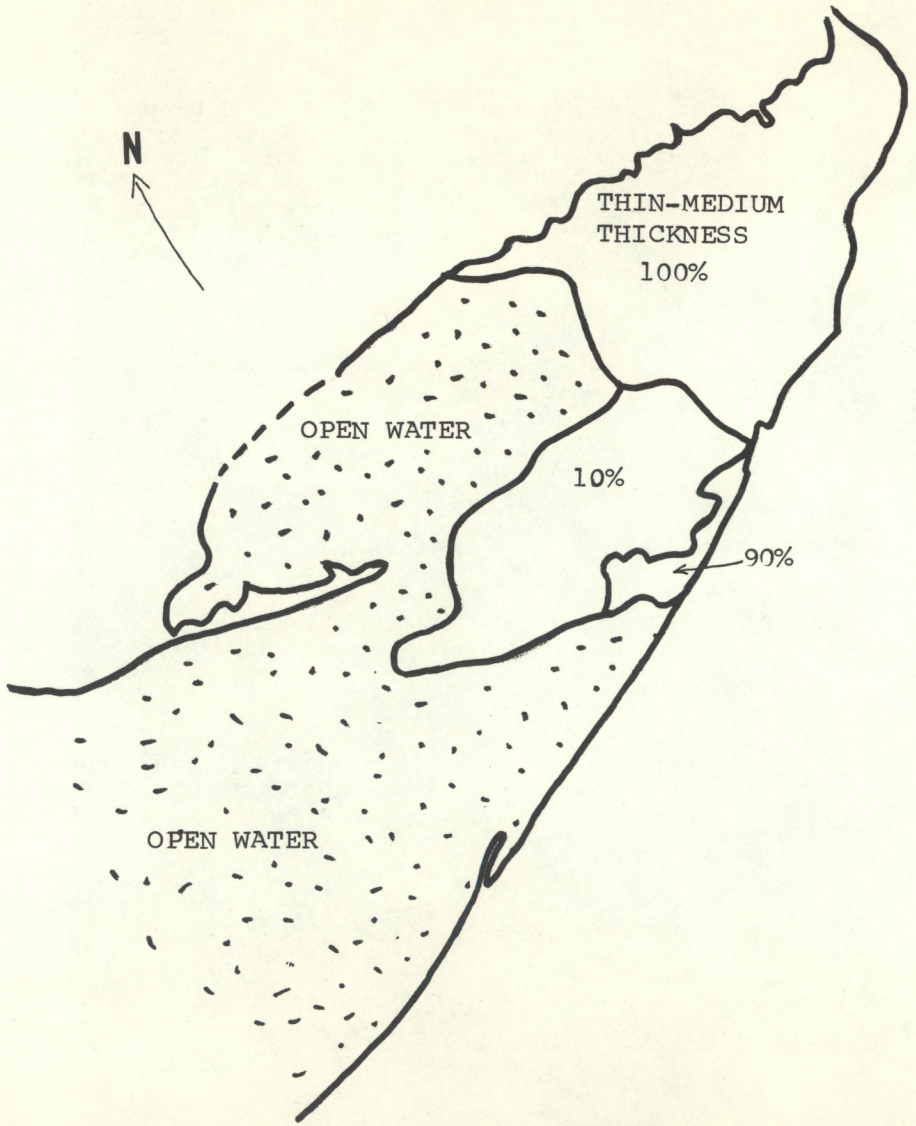

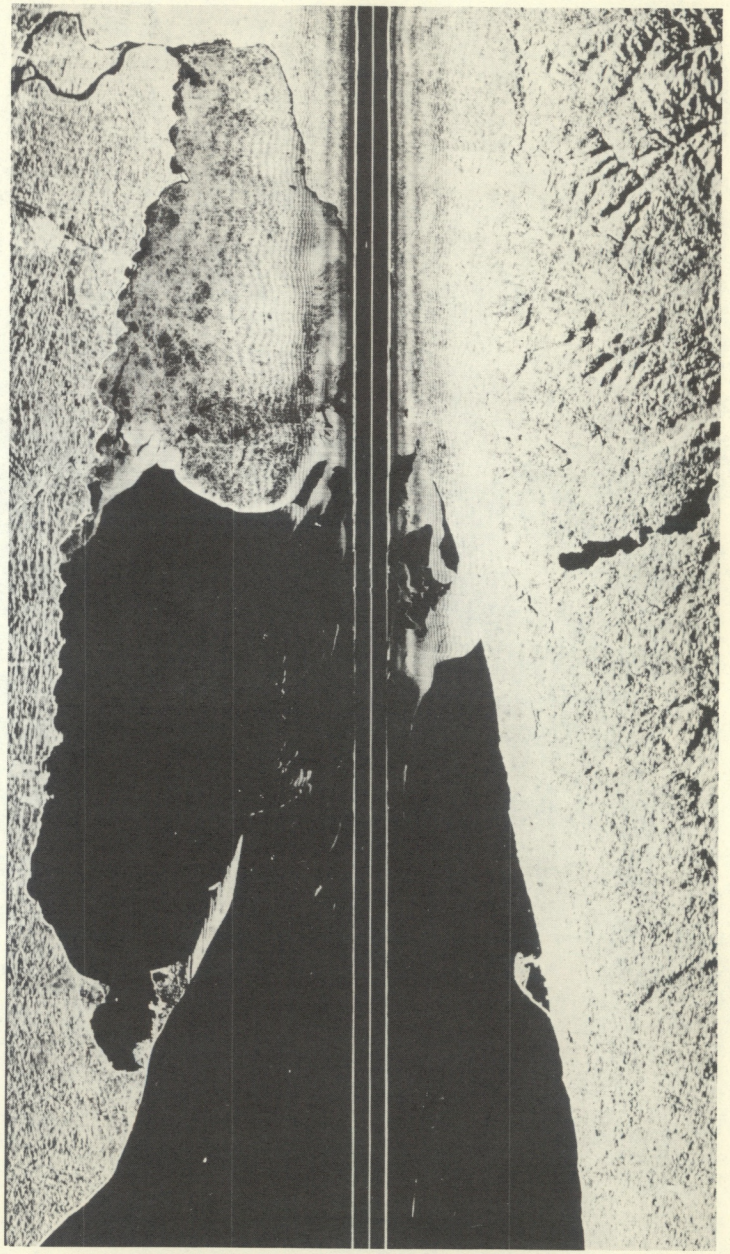

Figure 31C.--SLAR image and interpretation chart of the east end of Lake Erie, March 15, 1976.

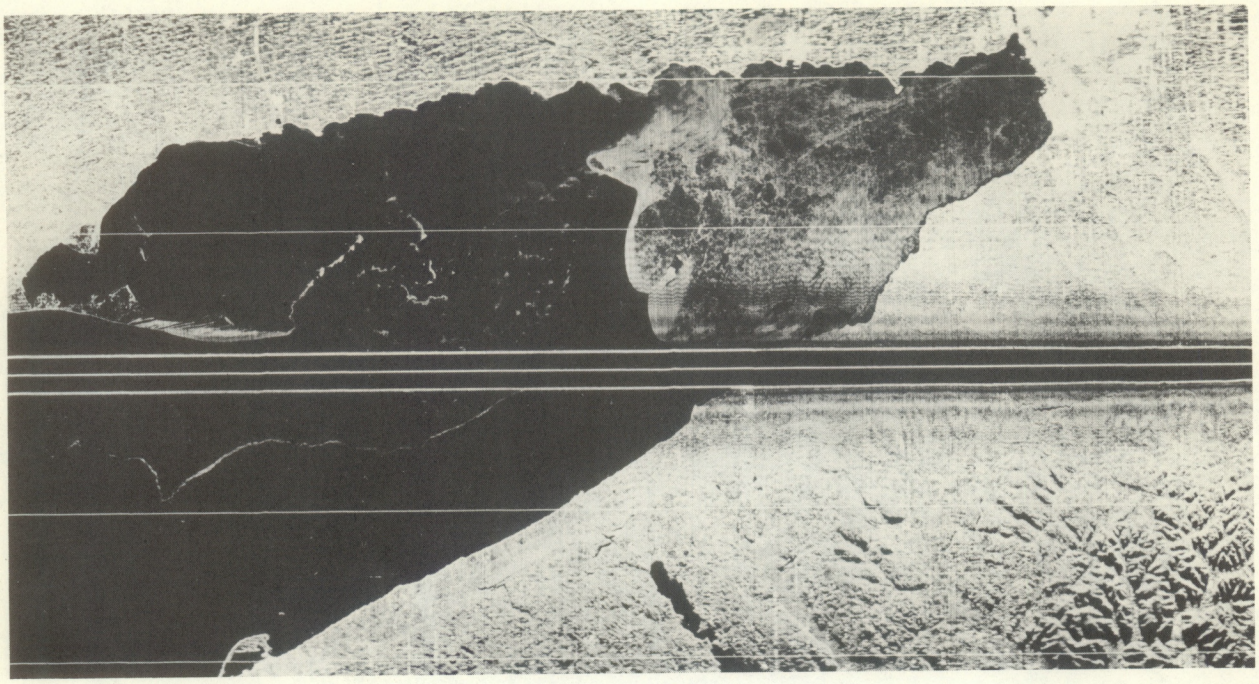

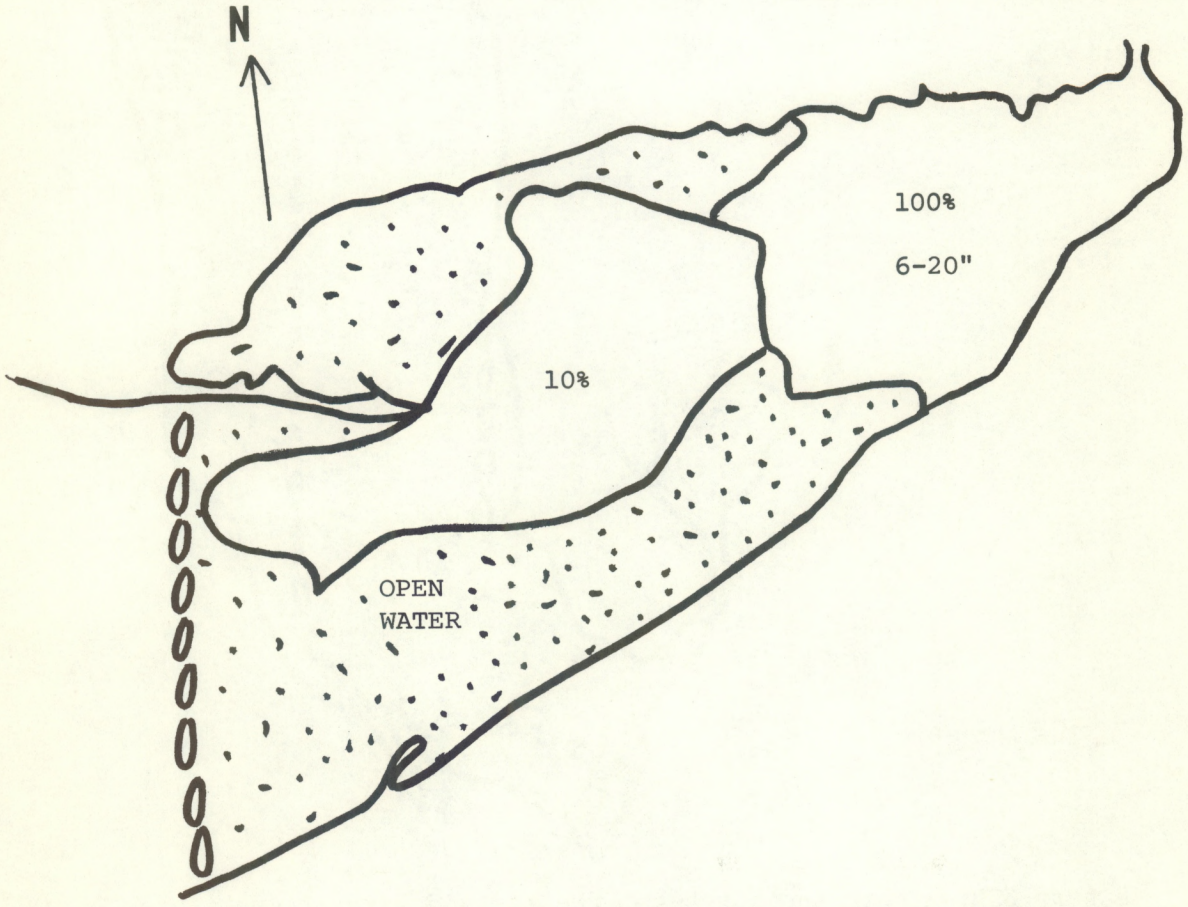

Figure 32A.--SLAR image and interpretation chart of the east end of Lake Erie, March 19, 1976.

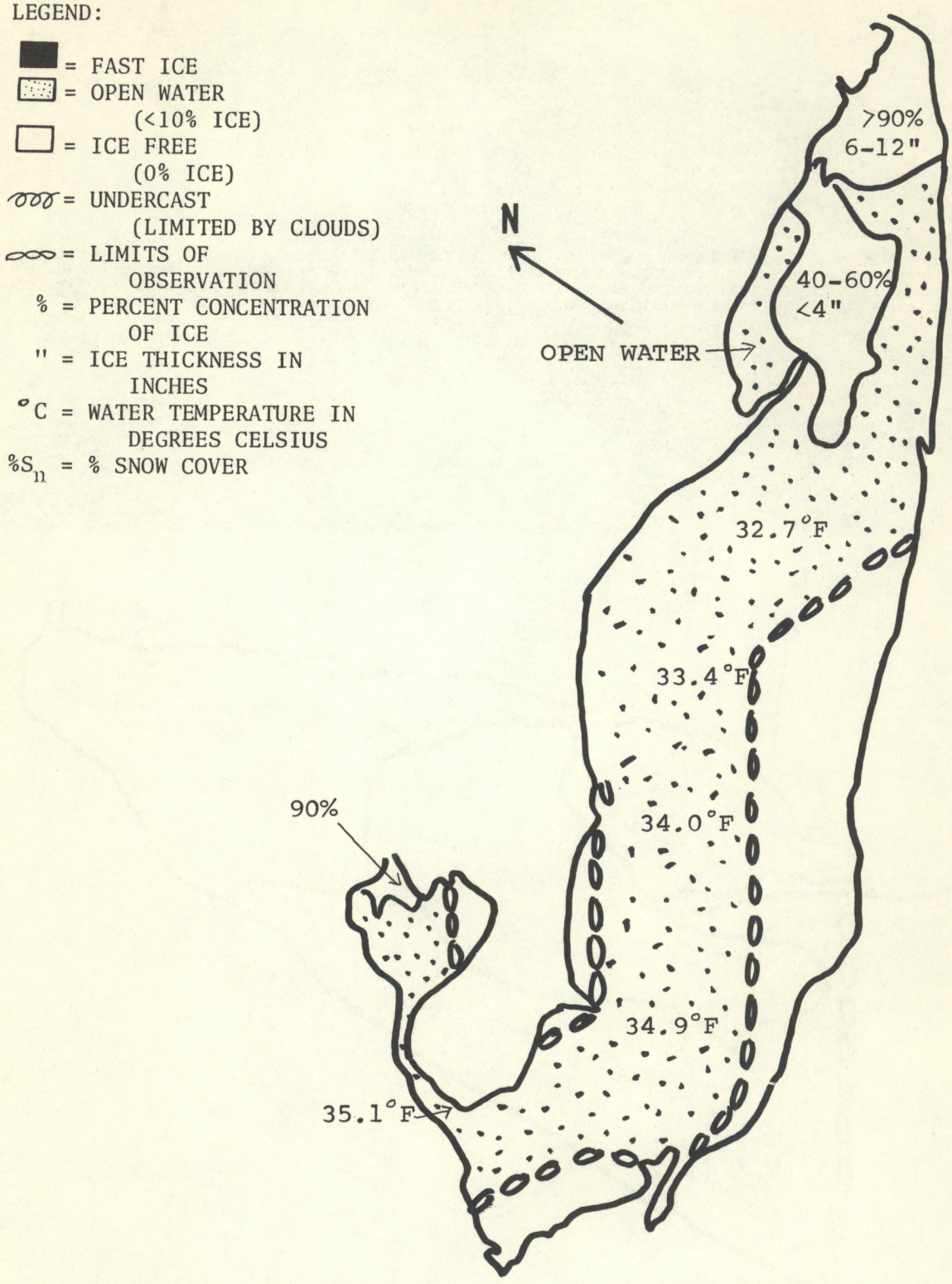

Figure 32B.--Chart showing Lake Erie ice and water temperatures, March 19, 1976. (Data from Atmospheric Environmental Service of Canada.)

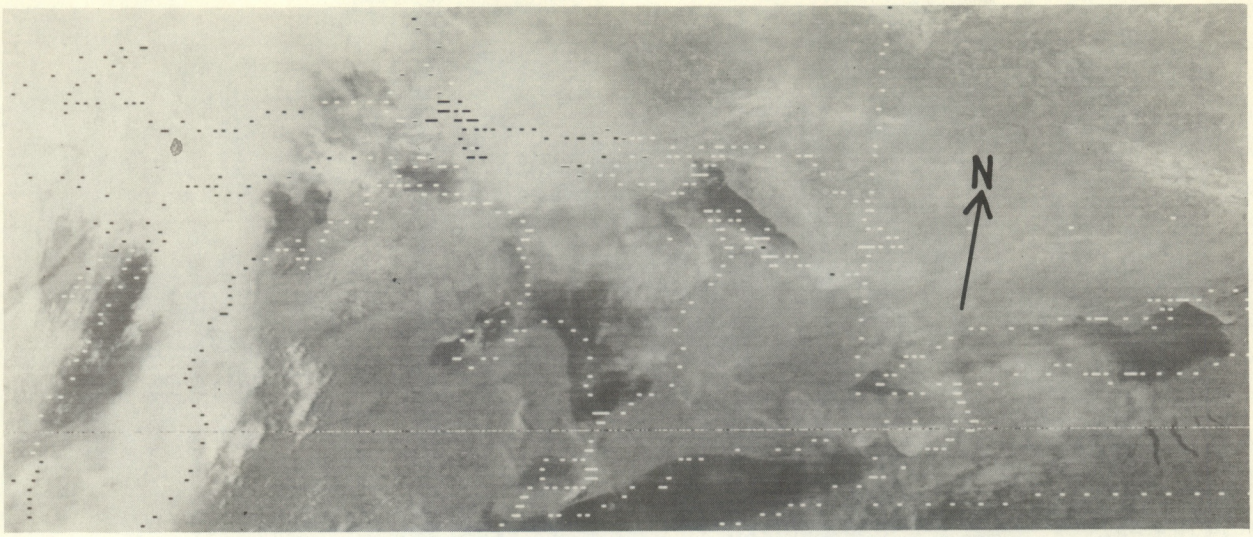

Figure 33A.--GOES image of Lake Erie, 1900 GMT, March 24, 1976.

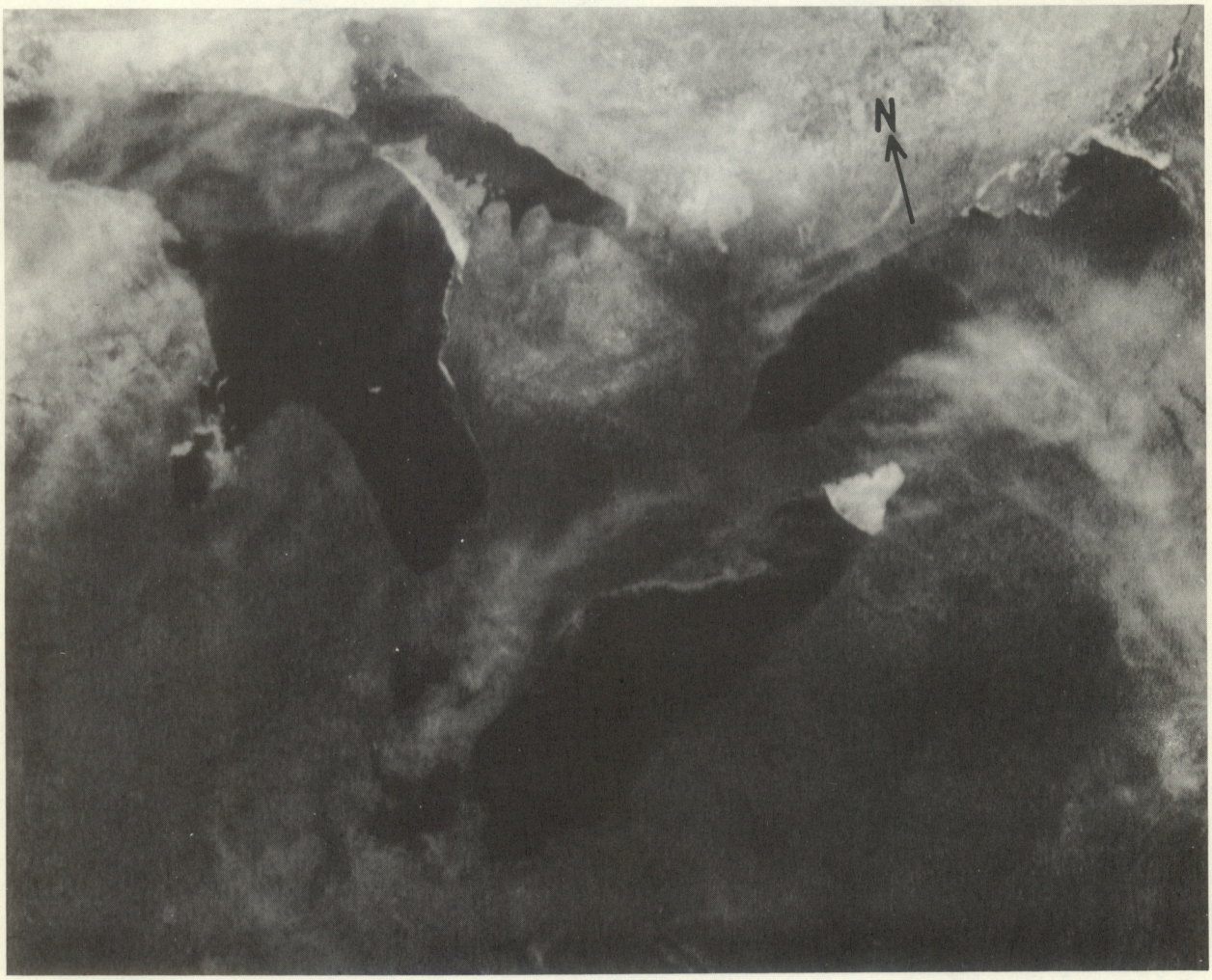

Figure 33B.--NOAA-4 VHRR (visible) image of Lake Erie, March 24, 1976.

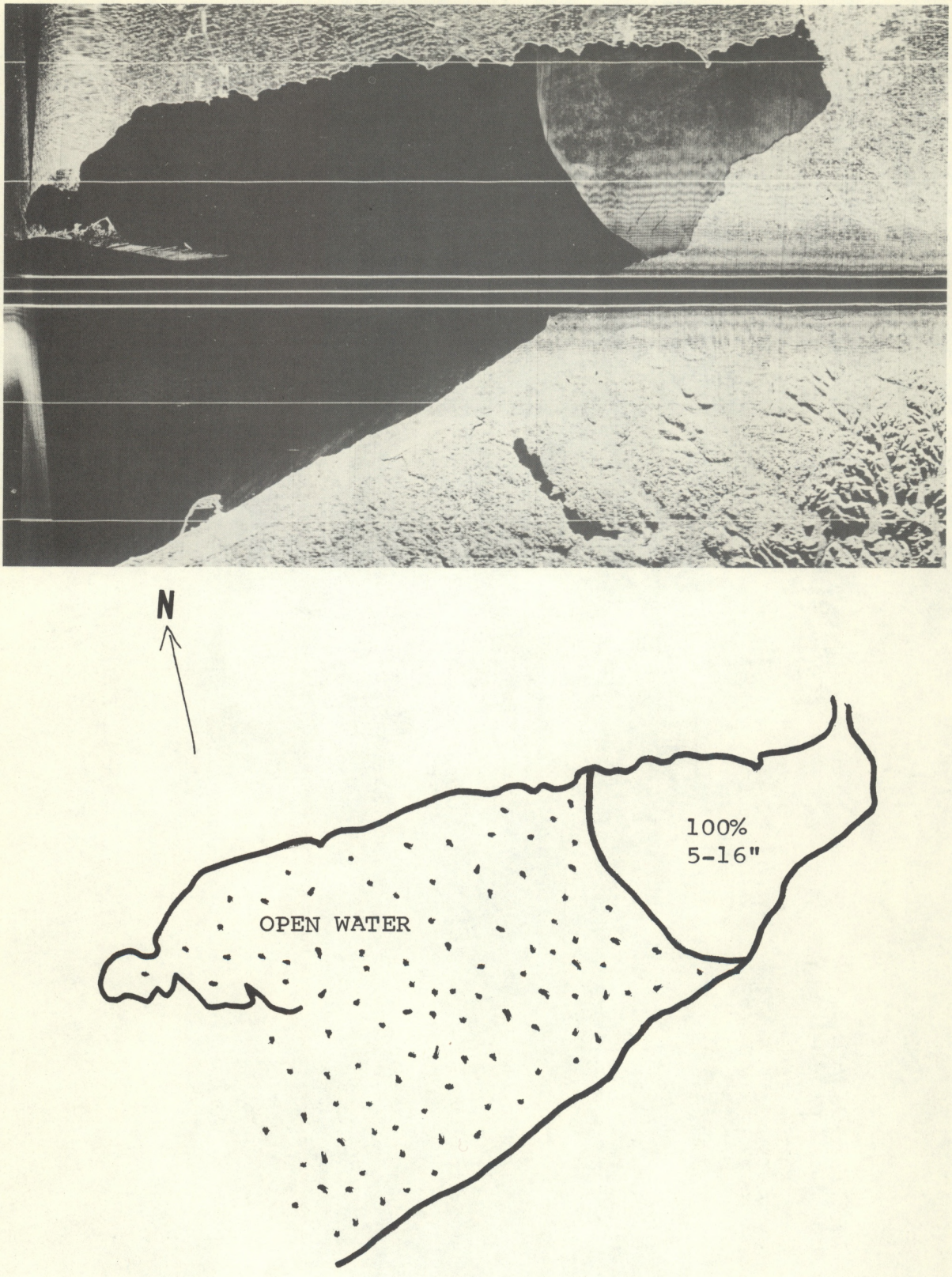

Figure 33C.--SLAR image and interpretation chart of the eastern end of Lake Erie, March 24, 1976.

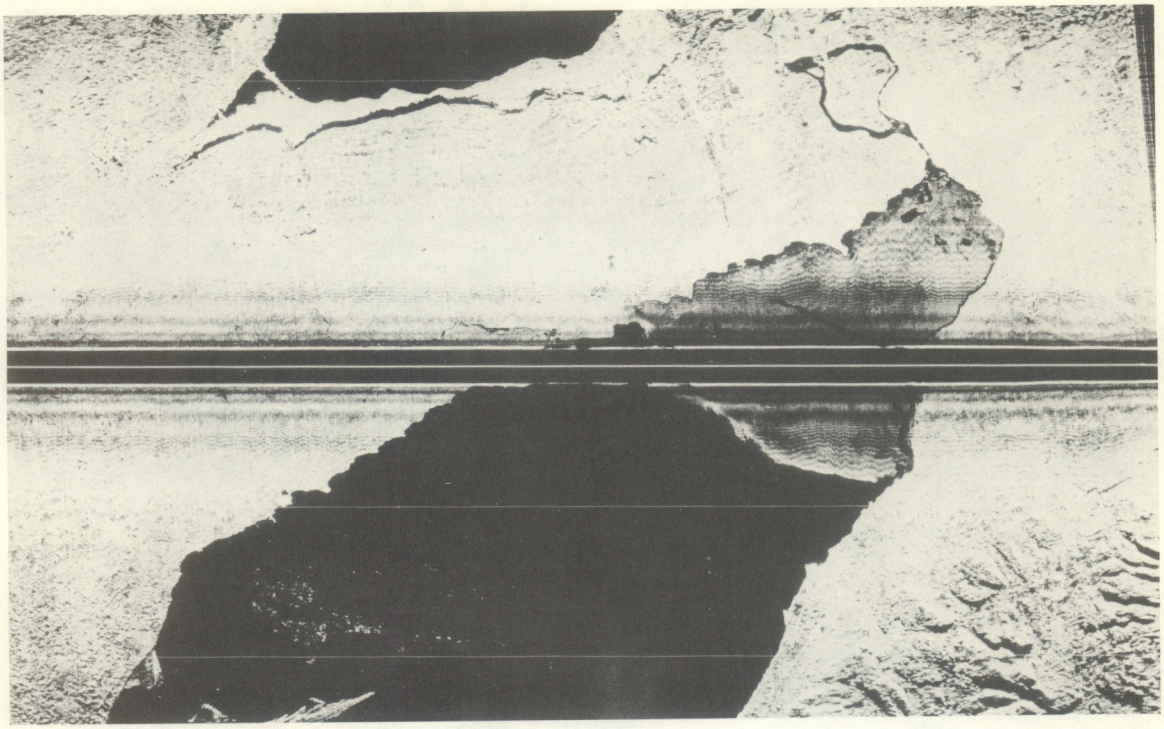

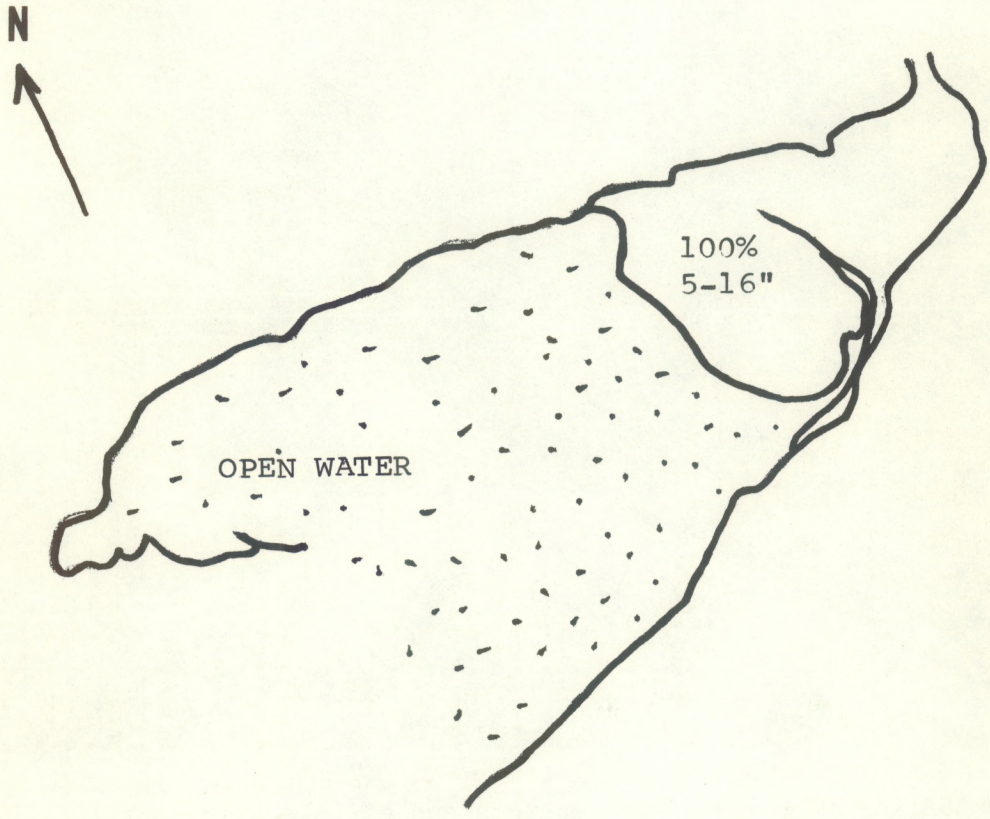

Figure 34.--SLAR image and interpretation chart of the eastern end of Lake Erie, March 26, 1976.

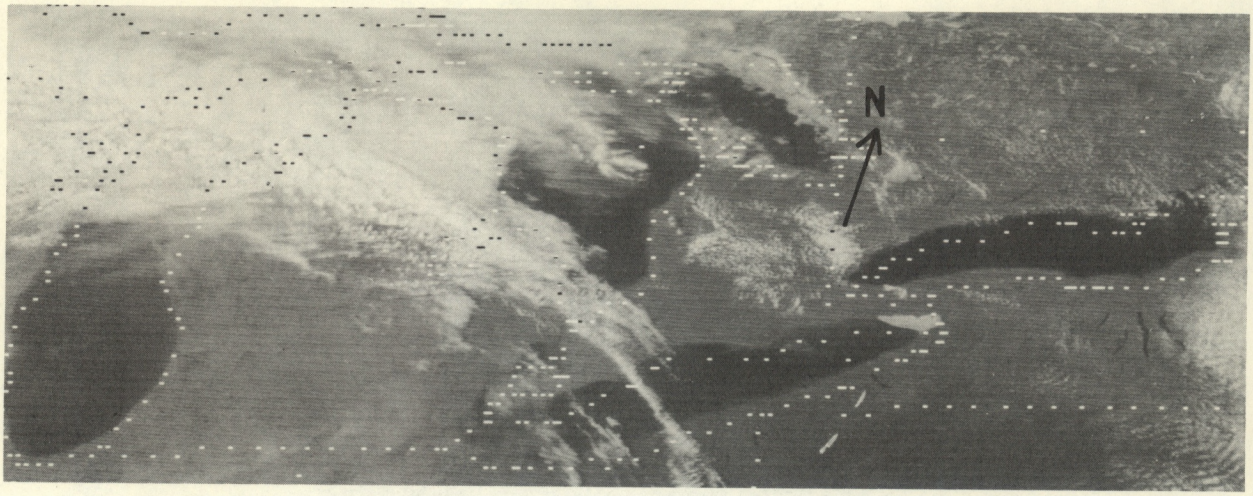

Figure 35A.--GOES image of Lake Erie, 2000 GMT, April 3, 1976.

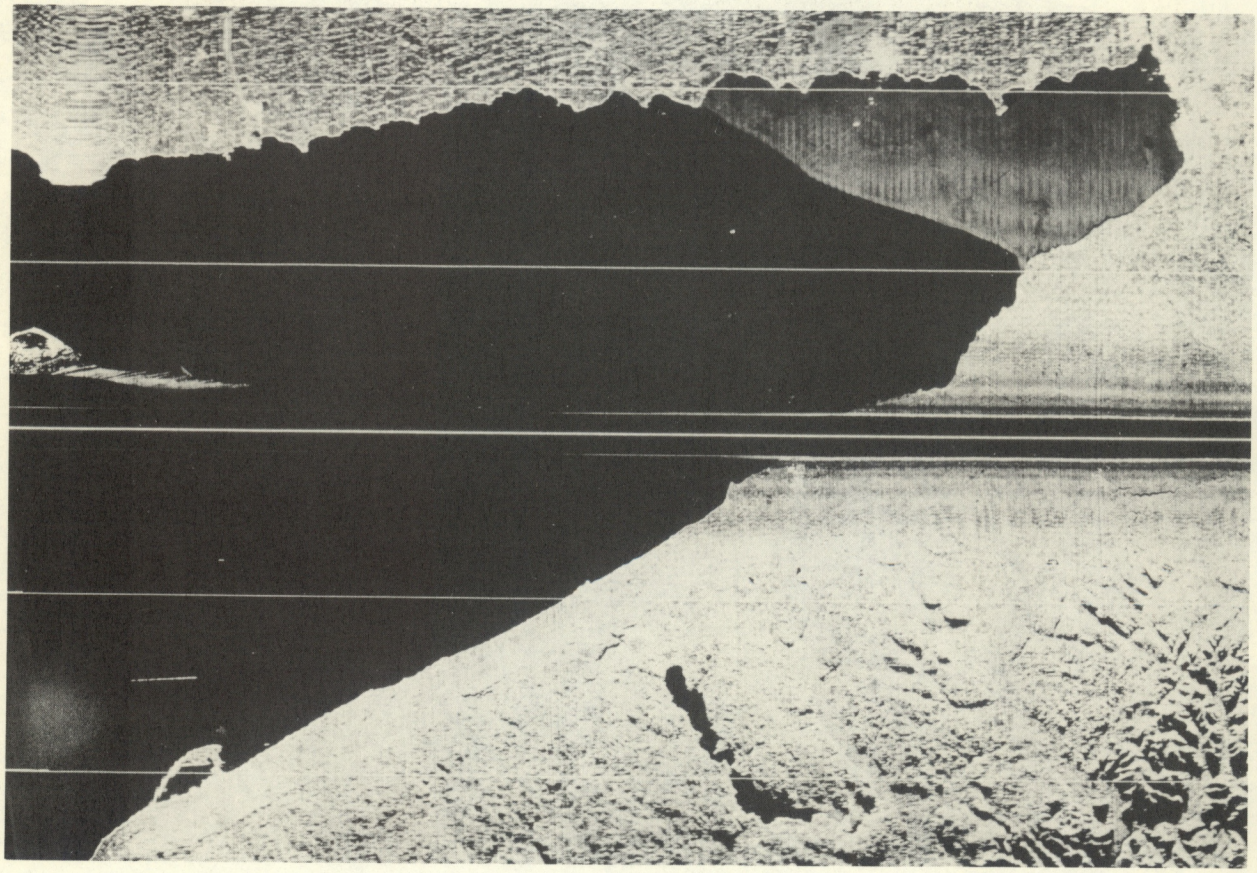

Figure 35B.--SLAR image of the eastern end of Lake Erie, April 3, 1976.

Figure 36A.--NOAA-4 VHRR (visible) image of Lake Erie, April 5, 1976.

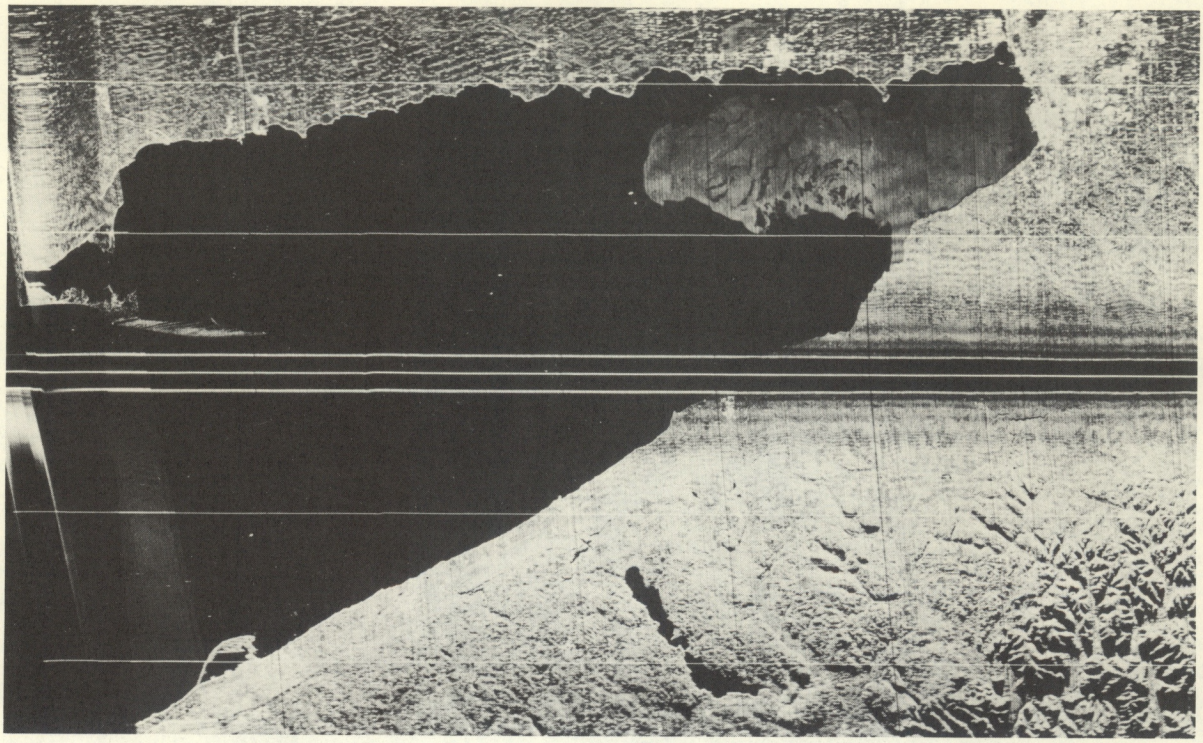

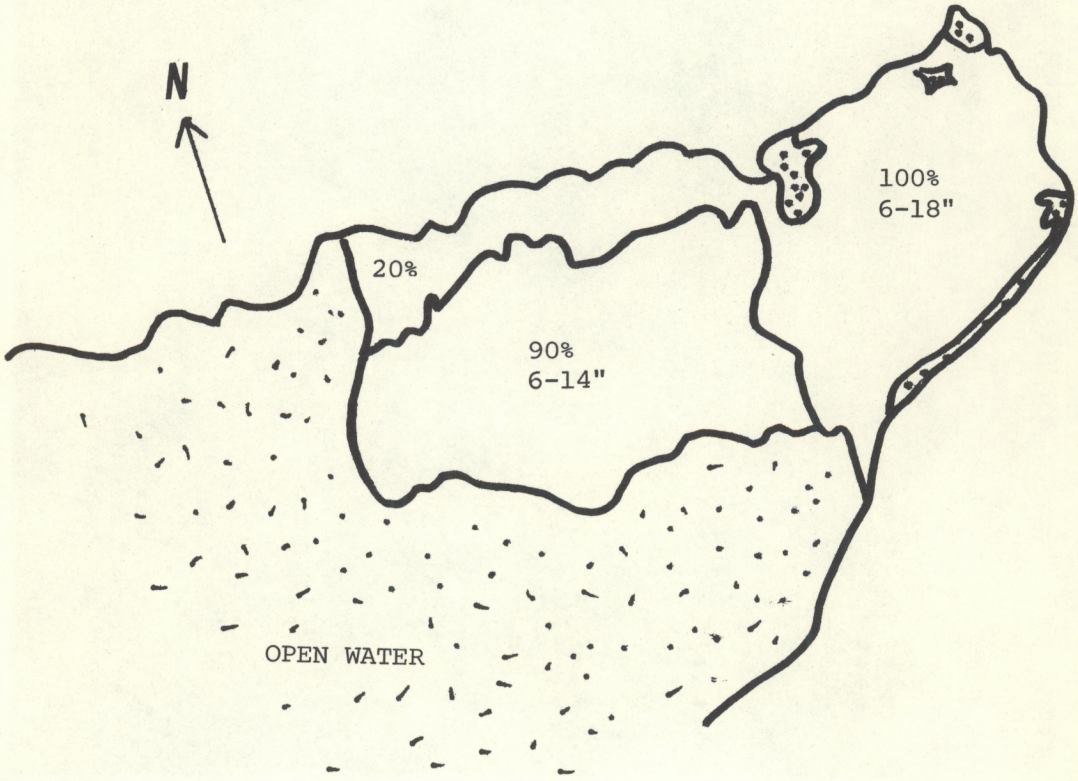

Figure 36B.--SLAR image and interpretation chart of the eastern end of Lake Erie, April 5, 1976.

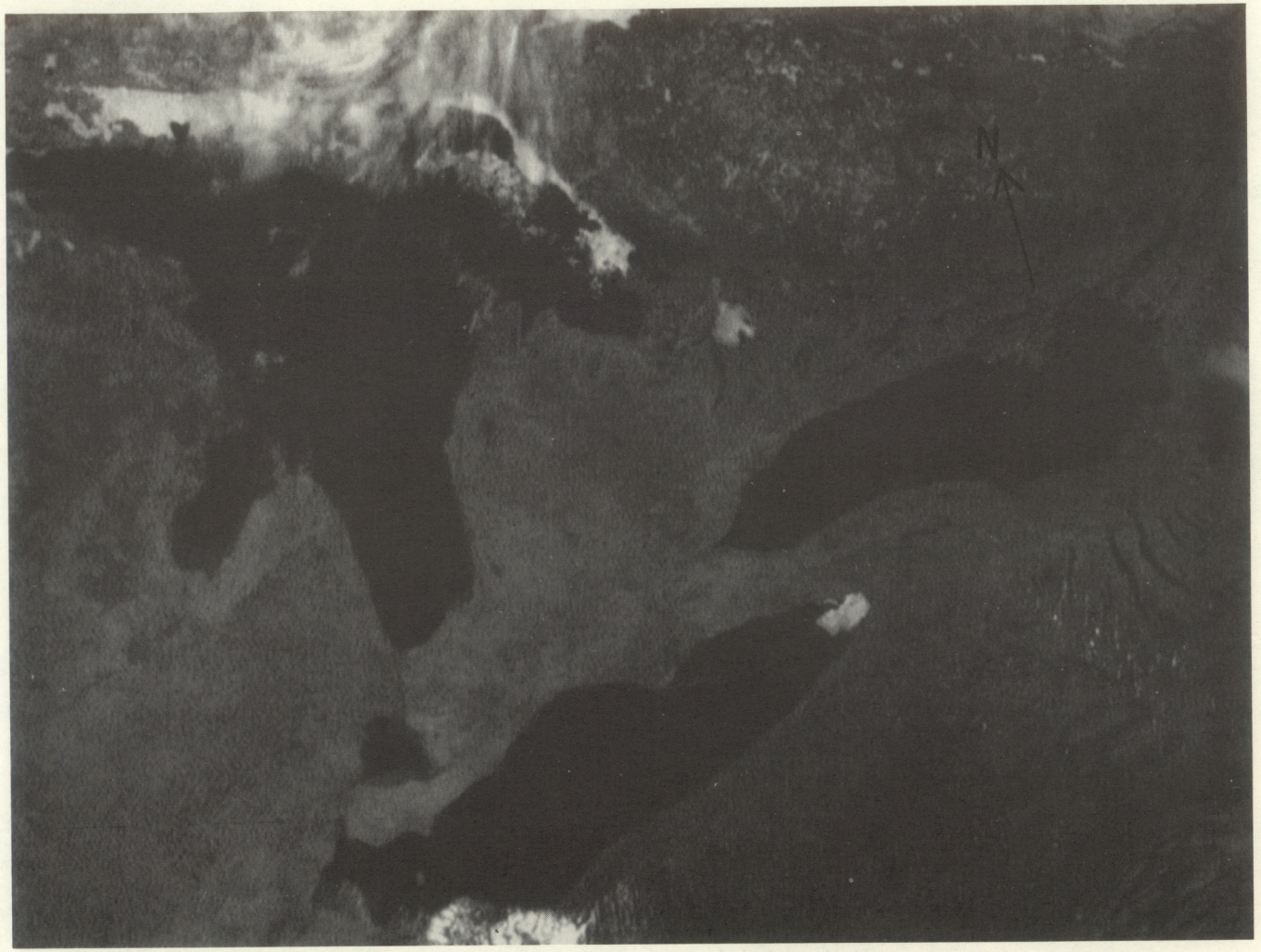

Figure 37A.--NOAA-4 VHRR (visible) image of Lake Erie, April 9, 1976.

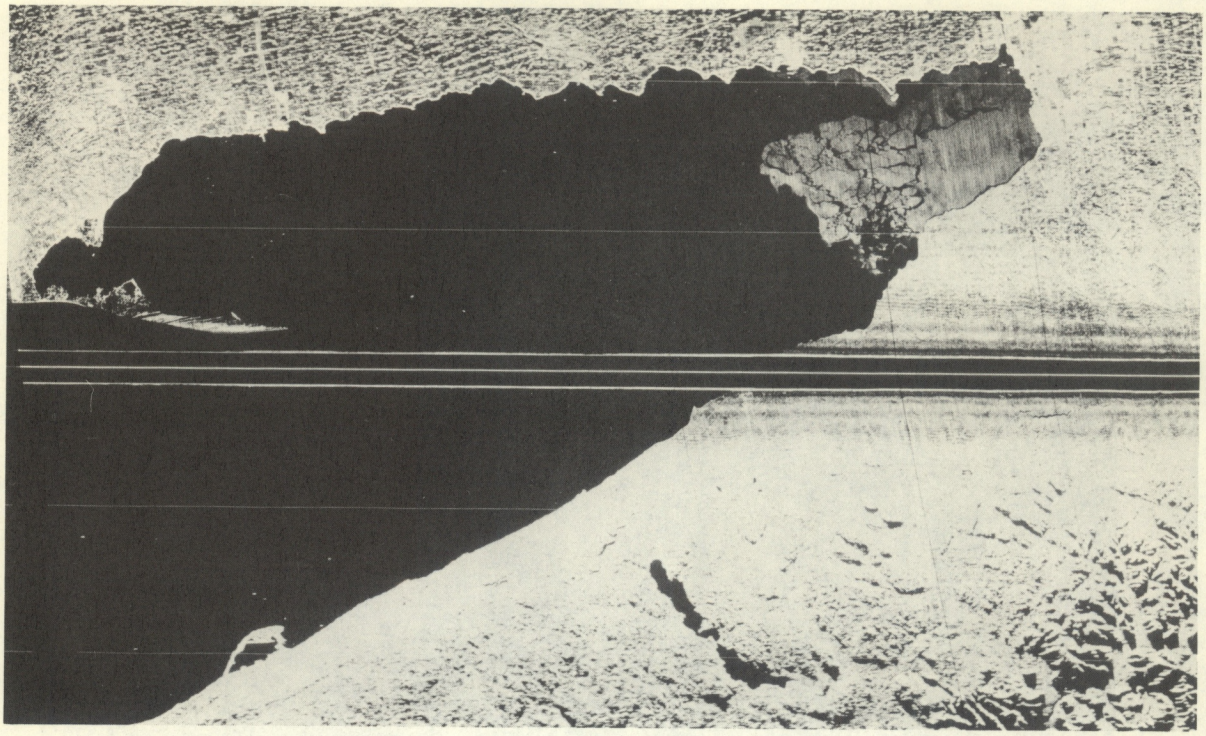

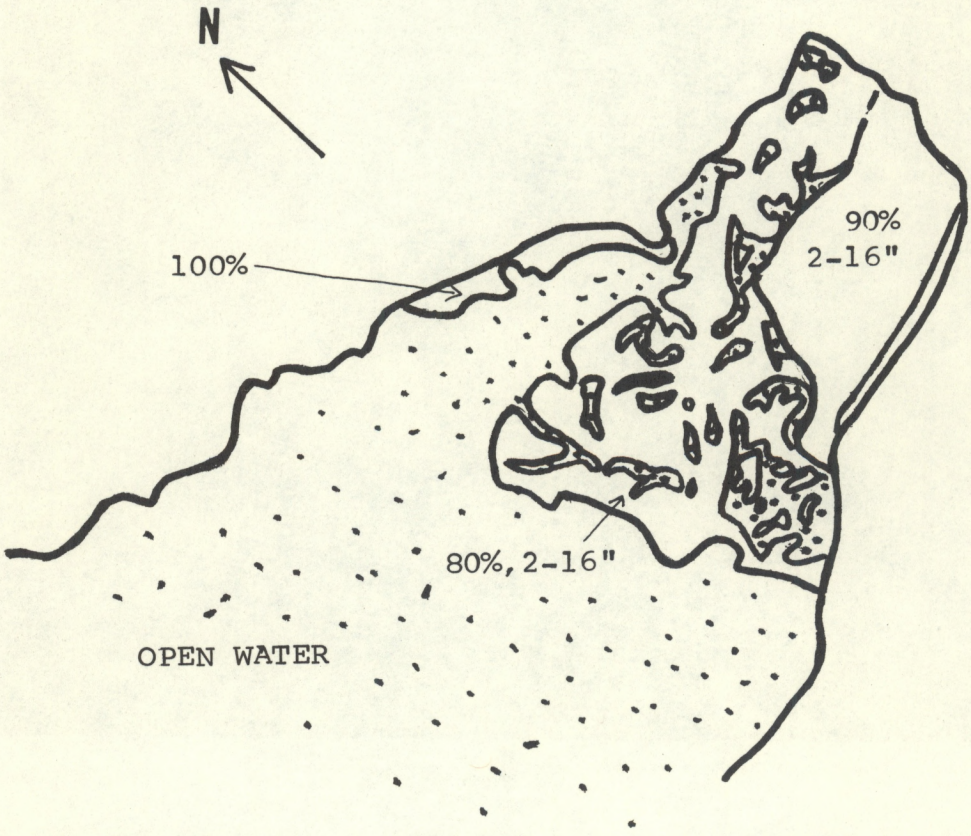

Figure 37B.--SLAR image and interpretation chart of the eastern end of Lake Erie, April 9, 1976.

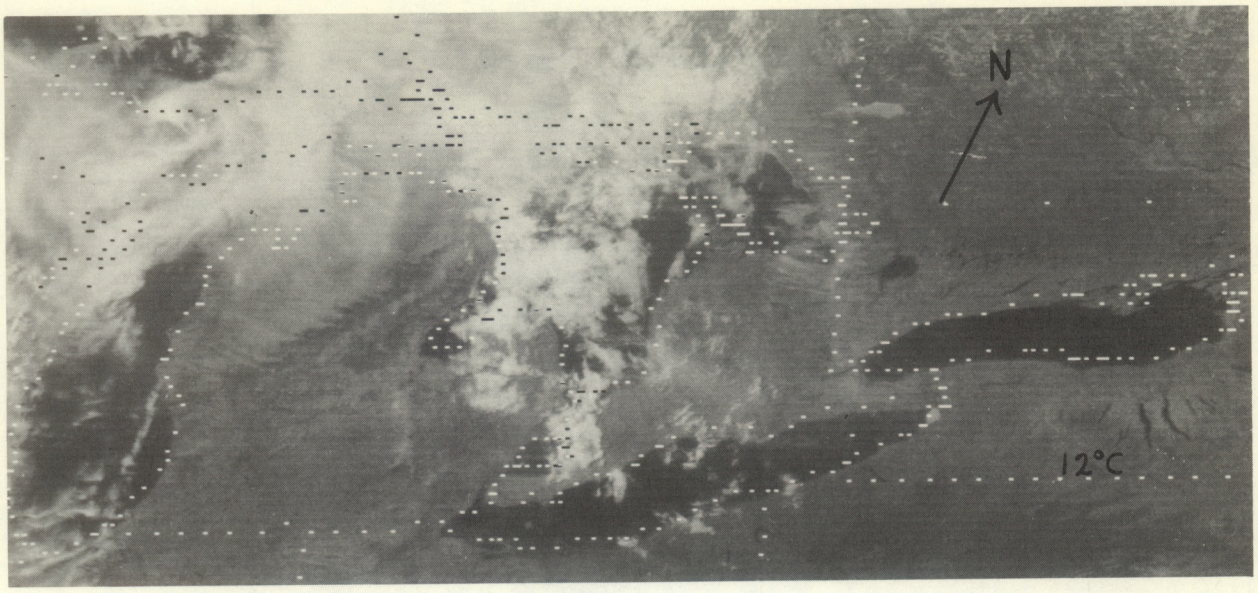

Figure 38.--GOES image of Lake Erie, 1800 GMT, April 14, 1976.

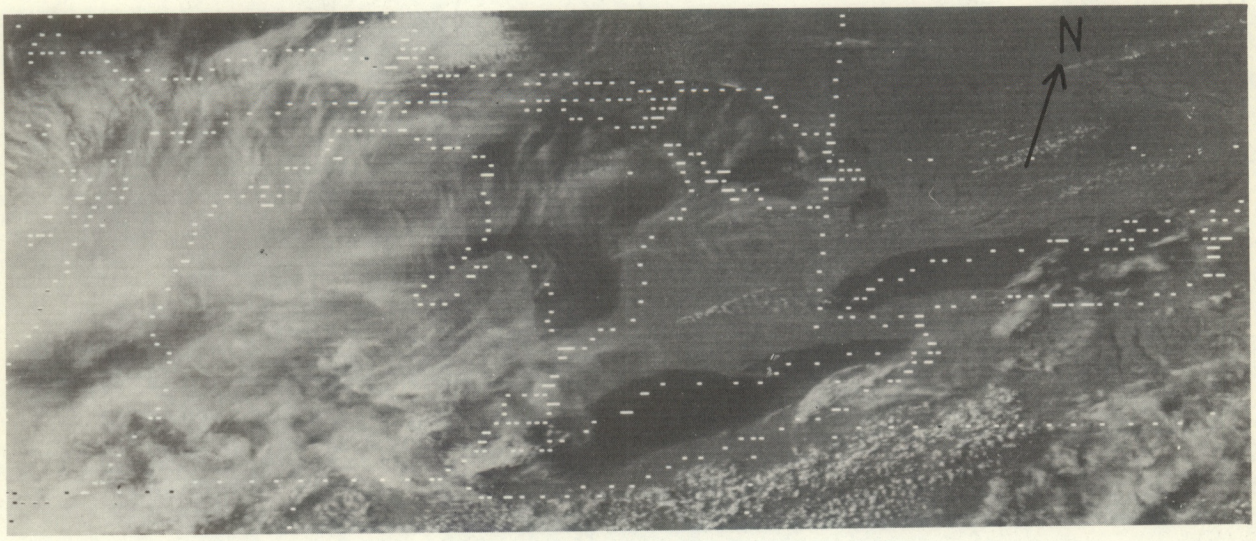

Figure 39.--GOES image of Lake Erie, 2130 GMT, April 19, 1976.

APPENDIX: CLIMATOLOGICAL DATA

MEAN DAILY WEATHER CONDITIONS

Buffalo, N.Y. January 1 - April 19, 1976

Date	$\overline{T}$ (°F)	Surface wind $\overline{dd}$	Surface wind $\overline{ff}$ (mi/h)	Date	$\overline{T}$ (°F)	Surface wind $\overline{dd}$	Surface wind $\overline{ff}$ (mi/h)
1/1	26	N	8	2/10	42	S	17
1/2	26	S	7	2/11	35	W	14
1/3	30	W	14	2/12	35	SW	12
1/4	19	W	17	2/13	37	W	14
1/5	16	W	7	2/14	28	W	6
1/6	23	S	12	2/15	40	S	16
1/7	25	SW	7	2/16	39	SW	2
1/8	12	W	9	2/17	40	SW	12
1/9	12	W	17	2/18	42	S	6
1/10	17	W	10	2/19	36	W	27
1/11	25	S	5	2/20	35	W	11
1/12	22	W	8	2/21	42	S	12
1/13	30	S	6	2/22	33	NW	13
1/14	27	W	22	2/23	19	W	9
1/15	17	W	10	2/24	38	SW	20
1/16	25	SW	10	2/25	48	S	12
1/17	6	N	8	2/26	46	SW	10
1/18	1	W	5	2/27	42	SW	10
1/19	15	S	13	2/28	40	W	11
1/20	31	W	18	2/29	41	S	9
1/21	24	W	12	3/1	31	E	12
1/22	6	NW	13	3/2	27	E	17
1/23	-3	E	5	3/3	32	E	5
1/24	10	NE	9	3/4	47	E	6
1/25	27	E	9	3/5	50	SW	21
1/26	41	S	13	3/6	30	W	18
1/27	28	W	5	3/7	29	W	17
1/28	22	SW	13	3/8	25	W	10
1/29	25	W	13	3/9	30	SE	6
1/30	16	N	4	3/10	36	SW	12
1/31	16	S	9	3/11	28	W	9
2/1	24	SW	14	3/12	34	S	13
2/2	3	W	22	3/13	36	W	20
2/3	16	SW	14	3/14	30	SW	17
2/4	24	W	13	3/15	31	W	9
2/5	19	E	4	3/16	25	N	7
2/6	16	W	7	3/17	16	W	15
2/7	19	W	16	3/18	24	S	8
2/8	25	W	18	3/19	47	SW	16
2/9	23	SW	7	3/20	62	S	16

Note: $\overline{T}$, mean temperature, 24-hr period.
$\overline{dd}$, mean wind direction, 24-hr period.
$\overline{ff}$, mean wind speed, 24-hr period, in miles per hour.

Buffalo, N.Y.--Continued

Date	$\overline{T}$ (°F)	Surface wind $\overline{dd}$	$\overline{ff}$ (mi/h)	Date	$\overline{T}$ (°F)	Surface wind $\overline{dd}$	$\overline{ff}$ (mi/h)
3/21	44	W	16	4/5	37	SW	15
3/22	23	W	5	4/6	43	SW	10
3/23	34	SW	11	4/7	40	NW	9
3/24	53	S	13	4/8	36	N	10
3/25	47	SW	14	4/9	37	W	4
3/26	51	S	8	4/10	42	SW	18
3/27	53	S	17	4/11	35	NW	16
3/28	37	W	12	4/12	30	W	11
3/29	43	E	11	4/13	42	SW	16
3/30	59	SE	10	4/14	49	SW	12
3/31	48	SW	9	4/15	61	SW	13
4/1	42	SW	14	4/16	62	SW	13
4/2	41	W	9	4/17	69	SW	10
4/3	41	W	8	4/18	68	S	7
4/4	40	N	11	4/19	63	SW	11

Erie, Pa. January 1 - April 19, 1976

Date	$\overline{T}$ (°F)	Surface wind $\overline{dd}$	$\overline{ff}$ (mi/h)	Date	$\overline{T}$ (°F)	Surface wind $\overline{dd}$	$\overline{ff}$ (mi/h)
1/1	28	NE	13	1/23	6	E	6
1/2	29	S	11	1/24	19	NE	4
1/3	28	W	15	1/25	29	SE	9
1/4	18	W	18	1/26	38	S	13
1/5	13	W	10	1/27	24	W	9
1/6	23	S	18	1/28	23	SW	14
1/7	27	W	6	1/29	25	W	12
1/8	14	W	5	1/30	20	E	5
1/9	5	S	22	1/31	18	S	10
1/10	13	S	14	2/1	20	W	11
1/11	26	S	12	2/2	3	W	20
1/12	25	W	13	2/3	16	S	12
1/13	31	S	16	2/4	24	W	11
1/14	27	W	20	2/5	20	E	9
1/15	22	W	13	2/6	17	NW	7
1/16	25	W	11	2/7	19	SW	16
1/17	12	N	14	2/8	24	W	14
1/18	7	NW	3	2/9	17	S	11
1/19	18	S	21	2/10	41	S	24
1/20	28	SW	14	2/11	36	W	16
1/21	20	W	16	2/12	35	S	18
1/22	13	NW	13	2/13	37	W	9

Date	$\overline{T}$ (°F)	Surface wind $\overline{dd}$	$\overline{ff}$ (mi/h)	Date	$\overline{T}$ (°F)	Surface wind $\overline{dd}$	$\overline{ff}$ (mi/h)
2/14	26	N	3	3/18	33	S	15
2/15	44	S	19	3/19	55	S	21
2/16	43	S	3	3/20	63	S	21
2/17	41	W	7	3/21	44	W	16
2/18	43	S	10	3/22	25	W	9
2/19	34	W	16	3/23	34	SW	10
2/20	35	W	6	3/24	54	S	18
2/21	44	S	15	3/25	47	SW	14
2/22	34	W	13	3/26	52	S	14
2/23	21	W	4	3/27	51	S	17
2/24	42	S	19	3/28	34	NW	8
2/25	56	S	17	3/29	44	SE	8
2/26	49	SW	11	3/30	59	S	18
2/27	45	W	7	3/31	43	W	6
2/28	42	W	8	4/1	38	SW	12
2/29	46	S	12	4/2	37	W	11
3/1	34	NE	14	4/3	43	N	2
3/2	30	NE	11	4/4	38	N	12
3/3	44	N	4	4/5	36	W	11
3/4	50	E	5	4/6	43	W	9
3/5	48	SW	19	4/7	38	N	4
3/6	30	W	17	4/8	33	N	8
3/7	31	W	19	4/9	31	N	4
3/8	26	W	8	4/10	41	SW	11
3/9	29	SE	9	4/11	39	N	14
3/10	36	S	11	4/12	32	NW	8
3/11	29	N	5	4/13	40	SW	10
3/12	37	S	20	4/14	51	SW	5
3/13	36	W	18	4/15	68	S	13
3/14	34	SW	18	4/16	67	W	10
3/15	32	NW	7	4/17	68	W	5
3/16	27	N	10	4/18	67	W	4
3/17	20	W	20	4/19	64	SW	8

Cleveland, Ohio January 1 - April 19, 1976

Date	$\overline{T}$ (°F)	Surface wind $\overline{dd}$	$\overline{ff}$ (mi/h)	Date	$\overline{T}$ (°F)	Surface wind $\overline{dd}$	$\overline{ff}$ (mi/h)
1/1	33	E	11	1/5	13	SW	10
1/2	35	S	11	1/6	24	S	16
1/3	27	W	16	1/7	28	W	2
1/4	14	W	18	1/8	10	NW	10

Date	$\overline{T}$ (°F)	Surface wind $\overline{dd}$	$\overline{ff}$ (mi/h)	Date	$\overline{T}$ (°F)	Surface wind $\overline{dd}$	$\overline{ff}$ (mi/h)
1/9	4	SW	17	2/24	48	SW	17
1/10	11	S	10	2/25	59	SW	14
1/11	28	SW	12	2/26	53	SW	11
1/12	25	W	13	2/27	50	SW	12
1/13	34	S	8	2/28	47	NW	5
1/14	26	W	17	2/29	56	SW	8
1/15	22	SW	10	3/1	41	NE	9
1/16	25	W	7	3/2	48	N	5
1/17	13	N	12	3/3	58	SW	7
1/18	7	W	4	3/4	57	S	3
1/19	18	S	18	3/5	53	W	21
1/20	24	W	14	3/6	36	W	16
1/21	19	W	10	3/7	36	W	16
1/22	15	N	10	3/8	30	N	6
1/23	14	SE	9	3/9	36	E	5
1/24	21	N	2	3/10	42	SW	8
1/25	29	SE	10	3/11	37	N	7
1/26	39	W	7	3/12	48	S	16
1/27	24	N	9	3/13	41	W	18
1/28	25	SW	13	3/14	38	SW	14
1/29	28	W	8	3/15	36	N	6
1/30	24	E	5	3/16	30	N	11
1/31	20	SW	9	3/17	23	W	13
2/1	16	W	8	3/18	36	S	14
2/2	5	W	12	3/19	58	SW	18
2/3	13	S	12	3/20	64	S	19
2/4	26	W	7	3/21	45	W	15
2/5	21	E	12	3/22	30	N	6
2/6	15	NW	9	3/23	43	SW	10
2/7	14	W	19	3/24	58	S	17
2/8	27	W	14	3/25	56	W	11
2/9	23	S	9	3/26	61	S	15
2/10	45	S	20	3/27	54	SW	17
2/11	37	W	17	3/28	42	N	6
2/12	37	S	15	3/29	50	S	10
2/13	37	NW	4	3/30	68	S	13
2/14	29	E	3	3/31	49	W	9
2/15	47	SW	17	4/1	42	W	13
2/16	46	SW	4	4/2	39	W	8
2/17	45	NW	7	4/3	50	S	4
2/18	50	SW	10	4/4	41	N	13
2/19	41	W	13	4/5	41	W	7
2/20	41	W	3	4/6	46	NW	3
2/21	51	S	14	4/7	42	NE	5
2/22	41	N	13	4/8	35	N	10
2/23	29	W	6	4/9	34	N	5

Cleveland, Ohio--Continued

Date	$\overline{T}$ (°F)	Surface wind $\overline{dd}$	$\overline{ff}$ (mi/h)	Date	$\overline{T}$ (°F)	Surface wind $\overline{dd}$	$\overline{ff}$ (mi/h)
4/10	44	W	9	4/15	69	SW	14
4/11	40	N	15	4/16	72	W	8
4/12	35	N	6	4/17	70	SW	8
4/13	42	W	4	4/18	69	SW	6
4/14	53	S	8	4/19	68	W	3

Toledo, Ohio January 1 - April 19, 1976

Date	$\overline{T}$ (°F)	Surface wind $\overline{dd}$	$\overline{ff}$ (mi/h)	Date	$\overline{T}$ (°F)	Surface wind $\overline{dd}$	$\overline{ff}$ (mi/h)
1/1	28	E	7	2/2	4	W	11
1/2	34	S	9	2/3	7	S	6
1/3	22	W	15	2/4	24	W	7
1/4	13	W	17	2/5	19	NE	12
1/5	12	S	9	2/6	14	W	10
1/6	24	S	11	2/7	13	SW	14
1/7	24	NW	5	2/8	27	W	14
1/8	6	W	10	2/9	20	S	8
1/9	5	SW	14	2/10	44	S	13
1/10	12	S	7	2/11	33	W	13
1/11	28	SW	9	2/12	37	S	12
1/12	23	SW	10	2/13	37	W	6
1/13	28	N	1	2/14	28	E	5
1/14	23	W	14	2/15	46	S	12
1/15	22	S	9	2/16	38	E	5
1/16	22	W	10	2/17	41	W	2
1/17	7	N	10	2/18	45	W	7
1/18	1	S	2	2/19	37	W	10
1/19	20	S	12	2/20	36	S	4
1/20	24	W	12	2/21	48	E	3
1/21	20	W	10	2/22	29	NW	14
1/22	12	W	10	2/23	22	W	7
1/23	14	E	9	2/24	46	S	14
1/24	20	N	1	2/25	55	S	12
1/25	31	E	9	2/26	50	SW	10
1/26	33	W	11	2/27	50	SW	10
1/27	17	W	7	2/28	45	W	3
1/28	21	SW	11	2/29	47	W	6
1/29	28	W	10	3/1	37	E	16
1/30	24	E	4	3/2	36	E	11
1/31	24	SW	8	3/3	53	W	2
2/1	16	W	7	3/4	53	E	7

Toledo, Ohio--Continued

Date	$\overline{T}$ (°F)	Surface wind $\overline{dd}$	$\overline{ff}$ (mi/h)	Date	$\overline{T}$ (°F)	Surface wind $\overline{dd}$	$\overline{ff}$ (mi/h)
3/5	50	W	19	3/28	42	E	3
3/6	33	W	17	3/29	45	E	9
3/7	32	W	15	3/30	61	S	12
3/8	27	N	2	3/31	42	W	9
3/9	35	E	7	4/1	39	W	11
3/10	36	SW	6	4/2	44	W	9
3/11	31	E	6	4/3	48	E	8
3/12	46	S	9	4/4	39	N	12
3/13	32	W	17	4/5	43	W	9
3/14	37	SW	11	4/6	51	W	8
3/15	34	NE	4	4/7	44	N	7
3/16	29	NW	11	4/8	35	N	9
3/17	23	W	13	4/9	35	NW	3
3/18	40	S	8	4/10	46	W	9
3/19	59	S	14	4/11	41	N	13
3/20	62	S	17	4/12	34	W	4
3/21	40	W	17	4/13	41	W	6
3/22	26	SW	3	4/14	56	S	8
3/23	41	SW	9	4/15	73	SW	12
3/24	56	S	13	4/16	74	SW	11
3/25	53	W	10	4/17	71	S	9
3/26	59	S	14	4/18	68	S	10
3/27	48	SW	11	4/19	70	W	8

Detroit, Mich. January 1 - April 19, 1976

Date	$\overline{T}$ (°F)	Surface wind $\overline{dd}$	$\overline{ff}$ (mi/h)	Date	$\overline{T}$ (°F)	Surface wind $\overline{dd}$	$\overline{ff}$ (mi/h)
1/1	31	E	9	1/15	24	S	6
1/2	35	S	12	1/16	24	W	8
1/3	28	W	16	1/17	11	NW	16
1/4	18	W	15	1/18	7	S	5
1/5	16	SW	10	1/19	24	S	15
1/6	27	S	16	1/20	29	W	16
1/7	25	NW	7	1/21	23	W	10
1/8	11	W	12	1/22	15	N	9
1/9	10	SW	17	1/23	12	E	10
1/10	15	S	8	1/24	19	NE	4
1/11	29	S	8	1/25	34	E	10
1/12	28	SW	11	1/26	37	W	10
1/13	31	SE	1	1/27	22	W	10
1/14	26	W	15	1/28	22	SW	15

Date	$\overline{T}$ (°F)	Surface wind $\overline{dd}$	$\overline{ff}$ (mi/h)	Date	$\overline{T}$ (°F)	Surface wind $\overline{dd}$	$\overline{ff}$ (mi/h)
1/29	29	W	11	3/10	36	SW	6
1/30	21	E	6	3/11	32	N	5
1/31	24	S	12	3/12	44	S	13
2/1	16	W	9	3/13	36	W	15
2/2	6	W	13	3/14	37	SW	17
2/3	16	S	11	3/15	34	N	2
2/4	26	W	9	3/16	30	NW	8
2/5	21	NE	8	3/17	23	W	13
2/6	19	W	10	3/18	39	S	13
2/7	21	SW	14	3/19	60	S	16
2/8	30	W	11	3/20	61	S	19
2/9	30	S	10	3/21	43	W	17
2/10	44	S	16	3/22	28	SW	4
2/11	35	W	15	3/23	44	S	13
2/12	38	S	15	3/24	58	S	18
2/13	38	NW	8	3/25	56	W	10
2/14	31	SE	4	3/26	59	S	13
2/15	47	S	14	3/27	49	SW	11
2/16	40	E	4	3/28	40	E	3
2/17	41	W	2	3/29	45	E	12
2/18	46	S	6	3/30	61	S	11
2/19	40	W	13	3/31	45	SW	11
2/20	41	S	6	4/1	40	W	12
2/21	40	NE	7	4/2	42	W	6
2/22	29	N	14	4/3	48	E	8
2/23	26	W	7	4/4	42	N	13
2/24	45	SW	14	4/5	47	W	9
2/25	58	S	17	4/6	52	NW	7
2/26	53	SW	9	4/7	46	NE	8
2/27	49	S	7	4/8	35	N	11
2/28	47	W	2	4/9	37	E	3
2/29	48	S	6	4/10	51	W	12
3/1	33	NE	14	4/11	39	N	16
3/2	34	E	9	4/12	40	W	8
3/3	39	E	3	4/13	50	W	8
3/4	49	NE	5	4/14	60	S	9
3/5	48	SW	16	4/15	73	S	14
3/6	33	W	14	4/16	75	SW	10
3/7	30	W	17	4/17	73	S	13
3/8	29	SW	2	4/18	71	S	12
3/9	36	E	8	4/19	70	W	10

(Continued from inside front cover)

NESS 67 Data Collection System Geostationary Operational Environmental Satellite: Preliminary Report. Merle L. Nelson, March 1975, 48 pp. (COM-75-10679/AS)

NESS 68 Atlantic Tropical Cyclone Classifications for 1974. Donald C. Gaby, Donald R. Cochran, James B. Lushine, Samuel C. Pearce, Arthur C. Pike, and Kenneth O. Poteat, April 1975, 6 pp. (COM-75-1676/AS)

NESS 69 Publications and Final Reports on Contracts and Grants, NESS-1974. April 1975, 7 pp. (COM-75-10850/AS)

NESS 70 Dependence of VTPR Transmittance Profiles and Observed Radiances on Spectral Line Shape Parameters. Charles Braun, July 1975, 17 pp. (COM-75-11234/AS)

NESS 71 Nimbus-5 Sounder Data Processing System, Part II: Results. W. L. Smith, H. M. Woolf, C. M. Hayden, and W. C. Shen. July 1975, 102 pp. (COM-75-11334/AS)

NESS 72 Radiation Budget Data From the Meteorological Satellites, ITOS 1 and NOAA 1. Donald H. Flanders and William L. Smith, August 1975, 22 pp. (PB-246877/AS)

NESS 73 Operational Processing of Solar Proton Monitor Data. Stanley R. Brown, September 1975. (Revision of NOAA TM NESS 49), 15 pp.

NESS 74 Monthly Winter Snowline Variation in the Northern Hemisphere from Satellite Records, 1966-75. Donald R. Wiesnet and Michael Matson, November 1975, 21 pp. (PB-248437)

NESS 75 Atlantic Tropical and Subtropical Cyclone Classifications for 1975. D. C. Gaby, J. B. Lushine, B. M. Mayfield, S. C. Pearce, and K. O. Poteat, March, 1976, 14 pp. (PB-253968/AS)

NESS 76 The Use of the Radiosonde in Deriving Temperature Soundings From the Nimbus and NOAA Satellite Data. Christopher M. Hayden, April 1976, 21 pp. (PB-256755)

NESS 77 Algorithm for Correcting the VHRR Imagery for Geometric Distortions Due to the Earth's Curvature and Rotation. Richard Legeckis and John Pritchard, April 1976, 30 pp. (PB-258027/AS)

NESS 78 Satellite Derived Sea-Surface Temperatures From NOAA Spacecraft. Robert L. Brower, Hilda S. Gohrband, William G. Pichel, T. L. Signore, and Charles C. Walton, June 1975, 74pp. (PB-258026/AS)

NESS 79 Publications and Final Reports on Contracts and Grants, 1975. NESS, June 1976, 18 pp. (PB-258450/AS)

NESS 80 Satellite Images of Lake Erie Ice: January-March 1975. Michael C. McMillan and David Forsyth, June 1976, 15 pp. (PB-258458/AS)

NESS 81 Estimation of Daily Precipitation Over China and the USSR Using Satellite Imagery. Walton A. Follansbee, September 1976, 37 pp. (PB-261970/AS)

NESS 82 The GOES Data Collection System Platform Address Code. Wilfred E. Mazur, Jr., October 1976, 26 pp. (PB-261968/AS)

NESS 83 River Basin Snow Mapping at the National Environmental Satellite Service. Stanley R. Schneider, Donald R. Wiesnet, and Michael C. McMillan, November, 1976, 27 pp. (PB-263816)

NESS 84 Winter Snow-Cover Maps of North America and Eurasia From Satellite Records; 1966-1976. Michael Matson, March 1977.

NESS 85 A Relationship Between Weakening of Tropical Cyclone Cloud Patterns and Lessening of Wind Speed. James B. Lushine, March 1977, 12 pp.

NESS 86 A Scheme for Estimating Convective Rainfall From Satellite Imagery. Roderick A. Scofield and Vincent J. Oliver, April 1977.

NESS 87 Atlantic Tropical and Subtropical Cyclone Classifications for 1976. D. C. Gaby, J. B. Lushine, B. M. Mayfield, S. C. Pearce, K. O. Poteat, and F. E. Torres, May 1977.

NESS 88 NOAA Catalogue of Products. Dennis C. Dismachek, Editor, June 1977.

NESS 89 A Laser Method of Observing Surface Pressure and Pressure-Altitude and Temperature Profiles of the Troposphere from Satellites. William L. Smith and C. M. R. Platt, July 1977, 38 pp.

NOAA SCIENTIFIC AND TECHNICAL PUBLICATIONS

NOAA, the *National Oceanic and Atmospheric Administration,* was established as part o ment of Commerce on October 3, 1970. The mission responsibilities of NOAA are to monitor an state of the solid Earth, the oceans and their living resources, the atmosphere, and the space environment of the Earth, and to assess the socioeconomic impact of natural and technological changes in the environment.

The six Major Line Components of NOAA regularly produce various types of scientific and technical information in the following kinds of publications:

PROFESSIONAL PAPERS — Important definitive research results, major techniques, and special investigations.

TECHNICAL REPORTS—Journal quality with extensive details, mathematical developments, or data listings.

TECHNICAL MEMORANDUMS — Reports of preliminary, partial, or negative research or technology results, interim instructions, and the like.

CONTRACT AND GRANT REPORTS—Reports prepared by contractors or grantees under NOAA sponsorship.

TECHNICAL SERVICE PUBLICATIONS—These are publications containing data, observations, instructions, etc. A partial listing: data serials; prediction and outlook periodicals; technical manuals, training papers, planning reports, and information serials; and miscellaneous technical publications.

ATLAS—Analysed data generally presented in the form of maps showing distribution of rainfall, chemical and physical conditions of oceans and atmosphere, distribution of fishes and marine mammals, ionospheric conditions, etc.

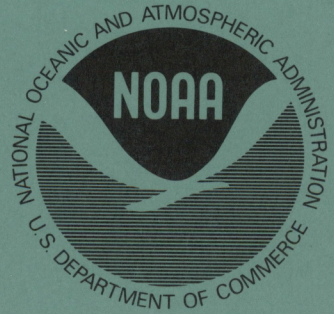

Information on availability of NOAA publications can be obtained from:

ENVIRONMENTAL SCIENCE INFORMATION CENTER
ENVIRONMENTAL DATA SERVICE
NATIONAL OCEANIC AND ATMOSPHERIC ADMINISTRATION
U.S. DEPARTMENT OF COMMERCE

3300 Whitehaven Street, N W
Washington, D C 20235

NOAA--S/T 77-2810